Apports des modèles de métapopulation hors équilibre : application à l'évaluation de la dynamique des plantes forestières

Etienne Lalechère

N° d'ordre : 827

UNIVERSITÉ CLERMONT AUVERGNE

U.F.R. Sciences et Technologies

ÉCOLE DOCTORALE DES SCIENCES POUR L'INGÉNIEUR

THÈSE

Présentée par

Étienne LALECHÈRE

pour obtenir le grade de

DOCTEUR D'UNIVERSITÉ

Spécialité : Informatique

Apports des modèles de métapopulation hors équilibre : application à l'évaluation de la dynamique des plantes forestières

Soutenue le 8 décembre 2017

Rapporteurs :

Déborah CLOSSET-KOPP (*Maître de Conférence, Université de Picardie Jules Verne*)

Hélène FRÉVILLE (*Chargée de Recherche, INRA, Montpellier)*

Examinateurs :

Kris VERHEYEN *(Professeur, Université de Gand)*

Christian DESVILETTES (*Professeur, Université Clermont Auvergne)*

Directeur :

Guillaume DEFFUANT (*Directeur de Recherche, IRSTEA, Clermont-Ferrand)*

Encadrants :

Franck JABOT (*ICPEF, IRSTEA, Clermond-Ferrand)*

Frédéric ARCHAUX (*ICPEF IRSTEA, Nogent-sur-Vernisson)*

Avant-propos

Cette thèse a été réalisée au centre IRSTEA (Institut national de Recherche en Sciences et Technologies pour l'Environnement et l'Agriculture) de Clermont-Ferrand au sein du LISC (Laboratoire d'Ingénierie des Systèmes Complexes). Elle a été financée par l'IRSTEA et la région Auvergne.

Résumé

Les modèles de métapopulations permettent de prédire l'occupation des habitats au sein desquels elles évoluent en fonction de la configuration spatiale du paysage. La destruction et la création d'habitats peuvent induire une dette d'extinction ou un crédit d'immigration, c'est-à-dire des dynamiques d'espèces qui ne sont pas immédiates mais décalées dans le temps par rapport cette rotation des habitats. La présence d'un délai temporel signifie que les espèces ne sont pas à l'équilibre avec les paysages actuels. Cette thèse a pour objectif d'évaluer l'apport de modèles de métapopulations hors équilibre pour comprendre ces dynamiques décalées dans le temps de façon théorique et à partir de données empiriques sur les plantes forestières.

A ces fins, nous avons évalué la robustesse d'une méthode d'inférence de paramètres de dynamique de métapopulations hors équilibre, adaptée à l'échelle régionale. Elle a ensuite été appliquée sur des données contemporaines de plantes forestières et de séries temporelles de cartographies des forêts dans les départements de la Seine-et-Marne et de l'Eure-et-Loir. A partir des modèles utilisés, nous avons pu reproduire certaines caractéristiques de la répartition des espèces qui sont dues à l'évolution historique des surfaces forestières. En effet, certaines espèces sont plus fréquentes en forêt anciennes et d'autres en forêt récentes, ce qui s'explique en partie par les traits des espèces et leurs affinités pour des conditions environnementales spécifiques. A partir de projections à long-terme de leurs dynamiques, nous avons montré que les délais de réponse de ces espèces peuvent être de plusieurs siècles et dépendent fortement de la connectivité fonctionnelle des habitats.

Des scénarios virtuels de rotation des habitats ont été simulés pour pallier l'analyse des seules zones d'études. Associé à des projections de dynamiques de métapopulations, qui permettent de contrôler les paramètres à étudier, nous avons testé l'importance relative de la distance de dispersion des espèces et de la configuration spatiale de la rotation des habitats sur ces dynamiques. Le temps de retour à l'équilibre des métapopulations ne s'explique pas uniquement par l'amplitude de la dette d'extinction ou du crédit d'immigration mais dépend aussi de ces deux facteurs. Ces résultats mettent en évidence l'importance d'approfondir nos connaissances sur les effets de perturbations successives qui rendent le retour théorique à l'équilibre des espèces très incertain.

Mots-clés : Dynamiques de biodiversité hors équilibre – Changements à long-terme – Dynamiques de paysage – Dette d'extinction – Crédit d'immigration – Métapopulation – Modèles stochastiques – Recrutement – Dispersion – Communauté – Plantes forestières

Abstract

Contributions of non-equilibrium metapopulation models: application to the assessment of forest plant dynamics.

Metapopulation models are used to predict the occupancy of habitats from landscape spatial configuration. Habitat destruction and creation can lead to an extinction debt or an immigration credit that are time-delayed species dynamics following habitat turnover. Such delays mean that species are not in equilibrium with the current landscape structures. The aim of this thesis is to evaluate the contribution of non-equilibrium metapopulation models to understand time-delayed dynamics theoretically and from empirical datasets about forest plants.

For this purpose, we assessed the robustness of the method used to infer metapopulation parameters at the regional scale. Then, we applied this method from contemporary plant inventories and time-series of forest maps of the Seine-et-Marne and the Eure-et-Loir french regions. Models satisfactorily reproduced some characteristics of forest plant spatial structure that are due to historical changes in forest areas. Indeed, some species are more frequent in ancient forests and some others are more frequent in recent forests notably due to species traits and their affinity for specific environmental characteristics. From long-term projections of species dynamics, we showed that the delays in forest plant dynamics are several centuries following habitat turnover and strongly depend on habitat functional connectivity.

Virtual scenarios of habitat turnover were simulated to assess other study cases than the two study areas. We projected metapopulation dynamics, while controlling for some metapopulation parameters, to test the relative effects of species dispersal distance and the spatial configuration of habitat turnover on these dynamics. Metapopulation return time towards equilibrium not only depends on the magnitude of the extinction debt or on the magnitude of the immigration credit but also on these two variables. These results put forward the need to improve our knowledge on the effects of successive perturbations that make species return towards equilibrium unsure.

Keywords: Non-equilibrium biodiversity dynamics – Long-term changes – Landscape dynamics – Extinction debt – Immigration credit – Metapopulation – Stochastic models – Recruitement – Dispersal – Community – Forest plants

Remerciements

Ce travail de thèse a été co-encadré par Franck Jabot et Frédéric Archaux que je remercie pour leur implication. Merci à Frédéric qui, depuis Nogent, est toujours resté disponible pour échanger et ce même en amont des résultats lorsque le dialogue et le débat sont indispensables à la construction d'une réflexion scientifique. Je souhaite également remercier pour son aide, Guillaume Deffuant, qui a dirigé cette thèse.

Merci à Laurent Bergès, Guillaume Decocq et Cécile Albert d'avoir accepté d'intégrer mon comité de suivi de thèse. Ces trois années consacrées à la recherche étant aussi une phase d'apprentissage, je vous remercie d'avoir assuré ce rôle.

Je remercie Déborah Closset-Kopp, Hélène Fréville, Kris Verheyen et Christian Desvilettes d'avoir accepté d'évaluer ce travail dont vous prendrez connaissance, je l'espère, avec intérêt.

Je remercie également tous ceux qui ont contribué à produire les données cartographiques utilisées dans ce manuscrit ainsi que l'Inventaire Forestier National (IFN) et le Conservatoire Botanique National du Bassin Parisien (CBNBP) pour avoir fourni les données d'inventaires.

Ces quelques années passées au LISC prenant fin, j'adresse une mention spéciale à tous les thésards avec qui j'ai partagé cette expérience.

C'est aussi grâce à tous les bons moments passés en dehors du labo que l'investissement nécessaire à la réalisation d'une thèse est digne d'intérêt. Merci à tous mes proches pour les moments de convivialité partagés. Je souhaite en particulier bon courage à celles et ceux pour qui la fin de thèse approche à grand pas. Enfin, je souhaite exprimer toute mon affection à ceux avec qui j'ai trop peu eu l'occasion de partager mon temps, votre présence restera toujours plus importante que le reste. Merci à mes parents pour les (trop rares) bons moments passés ensemble durant ces trois ans et pour la bouffée d'oxygène que procure un retour dans les Alpes. Enfin, merci Marianne...

Table des matières

Chapitre I : Introduction

I.1. Contexte général

Parmi les activités humaines, les changements d'usage des sols constituent un facteur majeur du déclin de la biodiversité à l'échelle planétaire (Sala et al. 2000, Newbold et al. 2015). Ils sont responsables de la destruction des habitats qui peut conduire des espèces ou des populations à l'extinction (Ceballos et al. 2017, Tilman et al. 2017). Cette destruction est associée à une réduction de la surface des habitats rémanents et une augmentation de leur isolement géographique (Forman 1995). Pour de nombreux taxons, ces changements induisent des dynamiques d'extinction progressives sur des temps longs (Kuussaari et al. 2009). Pour y faire face, la création d'habitats peut être planifiée par l'homme avec la mise en place de réseaux ou de compensations écologiques par exemple (Boitani et al. 2007, Bull et al. 2015). La création d'habitats peut aussi être spontanée, c'est le cas de la reforestation qui est en cours en Europe de l'Ouest depuis deux siècles (Hermy et Verheyen 2007). Le turnover des habitats, c'est-à-dire leur rotation au cours du temps, comprend donc à la fois une part de destruction et une part de création. Les dynamiques de biodiversité induites par ces changements peuvent être immédiates ou décalées dans le temps (Jackson et Sax 2010). La présence de tels décalages temporels indique que les espèces ne sont pas à l'équilibre avec les paysages actuels dans lesquels elles évoluent. Dans ce cas, leur répartition spatiale dépend encore en partie des paysages tels qu'ils étaient avant le turnover des habitats.

De nombreuses études empiriques ont contribué à établir que certaines communautés ne sont pas à l'équilibre. Pour ce faire, des méthodes statistiques ont été développées à cette échelle d'organisation à partir de l'utilisation de données historiques (Vellend et al. 2013, Kuussaari et al. 2009). Elles consistent, par exemple, à démontrer que le nombre d'espèces d'une communauté s'explique davantage par la structure des paysages passés plutôt que par celle des paysages actuels (Lindborg et Eriksson 2004, Adriaens et al. 2006). À un niveau d'organisation plus fin, des modèles de métapopulations (ensemble de populations) hors équilibre ont été développés (Verheyen et al. 2004, Ruete et al. 2014). Ils ont l'avantage de permettre l'étude du processus de relaxation, qui caractérise les dynamiques de biodiversité qui font suite à une perturbation (*e.g.* le turnover des habitats) jusqu'à un nouvel équilibre (Hylander et Ehrlén 2013). Ces modèles permettent de mesurer le temps de relaxation, qui est la durée de ce processus, et d'identifier ses déterminants. Ils n'ont cependant pas été utilisés en ce sens jusqu'ici. La capacité de ces modèles à répondre à cet objectif dépend de la robustesse des méthodes d'estimation des paramètres qui leurs sont associées.

Les forêts tempérées d'Europe de l'Ouest et de l'Est de l'Amérique du Nord ont connu des phases de déforestation et de reforestation successives durant les siècles précédents (Flinn et Vellend 2005, Hermy et Verheyen 2007). Depuis le début de l'industrialisation, il y a deux siècles, une reforestation importante est en cours sur d'anciennes terres agricoles. En parallèle de cette reforestation les forêts anciennes peuvent être en partie érodées, notamment à cause de l'urbanisation. L'interaction entre ces deux processus antagonistes reste peu connue (Jackson et Sax 2013). Les plantes forestières, qui sont soumises à ce turnover d'habitat, ont des dynamiques de colonisation et d'extinction très lentes dans l'espace et dans le temps (Cronk 2016). Ce sont donc des organismes particulièrement susceptibles de présenter des décalages temporels importants. Par conséquent, ce sont des modèles biologiques appropriés pour étudier les dynamiques de biodiversité hors équilibre.

L'objectif des travaux présentés dans ce manuscrit est d'évaluer l'apport des modèles de métapopulation hors équilibre pour comprendre les dynamiques qui font suite au turnover des habitats au sein desquels elles évoluent. Il s'agit de comprendre comment ces dynamiques sont influencées par les caractéristiques des espèces et des paysages, à partir de données empiriques et simulées. La suite de cette introduction décrit plus précisément (i) l'évolution des connaissances qui a conduit à considérer des dynamiques de biodiversité hors équilibre puis, (ii) l'apport des modèles de métapopulations hors équilibre et enfin (iii) les conséquences du turnover des forêts depuis le milieu du XIX^{ème} siècle sur la dynamique des plantes de sous-bois. Cette introduction a pour objectif de contextualiser et de problématiser les questions de recherches qui sont énoncées en fin de section. Les travaux qui ont pour objectif de répondre à ces questions sont présentés dans les trois chapitres qui suivent l'introduction et une discussion générale clôt le document.

I.2. Dynamiques de biodiversité hors équilibre

I.2.1 Processus de relaxation

I.2.1.1 Origines du processus

Les dynamiques de biodiversité étudiées dans ce manuscrit ont pour origine un turnover des habitats (ou patchs) qui modifie leurs connectivités. La connectivité est définie à l'échelle du patch (Hanski 1998) et prend en compte à la fois une modification de la surface des patchs (gains et pertes) et de leur isolement géographique, c'est à dire du degré de fragmentation (Figure 1). Dans ce manuscrit, on s'appuie sur le concept de connectivité, utilisé pour comparer la configuration spatiale de différentes zones

géographiques, et sur le concept de connectivité fonctionnelle qui prendra également en compte la capacité de dispersion des espèces (Kindlmann et Burel 2008). Dans le chapitre III, on s'intéresse plus particulièrement à comparer des scénarios de turnover d'habitat où la surface totale d'habitat est constante et le degré de fragmentation variable ou l'inverse. Dans un paysage donné, une telle reconfiguration spatiale se produit lorsque des patchs sont détruits et/ou créés (Figure 1).

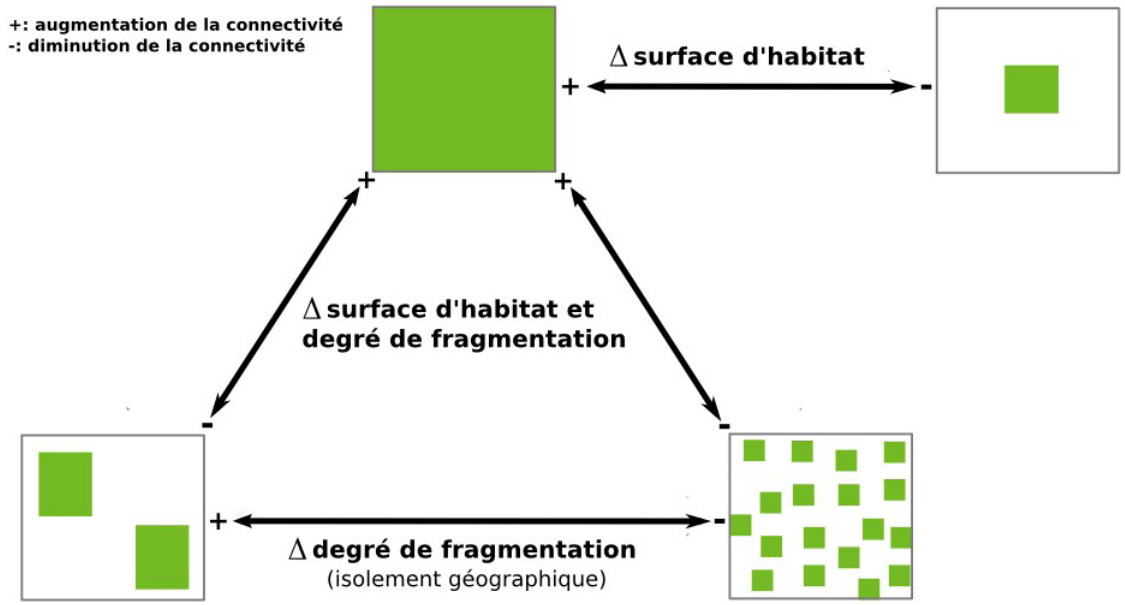

Figure 1 : Evolution de la connectivité en fonction de la surface d'habitat et du degré de fragmentation (isolement géographique). Les patchs (en vert) sont incorporés dans une matrice inhabitable (en blanc). Chaque flèche indique un changement de la configuration spatiale des patchs. Dans un paysage donné, ce changement se produit lorsque des patchs sont détruits et/ou créés. Dérivé de Fahrig et al. (2017).

La connectivité est un concept issu de l'écologie du paysage, discipline scientifique qui s'est développée en parallèle des systèmes d'information géographique avec l'objectif de mieux comprendre la dimension spatiale des processus écologiques en lien avec leur environnement (Burel et Baudry 1999). La généralisation de la photographie aérienne et des systèmes d'information géographique, qui permettent de les exploiter, ont fortement contribué à faire évoluer la discipline à partir des années 1980. Un des aspects fondamentaux est de caractériser, par des métriques, l'hétérogénéité du paysage en termes de composition et de configuration spatiale. Le paysage est perçu à travers le prisme des espèces, ce qui conduit à le représenter par des cartographies qui dépendent de celles-ci. Par exemple, cartographier la surface d'habitat disponible pour une espèce donnée permet de quantifier le risque d'extinction en fonction des besoins de cette espèce par rapport à ce critère (Vos et al. 2001). Cette vision du paysage se traduit par

différents modèles de représentation. Par exemple, le paysage peut être représenté par une cartographie de l'occupation des sols qui définit l'habitat d'une espèce, c'est à dire par une cartographie d'un ensemble de patchs. C'est la représentation qui est utilisée dans ce manuscrit. Parmi les représentations du paysage alternatives, les graphes paysagers sont également très fréquemment utilisés. Ils représentent le paysage comme un ensemble de nœuds interconnectés par des liens évalués selon l'intensité de ces connexions. Par exemple, les nœuds peuvent représenter des patchs et les liens entre les nœuds la connectivité fonctionnelle entre ceux-ci (Urban et Keitt 2001).

I.2.1.2 Dette d'extinction et crédit d'immigration

Plusieurs études (Stork 2010, Cronk 2016) rapportent que le nombre d'extinction d'espèces observés par l'IUCN (International Union for Conservation of Nature) est faible par rapport aux prédictions (*e.g.* Pimm et Raven 2000), quel que soit le taxon considéré. Les prédictions évoquées dans ces études (Stork 2010, Cronk 2016) reposent notamment sur la relation aire-espèce qui postule que le nombre d'espèces est une fonction positive de la surface d'habitat disponible (Connor et McCoy 1979). La surestimation du nombre d'extinction prédit, à partir des destructions d'habitats récentes observées, peut être en partie imputée aux limites de ces modèles (He et Hubell 2011, Halley et al. 2013a). Une autre explication est que l'extinction des espèces est progressive et très lente dans le temps (Cronk 2016) notamment à cause des réponses microévolutives à la pression de sélection, du développement de formes de résistance au cours du cycle de vie des organismes, de la stochasticité démographique qui implique qu'une population qui comprend peu d'individus ne s'éteint pas immédiatement et de la colonisation qui contrebalance l'extinction des populations (Hylander et Ehrlén 2013).

Les dynamiques de biodiversité hors équilibre sont définies par Jackson et Sax (2010) comme des dynamiques à long terme qui font suite à l'événement qui les a initiées. Cet événement est définit par Hylander et Ehrlén (2013) comme une diminution de la connectivité (Figure 1) ou de la qualité des habitats. Dans ce contexte, la dette d'extinction (Figure 2) a été définie comme le nombre d'espèces qui sont amenées à s'éteindre suite à cet événement (Tilman 1994). Au vu de l'importance de la destruction des habitats à l'échelle planétaire (Newbold et al. 2015), la littérature est principalement centrée sur l'étude de la dette d'extinction. Le crédit d'immigration (Figure 2) a donc été défini, plus tardivement, comme le nombre d'espèces amenées à immigrer suite à une augmentation de la connectivité ou de la qualité des habitats (Nagelkerke et al. 2002, Jackson et Sax 2010).

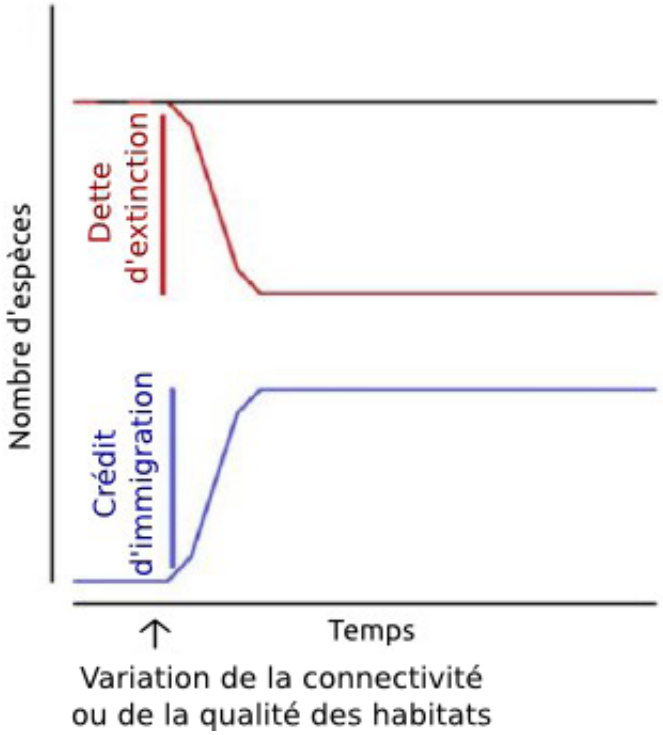

Figure 2 : Dette d'extinction et crédit d'immigration définis à l'échelle de la communauté. Dérivé de Jackson et Sax (2010).

I.2.2 Intérêt de l'échelle de la métapopulation pour évaluer le processus de relaxation

I.2.2.1 La théorie des métapopulations

La théorie des métapopulations (Levins 1969, 1970) prend racine dans la volonté de transférer aux écosystèmes terrestres la théorie de la biogéographie insulaire (MacArthur et Wilson 1967), qui a pour objectif d'expliquer les patrons de diversité entre îles et continents. Il en découle une vision simplifiée du paysage (Figure 3) où des patchs d'habitats discontinus (îles) sont intégrés au sein d'une matrice inhabitable (océan). Dans ce contexte, une métapopulation est un assemblage de populations d'une espèce, interconnectées par des événements de dispersion (Levins 1970). Dans le modèle classique de Levins, tous les patchs sont source d'immigration (Figure 3A). Dans le modèle île-continent (MacArthur et Wilson 1967, Boorman-Levitt 1973), les patchs sources sont occupés par une population de taille infinie à partir desquels les patchs puits sont colonisés (Figure 3B). Parmi les différentes représentations possibles d'une métapopulation, ces deux modèles sont des situations extrêmes le long d'un gradient d'hétérogénéité de la taille des patchs (Driscol 2007).

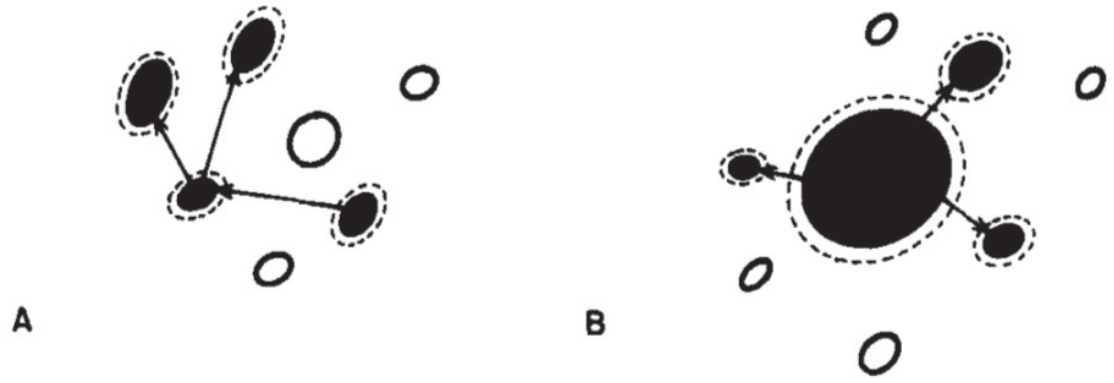

Figure 3 : Différents types de métapopulations (Harrison 1991). Les cercles pleins et vides représentent respectivement des patchs occupés ou vides incorporés dans une matrice inhabitable. Les cercles discontinus représentent des populations. A : Modèle classique de Levins (1970), B : Modèle île-continent (Boorman-Levitt 1973).

L'idée clé de cette théorie est qu'une métapopulation persiste à l'échelle du paysage si la colonisation de patchs inoccupés compense l'extinction locale des populations. Hanski (1994) relie la probabilité de colonisation d'un patch à la distance au patch source et à la surface de ce dernier, utilisée comme proxy du nombre de migrants potentiels. L'hypothèse d'une relation entre la surface du patch et le nombre d'individus est également utilisée pour définir la probabilité d'extinction d'une population comme fonction inverse de la surface du patch. Le nombre de populations d'une métapopulation dépend donc du nombre de patchs, de leurs surfaces et de leur isolement géographique, autrement dit de leurs connectivités. Dans ce manuscrit, on fait l'hypothèse que la résistance à la dispersion ne dépend pas de la nature de la matrice. Il est cependant peu probable que différents usages des sols freinent la dispersion des organismes de façon équivalente (Prugh et al. 2008).

I.2.2.2 Dynamiques de biodiversité hors équilibre selon le niveau d'organisation

A partir d'une synthèse de la littérature, Hylander et Ehrlén (2013) ont identifié certains mécanismes qui peuvent être à l'origine d'un déclin de biodiversité décalé dans le temps à différents niveaux d'organisation. La survie d'un individu dépend de la qualité du patch et des interactions biotiques. Chez les plantes, par exemple, les conséquences d'un stress environnemental peuvent être retardées par la présence de banques de graines ou de rhizomes. La présence d'un individu d'une espèce longévive peut s'expliquer par des conditions passées favorables à la germination et au développement mais qui n'ont plus cours. La compétition pour les ressources du sol ou la lumière peut amener à exclure progressivement les individus les moins compétitifs. Ces changements à l'échelle des

individus se répercutent sur la taille et la répartition des populations. Une population qui comprend peu d'individus ne s'éteint pas immédiatement mais est davantage exposée à la stochasticité démographique et environnementale. La dérive génétique peut également affecter la persistance à long terme d'une population qui comprend peu d'individus. À l'échelle de la métapopulation, l'équilibre entre la colonisation et l'extinction des populations est source de décalages temporels. Ils peuvent être dus à la colonisation de patchs inoccupés ou à un effet de sauvetage, c'est à dire à l'immigration d'individus qui préviennent une population de l'extinction (Brown et Kodric-Brown 1977). Un taux d'extinction très faible, chez des espèces plus tolérantes au stress par exemple, peut expliquer la lenteur du processus d'extinction à l'échelle de la métapopulation. Finalement, la composition des communautés dépend des dynamiques de métapopulation sous-jacentes. Plus généralement, les délais temporels à un niveau d'organisation sont susceptibles de s'accumuler aux niveaux d'organisation supérieurs (Essl et al. 2015). La notion de dette d'extinction peut donc être transposée à ces différents niveaux.

I.2.2.3 Dynamiques hors équilibre à l'échelle des communautés

L'étude des dynamiques de biodiversité hors équilibre est principalement centrée sur la dette d'extinction à l'échelle des communautés (Kuussari et al. 2009, Hylander et Ehrlén 2013). Tilman et al. (1994) ont proposé le concept de dette d'extinction et ont fortement influencé les travaux ultérieurs. Dans ce modèle théorique, le nombre de populations dépend de la compétition entre espèces et de la destruction d'habitats qui entraîne un déclin progressif du nombre de populations de certaines espèces jusqu'à l'extinction. La formalisation de ce modèle de patch repose sur la théorie des métapopulations mais la dette d'extinction est définie à l'échelle de la communauté en fonction du déclin de la richesse spécifique. Tilman précise que les extinctions à venir représentent une dette et donc un coût écologique qui sera payé progressivement après la destruction des habitats. Les travaux empiriques ultérieurs se sont majoritairement attelés à identifier un déclin de la richesse spécifique de communautés suite à la destruction des habitats. À ce niveau d'organisation, des dettes d'extinction ont été détectées pour des taxons très divers tels que les plantes, les oiseaux, les arthropodes, les poissons ou encore les primates (Kuussari et al. 2009).

I.2.2.4 Intérêt de l'échelle de la métapopulation

Selon Hylander et Ehrlén (2013), pour comprendre les processus qui sous-tendent les dynamiques de communauté hors équilibre, il faut changer de point de vue et considérer

l'échelle de l'espèce. À cette échelle, ils définissent la dette d'extinction comme le nombre de populations amenées à s'éteindre suite à une diminution de la connectivité ou de la qualité des habitats (Figure 4). Dans ce contexte, le temps de relaxation est défini comme la durée du paiement de la dette d'extinction qui prend fin lorsqu'un nouvel équilibre est atteint (Figure 4). Cet équilibre est un état dynamique de la métapopulation où le nombre de populations reste stable, malgré des événements de colonisation et d'extinction qui se compensent. Il reflète le patron spatial d'occupation des patchs à long terme (Moilanen 1999). On peut également transposer le concept de dette d'extinction, défini à l'échelle de l'espèce par Hylander et Ehrlén (2013), au crédit d'immigration qui est le nombre de populations amenées à se constituer suite à une augmentation de la connectivité ou de la qualité des habitats.

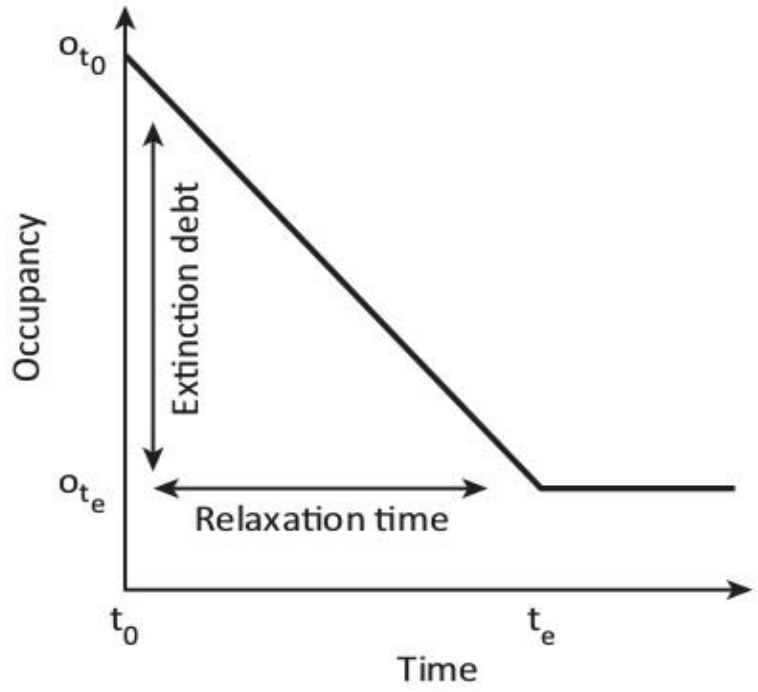

Figure 4 : Dette d'extinction et temps de relaxation définis à l'échelle de la métapopulation. Une modification de la qualité ou de la connectivité des habitats se produit à t_0 *et induit des extinctions de population jusqu'à* t_e *où un nouvel équilibre est atteint.* Ot_o *et* Ot_e *représentent l'occupation (le nombre de populations) à* t_0 et t_e *respectivement (Hylander et Ehrlén, 2013).*

Les travaux présentés dans ce manuscrit se focalisent sur des dynamiques hors équilibre à l'échelle des métapopulations et sur leurs conséquences sur la composition des communautés. Il est à noter que la qualité des patchs et les interactions interspécifiques, qui peuvent également impacter la dynamique des métapopulations, ne sont pas pris en compte dans le canevas de modélisation.

I.3. Apport des modèles de métapopulations hors équilibre pour évaluer le processus de relaxation

I.3.1 Limites des approches corrélatives couramment utilisées

Les dynamiques de biodiversité hors équilibre s'expliquent à partir de changements intervenus dans le passé. Ainsi, comprendre l'influence à long terme de ces changements permet d'anticiper ceux qui adviendront dans le futur. C'est l'objectif de « l'écologie historique » qui implique d'identifier les données historiques disponibles pour étudier l'évolution de la biodiversité sur des temps longs (Vellend et al. 2013). Parmi ces données, les inventaires de biodiversité anciens et les cartes historiques sont utiles pour faire le lien entre les patrons de biodiversité et la configuration spatiale des paysages. Différentes approches ont été utilisées pour détecter des dynamiques de biodiversité hors équilibre (Kuussaari et al. 2009). Le choix de l'approche dépend beaucoup des données disponibles. Certains travaux sont basés sur l'utilisation de séries temporelles d'inventaire de biodiversité et de paysage synchrones (Hautekèete et al. 2015, McCune et Vellend 2015). Cependant, il est rare de disposer de données d'inventaire de biodiversité sur des temps longs, même si les réseaux de recherche écologique à long terme ont été mis en place notamment pour répondre à cet objectif (Parr et al. 2002). Dans ce manuscrit, on se focalise donc sur les méthodes qui nécessitent un inventaire de biodiversité ponctuel dans le temps, l'information historique étant issue des cartographies. Ces méthodes ont été principalement appliquées pour détecter des dettes d'extinction. Cependant, elles sont également applicables au concept de crédit d'immigration.

Une première approche consiste à comparer des paysages actuels stables et instables (Figure 5b). Par exemple, Vellend et al. (2006) ont ajusté des modèles de régressions logistiques, à partir de données de présence-absence de plantes forestières (un modèle par espèce) dans un paysage du Royaume-Uni qui est resté relativement stable durant le dernier millénaire. Ces modèles sont ensuite utilisés pour prédire l'occupation des patchs des mêmes espèces dans un autre paysage, situé en Belgique, qui a connu une fragmentation importante entre le milieu du XIII^{ème} siècle et la fin du XIX^{ème} siècle et qui présente aujourd'hui une surface boisée totale équivalente à celle du paysage anglais. Il ressort que les modèles extrapolés à la Belgique sous-estiment le taux d'occupation des espèces qui ont des dynamiques de colonisation lentes. Il y a donc plus de populations qu'attendu sous l'hypothèse que les espèces sont à l'équilibre avec le paysage actuel. Une seconde approche couramment utilisée est de comparer le pouvoir explicatif de métriques paysagères, calculées à partir de paysages actuels et anciens, sur la diversité actuelle de communautés (Figure 5a). Par exemple, Kimberley et al. (2016)

ont étudié la composition de communautés de plantes de sous-bois, échantillonnées dans 82 patchs forestiers déjà présents à la fin XIX^{ème} siècle. Les métriques paysagères ont été calculées à partir de cartographies des habitats, qui témoignent d'une fragmentation ancienne. Les auteurs concluent à la présence d'une dette d'extinction car que la richesse spécifique des espèces rares est plus fortement corrélée aux métriques paysagères anciennes plutôt qu'aux actuelles. Cette diversité s'explique donc davantage par la configuration spatiale du paysage ancien. Par conséquent, la fragmentation continuera à induire l'extinction de certaines espèces jusqu'à ce que la dette d'extinction soit payée. Ces deux approches sont utilisées pour tester l'hypothèse que la richesse spécifique ou l'occupation des patchs s'expliquent davantage par les paysages historiques que par les paysages actuels. Elles ne permettent cependant pas de projeter des dynamiques de biodiversité, depuis le turnover des habitats jusqu'au temps de relaxation, pour mesurer leurs amplitudes et leurs durées. Le développement de modèles mécanistes permet de pallier ces limites (Essl et al. 2015).

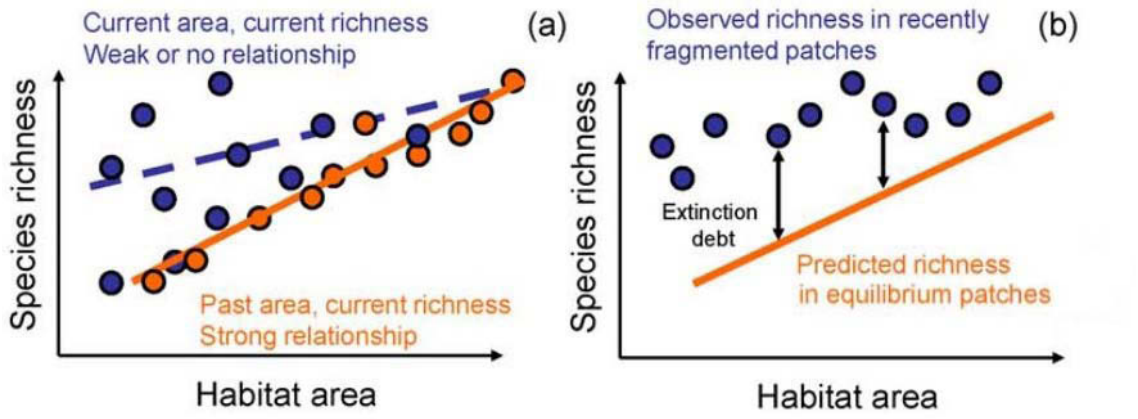

Figure 5 : Exemple d'approches utilisées pour évaluer la dette d'extinction à partir des caractéristiques passées et actuelles des paysages (a) ou de la comparaison de paysages actuels stables et instables (b). Dérivé de Kuussaari et al. (2009).

I.3.2 Modèles stochastiques d'occupation des patchs et inférence statistique

I.3.2.1 Cas des paysages statiques et dynamiques

Dans le cadre de la théorie des métapopulations, des modèles stochastiques d'occupation des patchs (Hanski 1994, Moilanen 1999) ont été développés pour des espèces supposées à l'équilibre avec le paysage. Ces modèles décrivent la dynamique d'occupation de patchs, incorporés dans une matrice inhabitable, à partir d'un processus markovien. Les patchs ont deux états d'occupation possibles et le changement d'état est

un processus stochastique qui dépend d'une probabilité de transition (Hanski 1994). Cette probabilité est liée à la surface des patchs et à leur isolement géographique. Différentes méthodes d'inférence ont été développées pour estimer les paramètres de colonisation et d'extinction utilisés dans ces modèles, dans des paysages statiques. Elles permettent également d'estimer des taux de colonisation et d'extinction à partir d'inventaires de biodiversité répétés dans le temps (Etienne et al. 2004).

Les inventaires de biodiversité répétés sur des temps longs étant rares, il convient de développer des approches alternatives. Verheyen et al. (2004) ont proposé d'estimer des taux de colonisation et d'extinction, à partir d'un inventaire de biodiversité ponctuel dans le temps, en utilisant comme information supplémentaire l'âge du patch accessible à partir de cartes historiques. Un intérêt notable de cette approche est d'introduire la création de patchs au cours du temps. Le paysage n'est alors plus considéré comme statique. Cependant, cette méthode requiert un échantillonnage exhaustif des patchs pour estimer les paramètres du modèle.

Récemment, Ruete et al. (2014) ont dépassé cette limite en utilisant une méthode d'inférence applicable à des inventaires incomplets. Comme Verheyen et al. (2004), ils s'appuient sur l'utilisation de séries temporelles de paysages et d'un inventaire de biodiversité ponctuel dans le temps. L'avantage de cette approche est qu'il n'est plus nécessaire de faire l'hypothèse que les espèces sont à l'équilibre avec le paysage. Les paramètres de dynamiques des espèces sont estimés en prenant en compte l'héritage des paysages historiques. Dans cette approche, ce ne sont pas uniquement les patchs créés qui sont pris en compte mais également les patchs disparus.

I.3.2.2 Verrous à lever liés à l'inférence statistique

L'approche de Ruete et al. (2014) comprend cependant certaines limites. Parmi celles qui sont liées à l'inférence statistique, le présent manuscrit en prend trois en considération.

Premièrement, les méthodes d'inférence bayésiennes ont l'inconvénient d'être coûteuses en temps de calcul (Etienne et al. 2004). C'est le cas de l'approche développée par Ruete et al. (2014), qui est appliquée à neuf métapopulations de lichens dans un réseau qui comprend une centaine de patchs. Il est difficile d'appliquer cette approche à un grand nombre d'espèces et de patchs (plusieurs centaines) ou à l'échelle régionale (plusieurs milliers). L'approche utilisée durant cette thèse reprend le canevas proposé par Ruete et al. (2014), qui consiste à estimer des paramètres de dynamique d'espèces à partir d'un

inventaire de biodiversité actuel et de données cartographiques actuelles et anciennes. L'inférence repose sur une méthode de maximisation de la vraisemblance approchée qui est plus efficace en temps de calcul que celle développée par Ruete et al. (2014). En appliquant les deux approches sur un même jeu de données, les tests réalisés montrent que le gain en temps de calcul, avec l'approche utilisée dans cette thèse, est supérieur à un facteur 10 pour une espèce à l'échelle du millier de patchs.

Deuxièmement, la probabilité de détecter une espèce lors de l'inventaire d'un patch dépend d'une interaction entre le nombre d'individus présents, le plan d'expérimentation et le processus d'observation qui peut introduire des fausses absences (Archaux et al. 2012). Par exemple, jusqu'à 19 % des espèces présentes peuvent échapper à la détection lors d'un relevé (Archaux et al. 2009). La détection imparfaite des espèces peut biaiser l'estimation des paramètres (Moilanen 1999). De nombreux modèles d'occupation des patchs intègrent une probabilité de détection (*e.g.* Sutherland et al. 2014) mais font l'hypothèse que les espèces sont à l'équilibre avec le paysage. Ruete et al. (2014) montre qu'il est aisé de prendre en compte une probabilité de détection sans l'appliquer cependant. Dans ce manuscrit, nous intégrons la détectabilité à la fonction de vraisemblance.

Troisièmement, la précision de l'estimation des paramètres des modèles stochastiques d'occupation des patchs n'a pas été évaluée. Les erreurs d'estimation des paramètres de ces modèles ne sont donc pas connues. L'incertitude qui leur est associée est par contre calculée et souvent associée de façon explicite aux résultats (*e.g.* Ruete et al. 2014). Plus généralement, les analyses de robustesse, qui ont pour objectif de quantifier les erreurs d'estimation et l'incertitude associées aux paramètres, sont rares (*e.g.* Moilanen 2002). Dans ce manuscrit, une analyse de robustesse est réalisée avant d'appliquer l'approche aux données empiriques.

I.4. Dynamique des forêts et des plantes de sous-bois dans l'espace et dans le temps

De nombreux habitats subissent un turnover important tel que les rivières intermittentes, des zones intertidales ou la mosaïque agricole (Ruiz et al. 2014, Datry et al. 2016, Bertrand et al. 2016). À des échelles temporelles plus importantes, les forêts continentales ont évolué suivant des phases de déforestation et de reforestation successives (Flinn et Vellend 2005). Les plantes de sous-bois inféodées à ces habitats ont des dynamiques de colonisation très lentes en comparaison d'organismes mobiles. Les propagules des plantes forestières sont dispersées de 20m à 100m par siècle selon

les estimations (Hermy et Verheyen 2007). La composition des communautés et la répartition spatiale des populations de plantes forestières sont donc susceptibles de porter les stigmates de l'évolution passée des surfaces forestières. Par conséquent, les plantes forestières sont des espèces particulièrement appropriées pour étudier des dynamiques hors équilibre.

I.4.1 Dynamique des forêts

I.4.1.1 Évolution de la surface des forêts au cours du temps

L'évolution des surfaces forestières est très fortement dépendante de l'évolution des surfaces agricoles (Crist et al. 2017). La première phase de défrichement de la forêt primaire qui a recolonisé l'Europe à la fin de la dernière glaciation a débuté au néolithique, avec la sédentarisation et les débuts de l'agriculture, pour prendre fin avec la chute de l'empire romain et le début des grandes invasions. Une seconde phase de déforestation a été initiée par la révolution agricole qui débute au XI^{ième} siècle. Par la suite, l'évolution des surfaces forestières a varié en fonction de l'utilisation du bois de chauffe et de la disponibilité de ressources alternatives telles que la tourbe et le charbon (Hermy et Verheyen 2007). En France par exemple, l'exploitation du bois s'intensifie au XVI^{ème} siècle pour répondre aux besoins des premières industries et de la construction navale. L'ordonnance de Colbert de 1669 régule l'exploitation des forêts et initie des plantations, en forêt de Fontainebleau notamment, pour répondre à la demande.

I.4.1.2 Dynamiques récentes des forêts et successions végétales

Depuis le début de l'industrialisation au XIX^{ème} siècle, une reforestation est en cours en Europe de l'Ouest et dans l'Est de l'Amérique du Nord (Flinn and Vellend 2005). En France par exemple, les surfaces forestières ont doublé depuis cette période (Koerner et al. 2000). La reforestation est à imputer à la déprise agricole qui permet à la forêt de se développer et atteindre un stade mature après une centaine d'années. Hermy et Verheyen (2007) décrivent les successions végétales initiées avec la colonisation de ces terres. L'implantation démarre avec des plantes rudérales typiques des milieux ouverts tel que *Capsella bursa-pastoris*. Des espèces plus compétitives (*e.g. Cytisus scoparius*) puis, des arbustes et arbres pionniers (du genre *Pinus*, *Betula* et *Salix*) leur succèdent au bout de 5 à 20 ans. L'ombrage apporté par ces espèces exclut progressivement les espèces les plus héliophiles. Les arbres typiques des derniers stades de succession (par exemple en plaine du genre *Fraxinus*, *Quercus*, *Tilia* et *Acer* et plus encore *Fagus)* remplacent les pionniers après une centaine d'années. La forêt actuelle est constituée de patchs d'âges variés, qui sont incorporés dans une matrice principalement agricole (Decocq et al.

2016).

I.4.1.3 Contrastes en fonction de la zone géographique

La déforestation pré-industrielle et la reforestation qui a suivi sont des tendances générales qui masquent des disparités régionales importantes. Par exemple, la déforestation pré-industrielle a réduit les surfaces forestières de 32% à près de 1% dans la région de Prignitz en Allemagne (Kolk et al. 2017) et de 13% à 5% en Flandre, dont la moitié sont actuellement présentes sur d'anciennes terres agricoles (Baeten et al. 2010). Bergès et al. (2015) comparent les surfaces forestières entre 1831 et 2002 dans plusieurs régions du nord de la France. Celles-ci ont diminué de 10.4% à 9.1% dans la région Nord alors qu'elles ont augmenté de 30.9% à 37.9% en Lorraine où la fragmentation est très réduite. Ces exemples montrent qu'une reforestation récente, importante en proportion, n'implique pas forcément des surfaces élevées ou une fragmentation réduite ce explique en partie la variabilité de l'héritage des paysages anciens sur la répartition actuelle des plantes forestières (De Frenne et al. 2011).

I.4.2 Les limites au recrutement

I.4.2.1 Différences de composition floristiques en fonction de l'usage passé des sols

Peterken, qui a conduit des travaux pionniers en écologie historique, classe les forêts en fonction de leur continuité temporelle (Peterken 1996). Les forêts primaires, qui existent de façon continue dans le temps depuis la dernière glaciation, sont distinguées des forêts secondaires qui n'ont pas été boisées en continue. Cette information n'étant pas forcément connue, les forêts anciennes qui sont présentes de façon continue depuis une date seuil, sont distinguées des forêts récentes qui se sont établies par la suite, souvent sur d'anciennes terres agricoles. La répartition spatiale des plantes dépend de l'âge des forêts dans lesquelles elles sont présentes (Hermy et al. 1999). Certaines espèces sont plus fréquentes dans les forêts anciennes et d'autres dans les forêts récentes. Ces espèces ont été identifiées mais les listes d'espèces de forêt anciennes et récentes ne sont pas forcément concordantes en fonction de la région (Hermy et al. 1999, Hermy et al. 2007, Matuszkiewicz et al. 2013). Une espèce classée comme espèce de forêt ancienne dans une région peut être classée comme une espèce de forêt récente dans une autre (*e.g. Listera ovata*). Ces listes sont établies en comparant les fréquences d'occurrence des espèces dans les deux types de forêts. Ces divergences peuvent s'expliquer par le fait que le recrutement ne dépend pas uniquement des traits des espèces mais aussi de propriétés extrinsèques (Figure 6). Le recrutement est limité par la capacité des espèces

à disperser leurs propagules jusqu'aux patchs de forêts récentes (filtre de dispersion), de la capacité de ces propagules à germer et se développer jusqu'au stade adulte fertile en fonction des conditions environnementales (filtrage environnemental) et des interactions entre espèces (filtre biotique).

Deux visions non exclusives s'opposent ici. La première est à relier à la théorie de la niche écologique (Hutchinson 1957) qui postule que la répartition spatiale des espèces s'explique par un ensemble de conditions environnementales (biotiques et abiotiques) qui leur sont favorables. Le concept de filtre de dispersion repose sur l'idée que la répartition spatiale des espèces s'explique par la configuration spatiale du paysage et les traits de dispersion des espèces. L'importance respective de ces filtres dans différentes zones géographiques n'a pas pu être complètement élucidée. Dans ce manuscrit, on cherche à identifier un filtrage environnemental et un filtrage lié à la dispersion en étudiant les corrélations entre les paramètres de dynamique des espèces inférés et leurs propriétés intrinsèques (dispersion et affinités pour certaines conditions environnementales). Les interactions biotiques et la qualité des patchs ne sont cependant pas modélisées.

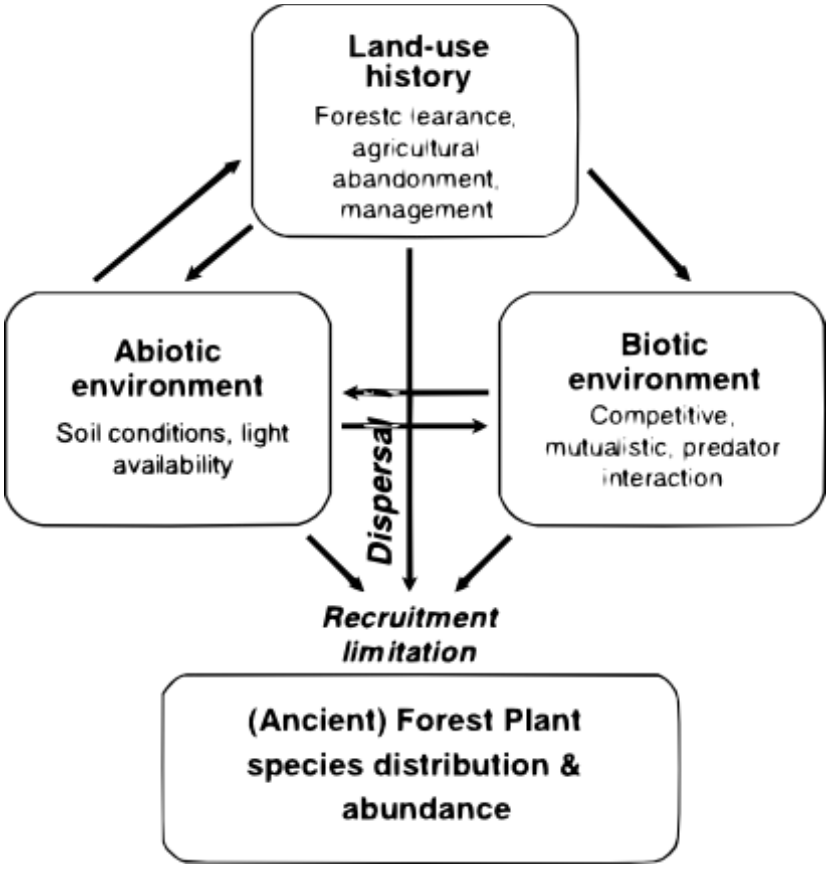

Figure 6 : Les filtres qui limitent le recrutement. Dérivé de Hermy et Verheyen (2007).

I.4.2.2 Filtrage environnemental

Des expérimentations ont permis de démontrer l'effet d'un filtrage environnemental sur le recrutement, en mesurant directement la variabilité des conditions environnementales entre les forêts anciennes et récentes (Dupré et Ehrlén 2002, Vellend 2005, Kimberley et al. 2014). La fertilité des sols, par exemple, a une large influence sur la composition des communautés. Les forêts récentes sont présentes sur des terres qui étaient initialement riches en azote ou bien qui ont été enrichies par fertilisation (Hermy et Verheyen 2007). Le recrutement des espèces de forêts anciennes, peu adaptées à ces conditions, est particulièrement limité par la teneur en azote élevée des forêts récentes (Hermy et al. 1999, Bergès et al. 2015). Par contraste, Brunet et al. (2012) ont montré que le filtrage environnemental ne limite pas forcément le recrutement. D'autres travaux ont expérimenté le semis de graines, d'espèces de forêts anciennes, en forêt récente pour tester l'hypothèse d'une limitation environnementale (Ehrlén et Eriksson 2000, Graae et al. 2004, Verheyen et Hermy 2004, Kolb et Barsch et al. 2010). Ces travaux ont conduit à minimiser l'importance d'un filtrage environnemental en démontrant que le recrutement des plantes de forêt anciennes en forêt récentes est très souvent effectif. La mise en place de mesures des conditions environnementales *in situ* n'est pas toujours possible. Les valeurs d'Ellenberg, qui définissent l'affinité des espèces pour certaines conditions environnementales (Ellenberg 1992), peuvent être utilisées comme proxy même si cette approche peut être discutée en raison d'une certaine circularité (la flore est utilisée pour comprendre sa propre distribution). En suivant cette approche, la présence d'un filtrage environnementale a pu être démontrée localement (Jacquemyn et al. 2003, Pellissier et al. 2013, Bergès et al. 2015) mais pas à large échelle (De Frenne et al. 2011).

I.4.2.3 Filtre de dispersion

L'importance du filtre de dispersion dans le recrutement a été clairement mise en évidence pour les plantes forestières (Jacquemyn et al. 2003, De Frenne et al. 2011, Brunet et al. 2012, Kimberley et al. 2014) et notamment à partir de méta-analyses à large échelle (Verheyen et al. 2003a, Vellend et al. 2007). Verheyen et al. (2003a) ont étudié la dispersion de 216 espèces en compilant 20 jeux de données Européen et Nord-Américain. Ils concluent que la dispersion est un facteur clé du recrutement pour la plupart des espèces. Vellend et al. (2007) démontrent que la composition des communautés en forêts récentes et anciennes dépend du filtre de dispersion indépendamment des conditions environnementales mais il faut noter qu'en moyenne, celles-ci ne varient pas entre les forêts anciennes et récentes dans les travaux inclus à leur méta-analyse. Peu d'études suggèrent au contraire que le rôle de la dispersion est

mineur. Cependant, des espèces qui ont une forte capacité de dispersion, certaines graminées par exemple, sont peu impactées par la configuration du paysage (Verheyen et al. 2003a).

I.4.2.4 Effet relatif des filtres qui limitent le recrutement

Les travaux qui comparent l'importance relative des filtres qui limitent le recrutement démontrent généralement l'importance du filtre de dispersion relativement au filtre environnemental (Verheyen et al. 2003b, Vellend 2007, De Frenne et al. 2011) voire à l'absence de ce dernier (Ehrlén et Eriksson 2000, Brunet et al. 2012). Cependant, Dupré et Ehrlén (2002) mettent en avant que la qualité de l'habitat, et plus particulièrement le pH, est plus importante que la dispersion pour une large majorité d'espèces. D'autres travaux (Jacquemyn et al. 2003, Kimberley et al. 2014) rapportent l'importance des deux types de filtres. Les résultats issus de ce type de comparaison dépendent fortement de la variabilité des conditions environnementales et de la configuration spatiale des paysages qui sont susceptibles de changer en fonction de la zone d'étude (Dupré et Ehrlén 2002, Vellend 2007). Finalement, des méta-analyses montrent que la diversité des patrons de répartition des espèces s'explique par une variabilité régionale de la connectivité, de l'âge des patchs et, dans une moindre mesure, des conditions environnementales (Verheyen et al. 2006, De Frenne et al. 2011).

I.4.2.5 Propriétés intrinsèques des espèces en lien avec le recrutement

la présence préférentielle des espèces en forêts récentes ou en forêts anciennes s'explique aussi par les traits des espèces qui caractérisent certaines de leurs propriétés intrinsèques qui peuvent être corrélées à la dispersion. Ce sont des caractéristiques morphologiques, physiologiques ou phénologiques mesurables à l'échelle de l'individu (Violle et al. 2007). Ces caractéristiques sont souvent moyennées à partir des attributs de plusieurs populations (*e.g.* Kleyer et al. 2008). Les traits sont définis dans ce manuscrit au sens large, en incluant l'affinité des espèces pour certaines conditions environnementales traduites par les indices d'Ellenberg. Les espèces de forêts anciennes sont, par exemple, plus tolérantes à l'ombrage et ont une affinité forte pour les sites qui ont une acidité ou une teneur en azote intermédiaire par rapport aux espèces de forêts récentes (Hermy et al. 1999). Elles sont également plus souvent tolérantes aux stress environnementaux par rapport aux espèces de forêts récentes (Hermy et al. 1999). Leur mode de dispersion est plus fréquemment myrmécochore (Hermy et al. 1999, Bergès et al. 2015). Les graines des espèces de forêts anciennes ont plus souvent une taille limitée et une masse importante, ces caractéristiques étant associées à une faible capacité de

colonisation (Brunet et al. 2012). Par comparaison, les espèces de forêts récentes ont généralement plus d'affinité pour les sols peu acides et plus riches en azote (Bergès et al. 2015). Le mode de dispersion est plus souvent endozoochores, ce qui facilite la dispersion à longue distance (Bergès et al. 2015). Ces espèces tendent également à être plus souvent rudérales que les espèces de forêts anciennes (Graae et Sunde 2000).

I.5. Objectifs de la thèse

I.5.1 Objectifs généraux

L'objectif des travaux présentés dans ce manuscrit est d'évaluer l'apport des modèles de métapopulation hors équilibre pour comprendre les dynamiques qui font suite au turnover des habitats au sein desquels elles évoluent. Pour cela, nous quantifions la robustesse de la méthode d'inférence et la capacité des modèles à reproduire les patrons de biodiversité observés. Puis, nous identifions les déterminants de la composition des communautés d'espèces de forêts anciennes et récentes à partir des paramètres de dynamique et des traits des espèces. Ensuite, nous utilisons des scénarios virtuels de turnover d'habitats pour comprendre quel est le rôle de la dispersion des espèces relativement à la configuration spatiale du turnover. À ces fins, des dynamiques de métapopulations sont simulées avec l'objectif d'estimer l'amplitude de la dette d'extinction ou du crédit d'immigration et le temps de relaxation. Finalement, les dynamiques des plantes forestières sont projetées à long terme dans l'un des réseaux de patchs, caractérisé par une reforestation importante associée à une érosion partielle des forêts anciennes. Ce contexte nous permet d'évaluer l'interaction entre la dette d'extinction et le crédit d'immigration et de quantifier le temps de relaxation à l'échelle du patch et du paysage.

I.5.2 Données utilisées

Afin de répondre à cet objectif, un unique inventaire de biodiversité actuel et des cartographies actuelles et historiques sont nécessaires pour un paysage donné.

Les cartes numériques utilisées (Figure 7) sont issues des cartes d'État-Major et de la BD TOPO de l'IGN (Institut National Géographique). Les cartes d'État-Major ont été réalisées au cours du XIX^{ème} siècle et couvrent le territoire français. Les versions aquarellées au 1:40000 ont été numérisées par l'IGN et sont disponibles en libre accès. À partir de ces données, les forêts ont été digitalisées dans plusieurs départements du Bassin Parisien dans le cadre du projet Distrafor (dispersion et persistance de la

biodiversité dans la trame forestière) qui a pris fin en 2014. Les cartes actuelles utilisées sont issues de la couche VEGETATION de la BD TOPO de l'IGN. Ces deux types de couches numériques représentent en moyenne les forêts en 1840 et en 2000.

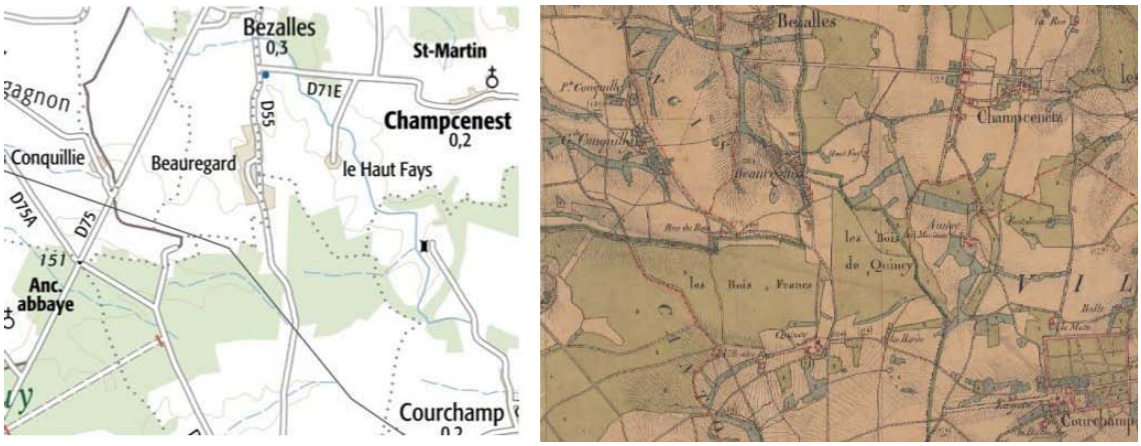

Figure 7 : Aperçu de la BD TOPO (à gauche) et d'une carte d'État-Major (à droite).

Les données floristiques utilisées sont issues de relevés de présence-absence réalisés par l'IFN (Inventaire Forestier National, IGN) et le CBNBP (Conservatoire Botanique National du Bassin Parisien). Les inventaires de l'IFN répondent à un échantillonnage standardisé de la flore forestière. La surface échantillonnée est de 700m^2 par relevé mais les espèces rares ne sont pas forcément inventoriées. Les surfaces des relevés du CBNBP sont très variables et l'exhaustivité est un critère plus important que pour les relevés IFN. Les relevés du CBNBP ont été réalisés en forêt entre 2000 et 2010 et ceux de l'IFN en 2004.

Dans ce manuscrit nous étudions les départements de la Seine-et-Marne et de l'Eure-et-Loir. Ils comprennent la proportion de patchs échantillonnés la plus importante, parmi les départements dont les cartes anciennes digitalisées étaient disponibles pour le Bassin Parisien. Les prétraitements des données cartographiques et des inventaires floristiques sont décrits dans le chapitre II.

Les travaux présentés dans ce manuscrit reposent également sur la simulation de dynamiques de métapopulations dans des paysages virtuels. Cette approche est couramment utilisée afin de contrôler les propriétés spatiales des paysages et de créer des réplicats, sans être limité par la disponibilité des données empiriques (*e.g.* Grilli et al. 2015). Nous utilisons un ensemble d'algorithmes proposé par Ethrington et al. (2015) pour générer des modèles de paysages neutres qui sont définis comme des paysages simulés, utilisés pour comparer des processus et des motifs écologiques (With et King 1997, Chipperfield et al. 2011, Ethrington et al. 2015). Nous développons ensuite un

algorithme simple pour dériver un modèle de paysage neutre à partir d'un autre afin de simuler une carte ancienne et une carte actuelle.

I.5.3 Questions de recherches et organisation du manuscrit

Pour répondre aux objectifs énoncés précédemment, la suite de ce manuscrit est organisée en plusieurs chapitres qui regroupent des articles scientifiques rédigés en anglais ainsi qu'une discussion générale. Le chapitre II vise à évaluer l'apport des modèles de métapopulations hors équilibre utilisés et à les appliquer aux plantes forestières de sous-bois, échantillonnées en Eure-et-Loir et en Seine-et-Marne. L'objectif de ce chapitre est de répondre aux questions suivantes :

(i) Quels sont les paramètres de dynamique qui peuvent être inférés de façon fiable à partir de la méthode utilisée et dans quelles conditions?

(ii) Les modèles qui en résultent permettent-ils de reproduire les patrons spatiaux observés ?

(iii) Les paramètres de dynamique des espèces sont-ils corrélés à leur présence préférentielle en forêts anciennes et en forêts récentes ?

(iv) Ces paramètres sont-ils consistants dans les deux réseaux de patchs étudiés ?

(v) Ces paramètres sont-ils prédictibles à partir des traits des espèces ?

Le chapitre III vise à étudier des dynamiques de métapopulations simulées en fonction de différents scénarios de turnover d'habitat. L'objectif de ce chapitre est de répondre aux questions suivantes :

(i) Comment l'effet d'un gain net ou d'une perte nette de surface d'habitat influence la dynamique des métapopulations ?

(ii) Comment l'agrégation spatiale du turnover des habitats, à surface totale constante, influence la dynamique des métapopulations ?

(iii) Le temps de relaxation estimé diffère-t-il en fonction des scénarios précédents ?

(iv) Quelle est l'influence de la distance de dispersion sur les conclusions aux questions précédentes ?

Le chapitre IV a pour objectif d'évaluer les projections à long terme des dynamiques d'espèces inventoriées en Seine-et-Marne. L'objectif de ce chapitre est de répondre aux questions suivantes :

(i) Comment l'équilibre entre la dette d'extinction et le crédit d'immigration impacte-t-elle la dynamique des espèces ?

(ii) Comment varie le temps de relaxation en fonction de la connectivité fonctionnelle et des caractéristiques des espèces ?

(iii) Existe-t-il un risque de déclin des espèces de forêts anciennes en dépit d'une reforestation importante ?

Chapitre II : Revoir le concept des espèces de forêts anciennes/récentes à partir de l'étude de dynamiques de métapopulations hors équilibre

Manuscrit correspondant :

Lalechère, E., Jabot, F., Archaux, F., & Deffuant, G. (2017). Non-equilibrium plant metapopulation dynamics challenge the concept of ancient/recent forest species. *Ecological Modelling*, *366*, 48-57.

Non-equilibrium plant metapopulation dynamics challenges the concept of ancient/recent forest species.

Étienne Lalechère [a1] , Franck Jabot [a] , Frédéric Archaux [b] , Guillaume Deffuant [a]

[a] UR LISC, Irstea, 9 avenue Blaise Pascal, F-63178 Aubière, France

[b] UR EFNO, Irstea, Domaine des Barres, F-45290 Nogent-sur-Vernisson, France

Corresponding author:

[1] E-mail address: lalechereetienne@gmail.com

Current address: UR LISC, Irstea, 9 avenue Blaise Pascal, F-63178 Aubière, France

Abstract

Previous analyses of the regional distribution of forest plants have revealed that some species have a biased distribution towards either ancient or recent forest patches. It has been therefore proposed to classify forest plant species according to their affinity for ancient or recent patches. In this contribution, we aimed at providing a dynamical perspective on this static concept of ancient/recent forest species. We developed an inference method to estimate the metapopulation dynamics of forest plants based on landscape history and static (and incomplete) biodiversity data accounting for false absence records. We assessed the power of this novel inference method using simulated metapopulation and landscape dynamics. We finally applied this method to occupancy data of 174 and 121 forest species in two networks of 9208 and 9201 forest patches respectively. These patch networks are located in two French regions, with corresponding landscape historical data based on two forest maps conceived in 1840 and 2000. Our analyses revealed that (i) the inference method enables to satisfactorily infer three parameters of the metapopulation model: the rates of colonization, extinction and decay of colonization with distance; (ii) this three parameter metapopulation model is sufficient to reproduce the occurrence spatial structure of 72% and 61% of the investigated species in the two regions; (iii) forest plant species are distributed along a spectrum of turnover speed, in which small (large) colonization capacity are associated with small (large) propensity to extinction; (iv) species position along this spectrum can be partially predicted from plant functional traits; and (v) species metapopulation dynamics are driven by the interaction between landscape and species intrinsic properties, suggesting that ancient/recent forest species lists are unlikely to be easily extrapolated to novel landscapes.

Keywords: Stochastic Patch Occupancy Model - Landscape dynamics - Dispersal limitation - Recruitment limitation - Species turnover - Parameter estimation.

1. Introduction

Since two centuries, reforestation occurs in many ancient agricultural lands in Western Europe (Koerner et al. 2000, Hermy and Verheyen 2007). Some plant species are better colonizers of these recent forests (hereafter called recent forest species RFS, Hermy et al. 1999), whereas some other species (hereafter called ancient forest species AFS, Hermy et al. 1999) are more confined to ancient forests, *i.e.* “forests that already existed before a certain threshold date”. Previous studies on ancient/recent forest species have delivered classification of plant species as AFS or RFS according to the age of forests where they are preferentially present (Hermy et al. 1999, Dupouey et al. 2002, Bergès et al. 2015). There is however no systematic agreement between the different AFS/RFS lists established in different regions (Hermy et al. 1999, Verheyen et al. 2006, Hermy et al. 2007, Matuszkiewicz et al. 2013). For instance, species classified as AFS may be typical of recent forests in another region (Hermy and Verheyen 2007). This suggests that the spatial distribution of these plant metapopulations is not solely triggered by species intrinsic properties.

Recruitment of plant individuals is indeed likely to be limited by both dispersal and post-dispersal environmental filters (Wang and Smith 2002). Biased distributions of plant species towards ancient forests can therefore be due to (i) their failure to disperse propagules to newly created forest patches, and (ii) the failure of their propagules to pass through local environmental filters encountered in recent forest patches. Biased distributions of plant species towards recent forests can in turn be due to (i) a more efficient dispersal into newly created forest patches than other plants, and (ii) a superior ability to pass through local environmental filters in these patches.

Regarding dispersal processes, several studies were able to detect distinct dispersal syndromes between AFS and RFS. For example, endozoochorous and epizoochorous species, that are good dispersers, are more frequent in recent forests (Brunet et al. 2012, Bergès et al. 2015). In contrast, AFS are more frequently small-size species with a high seed weight and a low seed terminal velocity (Kimberley et al. 2013). Regarding abiotic filters, AFS tend to be more present in unfertile soils and when soil acidity are intermediate, while RFS tend to be more present when soils are richer in nitrogen and when they are slightly acidic (Brunet et al. 2012, Bergès et al. 2015). Finally, RFS are poorly tolerant to shade and are more able to survive in open woodlands contrary to AFS (Kimberley et al. 2014, Bergès et al. 2015).

To understand how these two components of recruitment limitation, dispersal and environmental filtering, translate into the dynamics of forest plant species, one needs to go beyond static analyses of geographical patterns, and to develop models of plant spatial dynamics (Hanski 1998, Freckleton and Watkinson 2002). Models of metacommunity dynamics in which all species are assumed to behave equivalently and to compete for space have been developed and have incorporated either environmental filtering (Jabot et al. 2008) or a spatially-explicit landscape representation (Economo and Keitt 2008, May et al. 2013). At a finer level of organization, metapopulation models have also been developed and can also integrate environmental filtering and spatially-explicit dispersal processes (Hanski 1998, Purves et al. 2007). They can be tuned independently for different species but they do not integrate interspecific competition. All these models can be parametrized with snapshot floristic data, under the strong assumption that species spatial dynamics is at equilibrium (Etienne et al. 2004).

However, landscape composition and spatial structure change over time with the creation or destruction of habitats patches (Meeus 1993, Hermy and Verheyen 2007) or with gradual changes in patch quality, *e.g.* following climatic changes (García-Valdés et al. 2015). If the timescale of landscape dynamics is comparable to or shorter than the timescale of a species metapopulation dynamics, this species dynamics cannot be assumed to be at equilibrium anymore (Verheyen et al. 2004, Vellend et al. 2006). Such species may be strongly affected by the turnover rate of patches over time and current occupancy may be better explained by past landscape structure rather than current landscape structure (Kuussaari et al. 2009, Jackson and Sax 2010, Hylander and Ehrlén 2013, Essl et al. 2015).

A first attempt to integrate landscape dynamics into a forest plant metapopulation model was proposed by Verheyen et al. (2004) by adding patch age in Hanski's incidence function model (Hanski 1994). They also integrated post-dispersal environmental filtering in their framework, through an ad hoc index of patch quality based on Ellenberg indices (Ellenberg et al. 1992). The main limitation of this approach is that it requires an exhaustive sampling of all the landscape patches, so that it is hardly applicable to large scale studies. More recently, Ruete et al. (2014) resolved this limitation by using a Bayesian approach that authorizes non-exhaustive sampling. They applied their methodology to nine lichen metapopulations spanning roughly one hundred patches. This Bayesian approach is however computationally intensive and is therefore difficult to apply to a large number of species in larger landscapes as those we are studying in this contribution.

We therefore developed an innovative inference method, based on an approximate likelihood computation that is faster and scalable to larger landscapes encompassing several thousands of patches. We first tested this novel method with simulated data to assess its reliability and precision. We then applied it to two large forest plant inventory datasets located in two French regions to answer to the following five main questions: (1) how many and which metapopulation parameters can be reliably inferred from this type of data? (2) Is the resulting metapopulation model studied sufficient to reproduce observed plant metapopulation patterns? (3) Are forest plant metapopulation parameters linked with the observed difference of plant occurrence towards recent or ancient forest patches? (4) Are these colonization-extinction parameters consistent between the two regions studied? And (5) can they be predicted from plant functional traits and environmental characteristics?

2. Materials and methods

2.1 The metapopulation model

We consider a patch occupancy model that is close to the one proposed by Verheyen et al. (2004). The occupancy dynamics of the network of patches is modelled as a discrete time process, with events of local extinction and colonization, and events of patch destruction and creation. At each time step *t*, each patch *i* is either occupied by the focal species ($OCC_i(t)=1$) or not ($OCC_i(t)=0$). If a patch is unoccupied, it is colonized between step *t* and step *t+1* by the focal species with probability $C_i(t)$. The time step was fixed to ten years. If it is occupied, the local population of the focal species can go extinct between step *t* and *t+1* with probability $E_i(t)$.

The extinction probability $E_i(t)$ is assumed to be constant through time and given by the following formula:

$$E_i(t) = min\left(\frac{\sigma}{A_i^{\theta}}, 1\right) \quad (1)$$

where σ is the extinction rate parameter and θ regulates the decay of this rate with the area A_i of patch *i*.

The colonization probability $C_i(t)$ is given by:

$$C_i(t) = \frac{CON_i(t)^2}{CON_i(t)^2 + 1} \quad (2)$$

where $CON_i(t)$ measures the level of connectivity between patch i and the other patches that are occupied at time t. Following Verheyen et al. (2004), it is given by:

$$CON_i(t) = \alpha \cdot \sum_{j \neq i} \left(A_j \times OCC_j(t) \times \exp^{-\beta d_{ij}} \right) \quad (3)$$

where d_{ij} is the geographical distance between patches i and j, α is a colonization parameter and β is a parameter assuming a decay of colonization with distance. Note that we did not introduce habitat suitability in this framework (although technically straightforward), contrary to what Verheyen et al. (2004) did. This choice was made to keep the model simple. We will see below that this parsimony is critical to get reasonably accurate inferences. Geographical distances between patches were Euclidian distances computed from patch edge-to-edge.

Finally the modelled landscape is dynamical itself, with events of patch destruction and creation. When a patch i is newly created at time step t, it is considered to be unoccupied ($OCC_i(t)=0$), until a first colonization event takes place.

2.2 Inference of model parameters

Our aim was to infer the parameters of the metapopulation model described above based on the combined use of two types of data: (i) present occupancy data collected in a subset of the landscape patches, and (ii) historical maps of landscape patches that inform on past landscape dynamics. We made use of an approximate likelihood method that presents the advantage of being computationally scalable to networks of several thousands of patches. This approximate inference method further proved to be reasonably accurate (see below). This method consists first in assuming that the metapopulation is at equilibrium at the oldest date for which a historical map is available. This assumption enables to compute the probability of occupancy of each patch (thereafter called the incidence of a patch, following Hanski 1994) at this oldest date.

Second, the dynamics of patch incidences $J_i(t)$ is computed from this oldest date until the time step t_{data} at which occupancy data collection takes place (Fig. 1). The dynamics of $J_i(t)$ is given by:

$$J_i(t+1) = J_i(t) \times \left(1 - E_i(t)\right) + \left(1 - J_i(t)\right) \times C_i(t) \quad (4)$$

Our approximation consists in computing $C_i(t)$ in equation 4 using patch incidences $J_i(t)$ instead of unknown patch occupancies $OCC_i(t)$ at date t. Concretely, this is done by replacing equation 3 by:

$$CON_i(t) = \alpha \cdot \sum_{j \neq i} \left(A_j \times J_j(t) \times \exp^{-\beta d_{ij}} \right) \quad (5)$$

Equations 1, 2, 4 and 5 enable to compute an approximation of the forward dynamics of patch incidences $J_i(t)$. These equations are also used to compute equilibrium patch incidences at the oldest date $J_i(t)$. To do this, we follow Etienne et al. (2004), and (i) initialize the incidence of all patches at one (*i.e.* all patches are occupied) τ time steps in the past $J_i(-\tau)=1$, (ii) compute the dynamics of $J_i(t)$ from $t=-\tau$ to $t=0$ using equations 1, 2, 4 and 5. Using a large value for τ, ensures that we get initial conditions $J_i(0)$ that are close to the metapopulation dynamic equilibrium (we discuss alternative methods in Appendix A). In the following, we used a τ value equal to 100.

Finally, the log-likelihood $Ln(L)$ of occupancy data is computed conditionally to the computed incidences $J_i(t_{data})$ using the following formula:

$$\ln(L) = \sum_{i=1}^{N} \left(J_i(t_{data}) \times OCC_i(t_{data}) \times [1 - F_i(t_{data})] + [[1 - J_i(t_{data})] + J_i(t_{data}) \times F_i(t_{data})] \times [1 - OCC_i(t_{data})] \right) \quad (6)$$

Where $OCC_i(t_{data})$ are the observed occupancies (0 or 1) in the sampled patches, N is the number of sampled patches and F_i is the probability of false absence fixed to 0.19 following Archaux et al. (2009). Note that the model parameters (α, β, σ, θ) enter into the likelihood formula indirectly, through their presence in the equations governing incidence dynamics, and hence $J_i(t_{data})$. The model parameter values leading to the maximum log-likelihood serve as model parameter estimates.

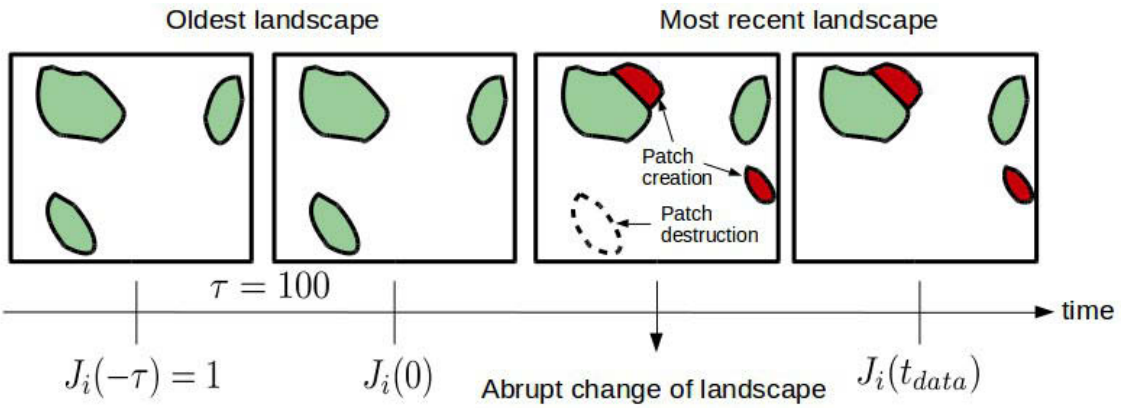

Figure 1: Schematic representation of the computed dynamics of patch incidences used in the inference method. Incidence *J* of each patch *i* of the oldest landscape is initialized at one and actualized during $\tau=100$ time steps to get initial conditions $J_i(0)$. The dynamics of patch incidences are then computed taking into account patch creations and destructions until the time step t_{data} at which occupancy data collection takes place.

2.3 Power analyses based on simulated data

2.3.1 Virtual landscape simulations

We assessed the reliability of the above inference method based on simulated metapopulation dynamics in virtual landscapes. Virtual landscapes of various characteristics were simulated to assess the robustness of the inference method. These virtual landscape characteristics were chosen to encompass the real characteristics observed in the French forest landscapes used in this study.

Virtual landscapes were simulated in 3 steps: (1) a square raster of 1000×1000 pixels was created corresponding to the simulated old map (m_{cont}^{old}) . Pixels values were randomly generated between 0 and 1. The python package nlmpy allowed us to simulate various levels of spatial autocorrelation in the generated pixel values thanks to an autocorrelation parameter α (Etherington et al. 2015). To transform this map into a binary map (m_{bin}^{old}) differentiating pixels of forests from matrix pixels (unsuitable habitat), pixels were classified as forest when the pixel value was above a chosen threshold. The threshold was fixed as the *np* percentile of the distribution of pixel values, which allowed us to control the proportion of forests in the landscape. (2) A transition map (m_{cont}^{trans}) was simulated with the same autocorrelation parameter *a* as the old map. (3) The recent map (m_{cont}^{rec}) was then simulated following the following equation:

$$m_{cont}^{rec} = m_{cont}^{old} + \varphi \times m_{expanded}^{trans} \quad (7)$$

where the parameter φ controls the pixel turnover rate and the $m_{expanded}^{trans}$ map corresponds to the m_{cont}^{trans} map rescaled between -0.5 (instead of -1) and 1 to mimic the increase of forest area in recent times observed in the study areas. A binary (forest/matrix) recent map (m_{bin}^{rec}) was produced from the m_{cont}^{rec} map following the same procedure as for the old map using the same threshold *np*. Finally, the recent and the old forest binary maps were vectorized to delineate patches from pixels. This step was realized with QGIS v.2.2 (Quantum GIS Development Team 2011). More details about virtual landscapes can be found in Appendix B.

We considered that the time interval between the old and recent maps was 160 years, *i.e.* the duration between the two real maps at our disposal (see next section). Number of time steps to actualize incidences between these dates was fixed to 16 periods of 10 years. For simplicity, we assumed that the patch turnover from old to recent maps occurred after 80 years. We will report in the main text the results associated with the median virtual landscape that most resembles the real landscapes. The results associated with the other virtual landscapes with patch turnover and connectivity that deviate from this median landscape are reported in Appendix B.

2.3.2 Metapopulation simulations

We simulated the metapopulation dynamics of virtual species that have different model parameter values (α, β, σ, θ). We expected the inference quality to rapidly decrease with the number of inferred parameters. We therefore considered five models of increasing complexity: a distance-independent colonization and no extinction model (α), a distance-dependent colonization and no extinction model (α and β), a distance-independent colonization and patch area-independent extinction model (α and σ), a distance-dependent colonization and patch area-independent extinction model (α, β and σ) and a colonization distance-dependent colonization and area-dependent extinction model (α, β, σ and θ). We simulated 200 virtual species for the α model, and at least 400 virtual species for the other models. For each simulated dataset, estimates of model parameters were computed by maximizing the log-likelihood (eq. 6 with $F_i(t_{data})=0$) and these estimates were then compared to the parameters used in the simulation of metapopulation dynamics.

2.3.3 Power analyses

To compare simulated and estimated values of model parameters, we first computed the relative estimation error:

$$error = \frac{|\hat{p} - p|}{p} \quad (8)$$

where $\hat{p}$ is the inferred parameter value and p is the parameter value used in the simulation. We also computed a 95% credible interval (CI) for the parameter estimates using a likelihood ratio test (Hilborn and Mangel 1997). Then parameter uncertainty was computed as:

$$uncertainty = \frac{|CI_{upper} - CI_{lower}|}{\hat{p}} \quad (9)$$

Where CI_{upper} and CI_{lower} are upper and lower limits of the credible interval.

2.4 Application to forest plant data

2.4.1 Study areas

The two study areas were the French administrative units of Seine-et-Marne (7144 km^2) and Eure-et-Loir (5880 km^2, Fig. 2). We had at our disposal historical forest shapefiles from 1840 digitized maps (military maps). In 2000, for the same departments, forest shapefiles were obtained from the French geographical national institute (IGN BD TOPO). We considered that the landscape turnover occurred in 1920. To make the two maps more comparable (for instance hedgerows were not vectorized on the ancient map) and to reduce the number of patches (respectively 49560 and 63174 in 2000 for the two study areas), we removed patches smaller than 1 ha on both maps. In 2000 in Seine-et-Marne and Eure-et-Loir, the number of patches was respectively reduced to 18.6% (9208 patches) and 14.6% (9201 patches) corresponding to a loss of forest area of 5.7% (9176 ha) and 14.1% (14763 ha) respectively. Then, old and recent maps were intersected to differentiate past old patches (present in 1840 but not in 2000), ancient patches (present in both 1840 and 2000) and recent patches (present in 2000 only). The Quantum GIS software (Quantum GIS Development Team 2011) was used for GIS manipulations.

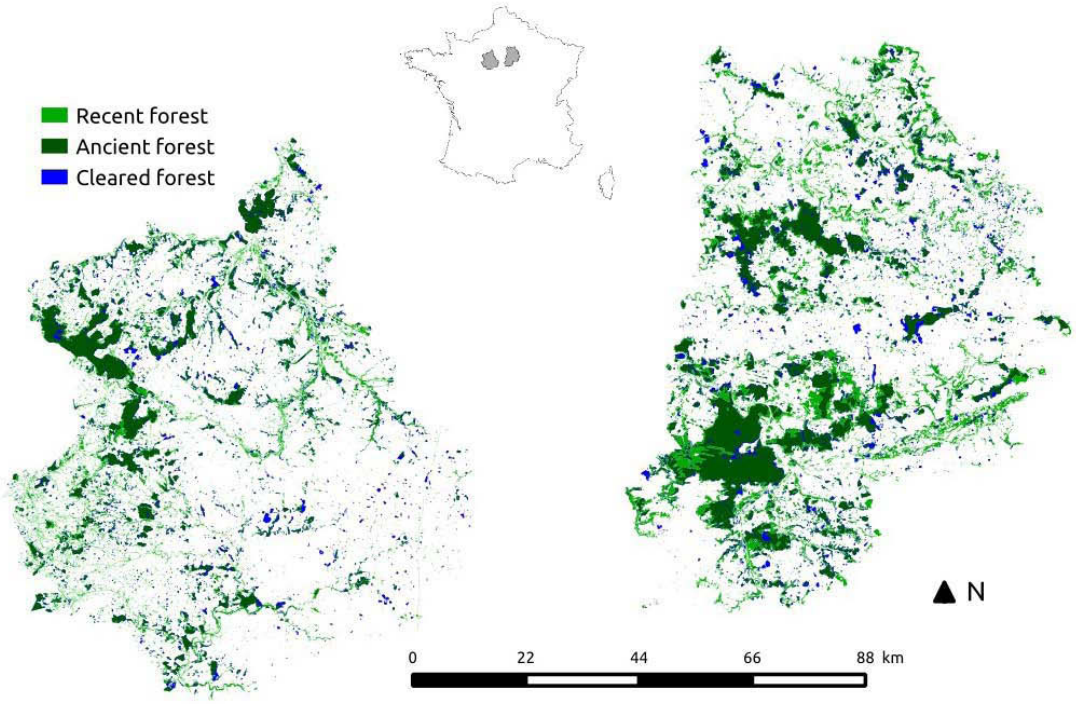

Figure 2: Eure-et-Loir (left) and Seine-et-Marne (right) study areas. Recent forests are patches present in 2000 only. Ancient forests are patches present in 1840 and 2000. Cleared forests are patches present in 1840 only.

The comparison of simplified maps showed that Eure-et-Loir was continuously less forested than the Seine-et-Marne study area (forest area was 62.6% lower in 1840 and 59.4% lower in 2000). Forest areas increased between 1840 and 2000 from 99920 ha to 151237ha in Seine-et-Marne (+51%), and from 62552ha to 89847ha in Eure-et-Loir (+44%). In the two study areas, respectively 78.3% and 76.2% of the forest in 1840 was preserved in 2000. New patches were often small and contiguous to ancient forests (Table 1), and represented 48.2% and 47.0% of the forest areas in 2000 in Seine-et-Marne and in Eure-et-Loir respectively.

Table 1: Description of forests present in 1840 and 2000. In 2000, we set apart ancient forest that are patches present in 1840 and 2000 and recent forest that are patches present in 2000. % s*tudy area*: forest area relatively to the Seine-et-Marne area (592428ha) or to the Eure-et-Loir area (592697ha). Median distance is distance to nearest neighboring patch in 1840 and distance to nearest neighboring ancient patch in 2000 (ancient and recent forests).

	1840 forest		2000 ancient forest		2000 recent forest	
Study area	*Seine-et-Marne*	*Eure-et-Loir*	*Seine-et-Marne*	*Eure-et-Loir*	*Seine-et-Marne*	*Eure-et-Loir*
Number of patches	3004	3359	2125	2235	7083	6966
Median area (ha)	3.1	3.0	3.3	3.2	2.6	2.1
% study area	16.7	10.6	13.2	8.0	12.3	7.1
Median distance (m)	153.2	125.7	113.9	129.7	187.8	184.5

2.4.2 Species data

We made use of presence / absence plant data collected by the French national forest inventory (IFN: Inventaire Forestier National) and the national botanic conservatory (CBNBP: Conservatoire Botanique National du Bassin Parisien). IFN sampling occurred in 2004 and was based on random selection of locations where flora was inventoried in 700m² quadrats. CBNBP data were collected between 2000 and 2010 and were stratified at a county level (commune); we selected only floristic censuses performed in forests. CBNBP sampling area was not fixed: it was 2.2 ± 5.3 ha in Seine-et-Marne and 2.1 ± 6.6 ha in Eure-et-Loir.

The shapefiles of sampling plots were intersected with ancient and recent forest shapefiles. Between 2000 and 2010, in Seine-et-Marne and Eure-et-Loir, respectively 10.6% and 7.0% of patches were sampled for 174 and 121 sampled species. Ancient forests were more often sampled (respectively 16.3% and 14.6%) than recent forests (8.9% and 4.6%). The median number of sampling sites per patch was 1.8 ± 4.7 for Seine-et-Marne and 2.0 ± 11.7 for Eure-et-Loir.

2.4.3 Inference and model checking

The maximization of the approximate log-likelihood was performed in two steps. First, the log-likelihood was computed on a grid of parameter values. Second, 100 local optimizations were carried out with the R function optim using the Nelder and Mead (1965) algorithm. Starting values for these local optimizations were the best set found in the first step.

We assessed the ability of the models to reproduce species occurrence in the sampled patches by a procedure of model checking (Rubin 1984). First, for each species, we compared the observed number of species occurrences in ancient (respectively recent) patches in the data (used as a reference) to the number of simulated occurrences in ancient (respectively recent) patches in the same set of patches. Species occurrences were simulated 100 times from inferred parameters. Then we checked if the observed number of occurrences was within the 95% of the range of the simulated numbers of occurrences. In addition, we compared the mean distance of recent patches occupied to their nearest ancient patch in the simulated datasets and in the data, checking that the observed mean distance fell within the range of 95% of the simulated distances. We considered that the model passed the model checking tests for a given species only if both the number of occurrences in recent and in ancient forest and the mean distance of occupied recent patches to nearest ancient forest patch were within the 95% ranges of the simulations.

2.4.4 Distribution of inferred dynamics and relation with species characteristics

We related colonization and extinction parameters with Spearman correlation coefficients, and to species life-history traits with linear regression analyses for continuous variables, with nonparametric Kruskal-Wallis tests for categorical variables or Wilcoxon tests for pairs of samples. Linear regressions were weighted with parameters uncertainties. AFS and RFS were identified from the literature (Hermy et al. 1999, Dupouey et al. 2002, Bergès et al. 2015) but only species similarly classified in the three studies (*i.e.* systematically typical of ancient forest or of recent forest) were selected in this classification. We constituted an alternative list of AFS/RFS from our sampling data with Fisher exact test for frequency comparison, AFS being those species statistically more frequent in ancient forest and RFS in recent forest. We selected plant trait data or variables in the LEDA database (Kleyer et al. 2008) for dispersal and in Julve (1998) for abiotic optima (see Appendix C for additional details). Statistical analyses excluded outliers species if parameters or traits were 5 times lower than the 1st quartile or 5 times upper than the 3rd quartile.

3. Results

3.1 Assessment of the inference method on virtual landscapes

Our novel inference method successfully inferred the metapopulation model parameters from landscape history and static biodiversity data with reasonable accuracy (Fig. 3). However, estimation errors increased as the number of inferred parameters increased (Fig. 3A-C). Estimation uncertainties similarly increased with the number of parameters (Fig. 3D-F). The full model with four parameters (α, β, σ, θ) was hence difficult to calibrate, the median estimation errors rising up to 100% for parameter α. We therefore only considered metapopulation models with up to three parameters ($\alpha\beta\sigma$) in the following. For such models, median estimation errors were below 58%, 60%, and 17%, for parameters α, β and σ respectively, and median estimation uncertainties below 92%, 131%, and 25% respectively. Estimation errors were qualitatively similar in landscapes with higher or lower patch connectivities, and higher or lower temporal turnover of patches, these two landscape characteristics having relatively little influence on inference efficiency (Appendix B).

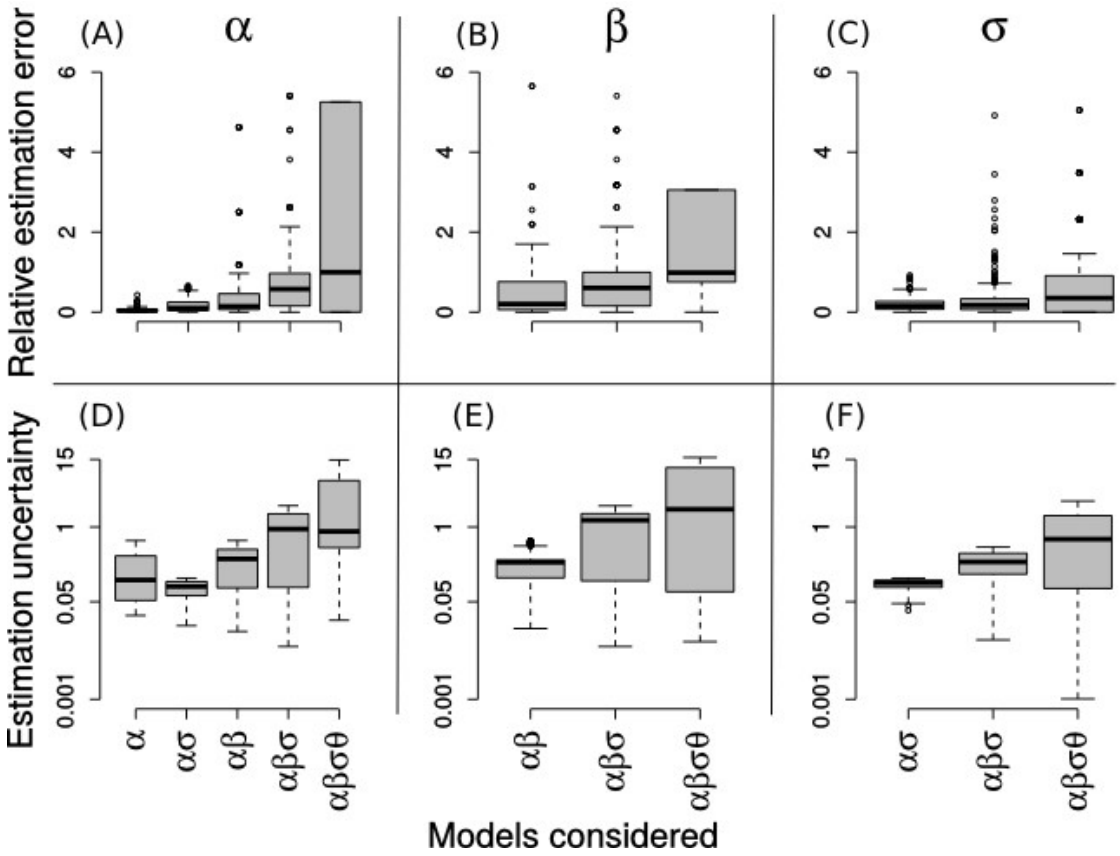

Figure 3: Parameter relative estimation error and estimation uncertainty (logarithmic scale) for five models of increasing complexity: a distance-independent colonization and no extinction model (α), a distance-dependent colonization and no extinction model (α and β,), a distance-independent colonization and patch area-independent extinction model (α and σ), a distance-dependent colonization and patch area-independent extinction model (α, β and σ) and a distance-dependent colonization and patch area-dependent extinction model (α, β, σ and θ). α: colonization rate parameter, β,: rate of colonization decrease with distance and σ: extinction rate parameter, θ: decay of the colonization rate with patch area. Some outliers do not appear (except for panel D, F) for clarity purpose.

Estimation error and uncertainty of colonization parameters (α and β) tended to be lower for the simulated metapopulations that had partially recolonized recent patches, compared to metapopulation that had recolonized either almost all recent patches or, conversely, almost none (Appendix D). Similarly, the extinction parameter (σ) was best estimated for metapopulations presenting intermediate extinction rates in ancient patches (Appendix D). We therefore excluded from the following analyses all species having an occurrence frequency below 5% or above 95% in either ancient or recent forest patches. 106 species out of the 174 species present in the dataset passed this criterion in Seine-et-Marne, 102 out of 121 in Eure-et-Loir.

3.2 Sufficiency of the metapopulation model for the studied forest plant data

The metapopulation model with three parameters ($\alpha\beta\sigma$) was sufficient to recover observed patterns for 72% of the studied species in Seine-et-Marne (n=76 species) and 61% in Eure-et-Loir (n=62 species). For these species, observed summary statistics (occurrence frequency in ancient forest patches, occurrence frequency in recent forest patches, mean distance of occupied recent patches to the nearest ancient patch) were within the 95% range of predicted values based on the fitted metapopulation model (*e.g.* Appendix E). When the model failed at reproducing observed species metapopulation patterns, it was generally due to an underestimation of the occurrence in recent patches. We also assessed the ability of a simpler metapopulation model with only two parameters ($\alpha\sigma$) to recover observed metapopulation patterns, but it was only validated for 21% of the species in Seine-et-Marne and 25% in Eure-et-Loir. We therefore only analyzed the three parameter metapopulation model ($\alpha\beta\sigma$) in the following. In both regions, median estimation uncertainties of the parameters α, β and σ were respectively below 28%, 63%, and 26% (Full species-level estimation results in Appendix F excluding two and three outliers species in Seine-et-Marne and Eure-et-Loir respectively).

3.3 Links between inferred metapopulation parameters and AFS/RFS status

Forest plant species were continuously distributed in the parameter space (Fig. 4). There was a positive correlation between α and σ values (Spearman's rho=0.95 and 0.75 in Seine-et-Marne and Eure-et-Loir respectively, see grey points on the bottom planes of Fig. 4). This indicates that some species have large propensity to both colonization and extinction (high α and σ values), and at the other extreme, some species have low propensity to both colonization and extinction (low α and σ values). The two colonization parameters (α and β) were positively correlated in Eure-et-Loir (Wilcoxon's test $p<0.001$, Spearman's rho=0.47, see grey points on the back right plans of Fig. 4) but were not in Seine-et-Marne. Finally, β was correlated with the extinction parameter σ neither in Seine-et-Marne, nor in Eure-et-Loir.

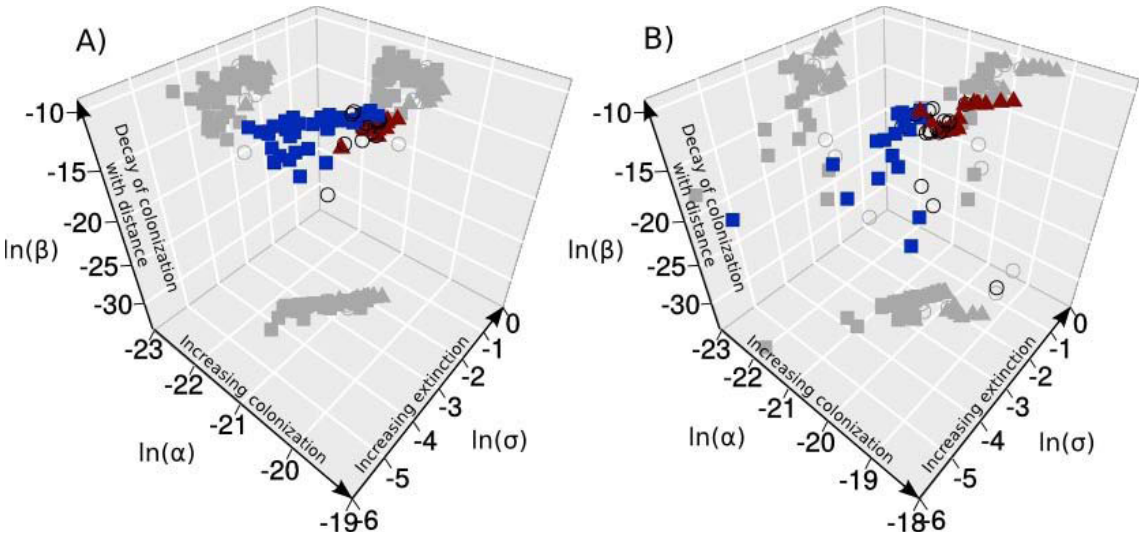

Figure 4: Inferred parameters ($\alpha\beta\sigma$) for forest plant species for A) Seine-et-Marne and B) Eure-et-Loir. Blue squares represent ancient forest species, red triangles represent recent forest species, open circles are species with no specific affinity for recent and ancient forests. Symbols are projected in 2D-planes in grey. Ancient/recent forest species were identified from sampling data with Fisher exact test for frequency comparison.

In both regions, AFS tended to have low propensity to both colonization and extinction, while recent forest species (RFS) tended to have large propensities to both colonization and extinction (Fig. 4). Indeed, AFS were found to have lower α and σ values than RFS (Wilcoxon's test $p<0.001$ in both regions), and larger β values in Seine-et-Marne (Wilcoxon's test $p<0.05$). This result was further confirmed by a complementary analysis evidencing a positive correlation between the ratio of occurrence frequency in recent forests versus ancient forests and the colonization parameter α (Spearman's rho=0.83 and 0.81 in Seine-et-Marne and Eure-et-Loir respectively) or the extinction parameter σ (Spearman's rho=0.88 and 0.80 in Seine-et-Marne and Eure-et-Loir respectively).

3.4 Between-region consistency of inferred metapopulation parameters

We evidenced strong differences (Wilcoxon's test $p<0.05$) in inferred model parameters between the two studied regions with overall higher α colonization parameter values and lower σ extinction parameter values in Eure-et-Loir than in Seine-et-Marne (Fig. 4, compare the locations of grey points in the bottom planes of the two panels). For the species analyzed in both regions, median α, β and σ values were respectively 1.8 times larger, 0.4 smaller and 1.3 times larger in Eure-et-Loir than in Seine-et-Marne. These

differences in inferred model parameters reflected observed differences in geographical distribution bias towards recent forests between the two regions. Indeed, species ratio of occurrence frequency in recent forests compared to ancient forests was larger (Wilcoxon one-tailed test $p<0.001$) in Eure-et-Loire (median=1.12) than in Seine-et-Marne (median=0.66).

We further assessed whether species ranks in terms of parameter values were the same in the two regions, and found only a positive correlation between the ranks in the two regions (Spearman's rho=0.46) for the parameter β.

3.5 Predictability of metapopulation parameters from plant functional traits

Given the high correlation value between α and σ, correlations with species traits were estimated only for α and β (the latter was log-transformed to improve normality). Specific leaf area and terminal velocity were positively correlated with the colonization parameter β in Eure-et-Loir (Fig. 5DE). Broader-sense plant functional traits, namely Ellenberg indicator values (EIV), were correlated with the parameters α and β. We found that species with higher nitrogen requirements had a lower β value in Seine-et-Marne and a larger α value in Eure-et-Loir (Fig. 5AC). Another correlation was region-specific, with a positive correlation between α and EIV for humidity in Seine-et-Marne (Fig. 5B).

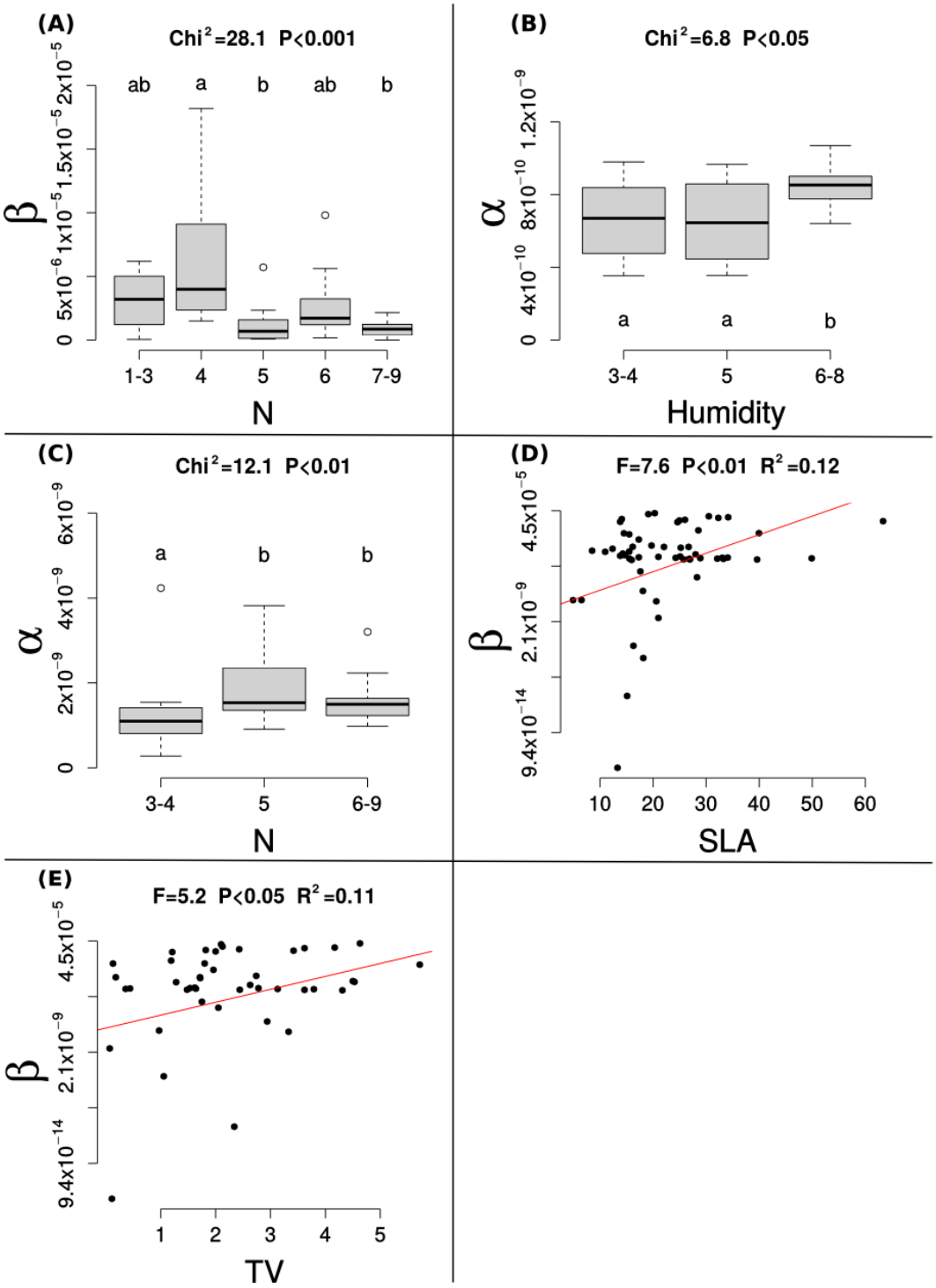

Figure 5: Significant relationships between parameters and broader sense plant functional traits in Seine-et-Marne (A: nitrogen requirement, B: affinity for soil humidity) and Eure-et-Loir (C: nitrogen requirement, D: specific leaf area, E: terminal velocity). *Chi²*: Chi squared, *P*: p-value. For ecological optimum, the abscissa represents Ellenberg's indicator value or group of values if the number of species was less than ten. Letters indicate significant differences in groups defined from a post hoc Kruskal analysis. P-values were computed with a Bonferroni correction. Linear regressions were weighted with parameter uncertainties.

4. Discussion

We developed an original inference method to calibrate a patch occupancy model of metapopulation dynamics from a combination of non-exhaustive static biodiversity data and landscape history data. This method was found to have a relatively good accuracy when used on moderately complex metapopulation models containing up to three colonization/extinction parameters (Fig. 3). Its main advantage over existing inference approaches (Ruete et al. 2014) is that it is scalable to large landscapes of several thousands of patches, as we evidenced here. We further demonstrated the robustness of the method to landscape characteristics using virtual landscapes (Appendix B). These properties of scalability and robustness make the proposed method suitable to be applied to common large scale non-exhaustive biodiversity inventory data (*e.g.*, Flemons et al. 2007, Pereira et al. 2013). For such applications, our simulation study points that the documented time window of landscape dynamics should be selected to correspond to an intermediate recolonization level of recent patches by the focal species, so as to maximize inference accuracy (Appendix D).

Our application to forest plant data showed that empirical uncertainties are lower than those reported in the power analyses due to the precautions taken that are (i) the exclusion of species having a large or a low occurrence frequency in either ancient or recent forest patches, (ii) the improvement of the maximization of the approximate log-likelihood with local optimizations and (iii) the exclusion of species, that have inaccurate combinations of parameters, thanks to model checking tests. Our analyses revealed that a patch-occupancy model with distance-dependent colonization and area-independent extinction was sufficient to account for observed spatial patterns of occurrence for most species (Appendix F). It further revealed a spectrum of metapopulation turnover speed, with species having strongly correlated values of colonization capacity and extinction propensity (Fig. 4). This spectrum of turnover speed explains the variability in responses of forest plant species to landscape dynamics that has been recurrently evidenced in the literature (Hermy et al. 1999, Dupouey et al. 2002, Bergès et al. 2015). The position of a species along this spectrum of turnover speed can be seen as a measure of recruitment limitation of this species in novel landscape patches, since species with large turnover speed are more likely to colonize novel patches. Our analyses thus revealed that the recruitment limitation experienced by forest plant species is both linked to its intrinsic functional properties (as measured by its functional traits) and to the environmental characteristics of novel patches (Fig. 5). More precisely, species having larger specific leaf area were found to have a lower dispersal distance in Eure-et-Loir (Fig. 5D) suggesting that they could be more confined

into ancient forests. Species having larger terminal velocity were also found to have a lower dispersal distance in Eure-et-Loir (Fig. 5E). This result is consistent with Kimberley et al. (2014) who found higher mean values for seed terminal velocity for species that are more confined in ancient patches. Besides, environmental preferences of species, as measured by Ellenberg indicator values (Julve et al. 1998), were found to be correlated with turnover speed (Fig. 5B, C) or dispersal distance (Fig. 5A). In particular, recent forest soils are generally enriched in nitrogen either due to intrinsic properties (forests on richer soils were more likely to be deforested than forests growing on poor soils) or to fertilization for agronomic purposes (Hermy and Verheyen 2007). It is thus consistent to observe a lower recruitment limitation of nitrophilous species in these recent forests (Fig. 5A, C), a result also consistent with previous studies (Hermy et al. 1999, Bergès et al. 2015). Finally, the turnover speed was also found higher when edaphic humidity (Fig. 5B) are intermediate or high, a pattern also evidenced by Hermy et al. (1999).

This dependence of recruitment limitation of forest plant species to both intrinsic colonization properties and environmental characteristics of patches challenges the concept of ancient/recent forest species, since the recolonization potential of a plant species cannot be solely predicted from its intrinsic properties but rather from an interaction between its properties and the environmental characteristics of the dynamical landscape. In this vein, we only found a significant positive correlation of the species dispersal parameter (β) between the two regions studied.

Our approach thus enables to get a compound quantification of recruitment limitation for the different species of the community, but not to tease apart the respective roles of dispersal limitation and post-dispersal environmental filtering processes. To achieve this, one possibility would be to explicitly model the quality of the different patches. For instance, Verheyen et al. (2004) proposed to define this patch quality as a distance in terms of Ellenberg indices between the focal species and the average of the species found in a patch. This approach that requires to sample all patches to estimate patch quality could not be applied in our context in which only a reduced subset of patches have been inventoried. It may however be possible to interpolate patch quality measures for unsampled patches or to predict patch quality based on complementary environmental data through niche modelling (Warren 2012).

Our modelling framework accounts for imperfect detection that is a reality for forest plant species: Archaux et al. (2008) showed that 19% of plant species may be undetected at the plot scale. However imperfect detection was fixed but not species-specific in our approach, although this would have been technically straightforward.

This choice was motivated by our preliminary simulation study that revealed that only up to three model parameters could be reasonably inferred from this type of data. Indeed, we point out here again the importance to quantify inference accuracy when introducing any new parameters.

Our inference approach has been used in this study to assess the concept of ancient/recent forest species, but it may be applied to other purposes. In particular, by providing a species-level calibrated model of metapopulation dynamics, our approach could be used to predict species spatial dynamics at regional scales, since it is operational at the scale of several thousands of patches. Such a metapopulation model with dynamical landscape is particularly appealing to study the time-delayed response of biodiversity following a modification of habitat quality, quantity or connectivity (Hylander and Ehrlén 2013) and to detect the presence of extinction debts or immigration credits following such a perturbation (Kuussaari et al. 2009, Jackson and Sax 2010, Essl et al. 2015). This inference approach could also be used to make cross-landscape comparisons to better understand environmental drivers of species spatial dynamics. The present study offered some first clues related to the fertility of recent forest patches compared to ancient ones, but application of this approach to much more contrasted landscape contexts should provide a deeper understanding of the processes at play. Finally, this approach could be applied to other types of habitat, like ephemeral ecosystems such as intermittent rivers (Datry et al. 2016), agricultural mosaics (Bertrand et al. 2016) or backwaters (Ruiz et al. 2014) to name a few.

Acknowledgements

This work was supported by the French national research institute of science and technology for environment and agriculture (IRSTEA). EL was supported by the Regional Council of Auvergne-Rhône-Alpes. We are grateful to the French national forest inventory (IFN: Inventaire Forestier National) and the national botanic conservatory (CBNBP: Conservatoire Botanique National du Bassin Parisien) for providing us with floristic inventory data. We also thank Hilaire Martin and Julien Fleury for having digitalized the thousands of forest patches present in old maps (research project “Distrafor” funded by the French Ministry of Environment through GIP Ecofor).

Appendix

Appendix A: Alternative methods to compute patch incidences at the time of the oldest map

In the Seine-et-Marne study area, we tested two methods that not required the assumption that species would be in equilibrium with the landscape configuration at the time of the oldest map, to compute patch incidences. First, initial incidences were randomly sampled from trials in the Bernoulli distribution with an arbitrary probability of 0.1. Second, as the ancient forest was partially cleared during the period 1820-2000, an extinction debt could be expected in 2000. Therefore we considered the hypothesis that present species frequencies f_i in ancient forests reflect the state of occupancy at the time of the oldest map and we initialized patch incidences accordingly, using Bernouilli trials with probability f_i. These two initialization methods were not good alternatives because species acceptance rates (model checking tests, section 2.4.3) were finally very low (<20%). Consequently, the equilibrium hypothesis (section 2.2) is the better in absence of maps older than the 1820 map. This hypothesis is sufficient to reproduce most of the present pattern of species occupancy (acceptance rate=72%) probably because it reflects fairly well the probability of occupancy in the old landscape according to connectivity.

Appendix B: Reliability of the inference method for virtual landscapes.

1. Realism of virtual landscapes.

The old and recent maps of virtual landscapes were created using the python package nlmpy (Etherington et al. 2015). For each landscape, an old map was generated from grid squares with various levels of spatial autocorrelation in the pixel values controlled thanks to an autocorrelation parameter *a* (Etherington et al. 2015). To transform this map into a binary map differentiating pixels of forests from matrix pixels (unsuitable habitat), pixels were classified as forest when the pixel value was above a chosen threshold. The threshold was fixed as the *np* percentile of the distribution of pixel values. Then, a transition map was created with the same autocorrelation parameter *a* as for the old map. Finally, the recent map derive from the old map and the transition map thanks to an algorithm (Fig B.1) that allowed to control patch turnover rates with a parameter (φ).

Virtual landscapes were confronted to real ones to test if patches dynamics and

connectivity were realistic using the French administrative units of Eure-et-Loir (5927km^2) of the Centre-Val de Loire region and the administrative units of Seine-et-Marne (7144km^2) and Essonne (2171km^2) of the Ile-de-France region.

Virtual landscape parameters (Table B.1) of autocorrelation *a*, proportion *np*, patch turnover rates φ were selected so that simulated patch dynamics (Table B.2) and connectivity (Fig. B.2) remained close to the ranges defined by the real landscapes. Connectivity (*CON*) was calculated following equation 3, of the materials and methods section, with $\alpha=1$ and β=0.001. Other virtual landscapes have various patches turnover and connectivity that deviate from the intermediate landscape. Total area of virtual landscapes was lower than real landscapes (1000km^2) thus patch dynamics was quantified in terms of proportion.

Table B.1: Landscape simulation parameters. *a*: patches autocorrelation, *np*: percentile used as threshold to differentiate patches and matrix, φ: changing rate between ancient and recent map. *Int*: intermediate landscape, *LC*: low connectivity landscape, *HC*: high connectivity landscape, *LT*: low patch turnover, *HT*: high patch turnover.

	Int	LC	HC	LT	HT
a	0.2	0.05	0.45	0.2	0.2
np	90	95	65	90	90
φ	0.25	0.25	0.25	0.05	0.7

Table B.2: Simulated and real landscape patch dynamics. Lost area is ancient forest area that was cleared relatively to total ancient forest area. New area is new forest area relatively to forest area always present over time. *28*: Eure-et-Loir, *77*: Seine-et-Marne, *91*: Essonne, *Int*: intermediate landscape, *LC*: low connectivity landscape, *HC*: high connectivity landscape, *LD*: low patches dynamic landscape, *HD*: high patches dynamic landscape.

	28	77	91	Int	LC	HC	LT	HT
Lost area	0.24	0.22	0.31	0.39	0.58	0.20	0.09	0.85
New area	0.89	0.93	1.01	0.64	1.14	0.25	0.09	5.68

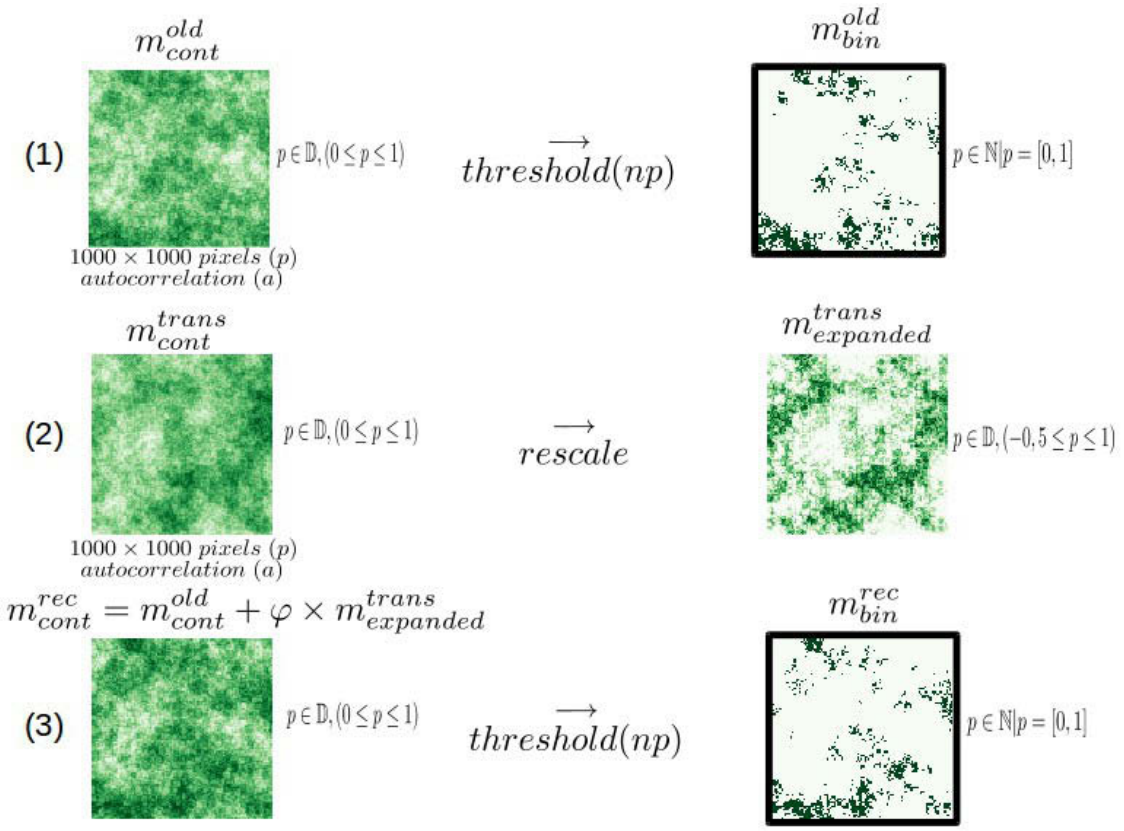

Figure B1: Summary of virtual landscape simulations. *(1)* An old map $\left(m_{cont}^{old}\right)$ was created from a square raster of 1000×1000 pixels (*p*) randomly generated between 0 and 1. The level of spatial autocorrelation in the generated pixel values (*p*) were controlled thanks to an autocorrelation parameter *a*. A threshold (*np*) was used to differentiate pixels of forests from matrix pixels and to create a binary map $\left(m_{bin}^{old}\right)$. *(2)* A transition map $\left(m_{cont}^{trans}\right)$ was simulated following the same procedure as for the old map and rescaled between -0.5 and 1 $\left(m_{expanded}^{trans}\right)$ to mimic the increase of forest area. *(3)* A recent map $\left(m_{cont}^{rec}\right)$ was created (from the algorithm below) using the parameter φ to control the pixel turnover rate. A binary (forest/matrix) recent map $\left(m_{bin}^{rec}\right)$ was produced from the m_{cont}^{rec} map using the threshold *np*.

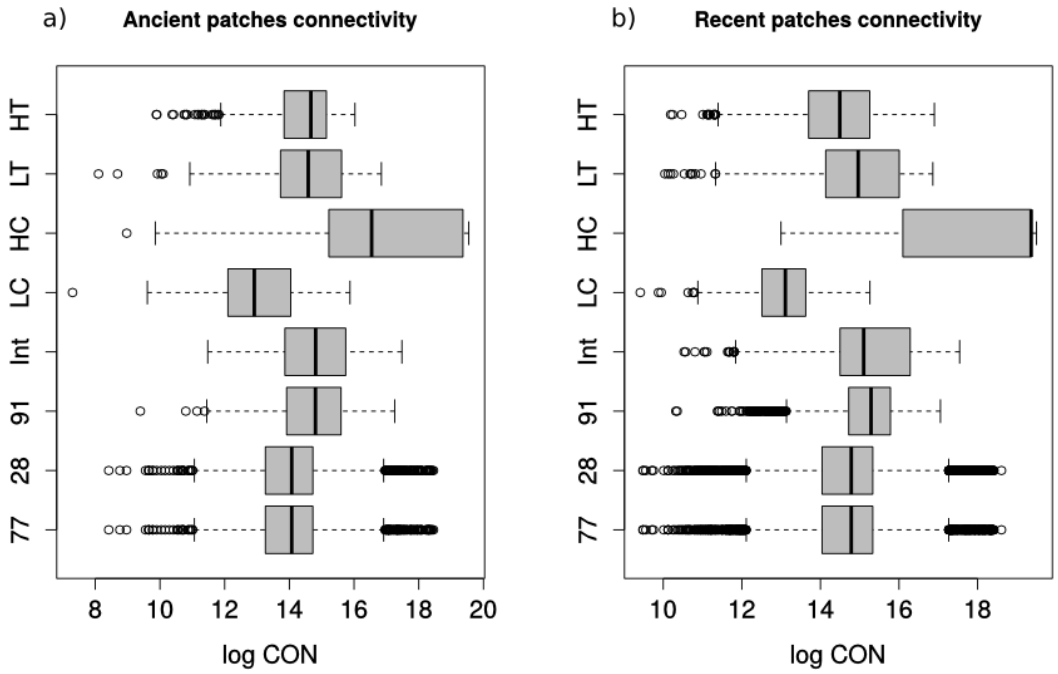

Figure B.2: Connectivity of ancient patches (a) and recent patches (b) for simulated and real landscapes. See Table A.2 for codes.

2. Prediction error and uncertainty estimations for virtual landscapes.

We examined in this section the effect of connectivity and temporal patch turnover, on the inference quality. For example, the α median estimation error (α model) ranged from 2.0 ± 4.0% (low turnover landscape) to 7.7 ± 12.2% (high turnover landscape) and from 5.7 ± 20.1% (low connectivity landscape) to 3.0 ± 7.1% (high connectivity landscape). These results indicate that inference quality did not vary much among landscapes with very different connectivity or patch turnover values. For the distance-dependent colonization and no extinction model (α and β) and the distance-independent colonization and patch area-independent extinction model (α and σ), estimation errors were rather stable among landscapes (Fig. B.3). Estimation error remained lower with one parameter to infer (α model) in comparison to models with more parameters: the α median estimation error ranged from 12.7 ± 38.4% (low turnover landscape) to 31.8 ± 117.8% (high turnover landscape) for the $\alpha\beta$ model and from 10.0 ± 15.6% (intermediate landscape) to 53.4 ± 43.8% (high connectivity landscape) for the $\alpha\sigma$ model.

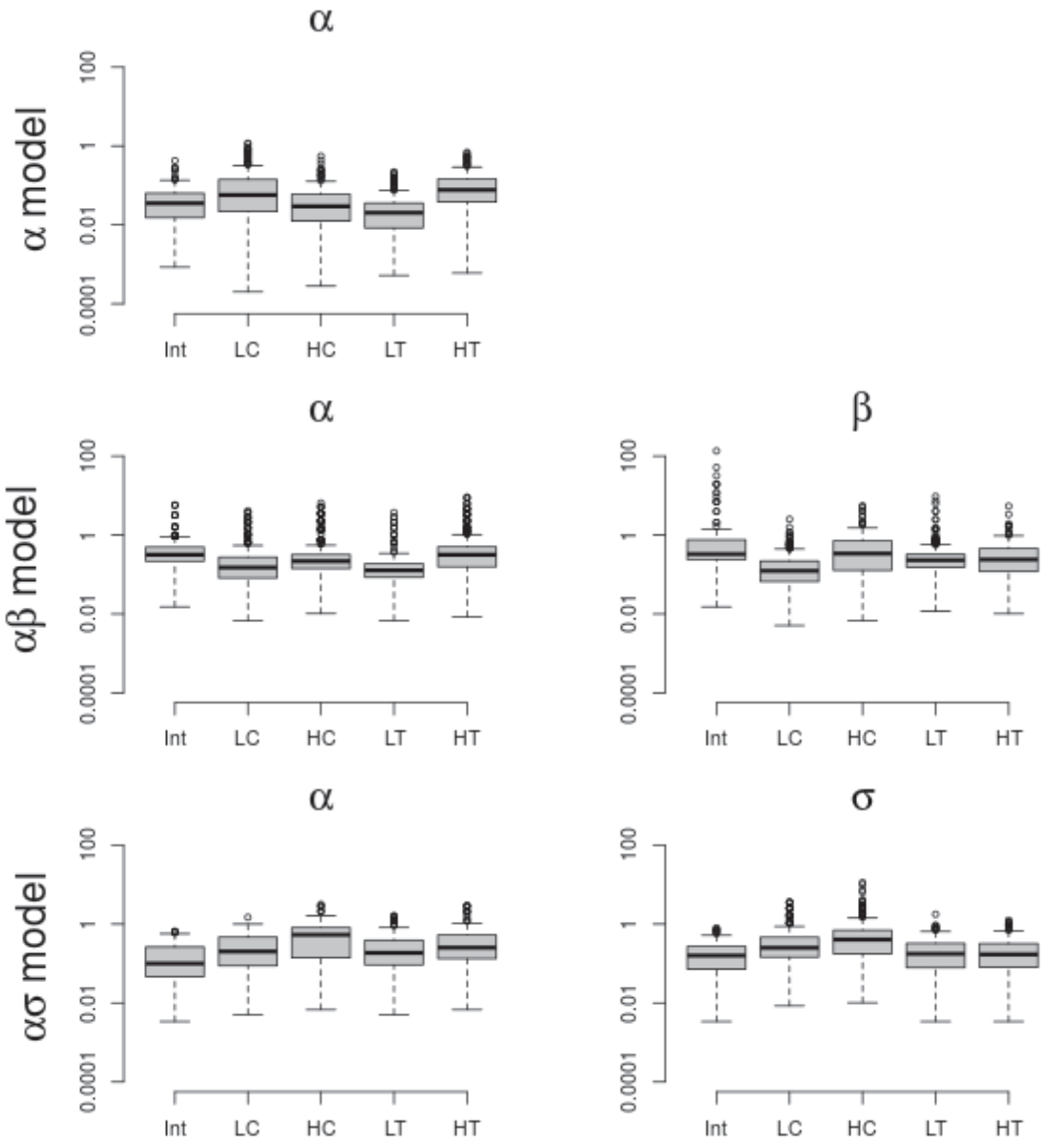

Figure B.3: Parameter estimation error (logarithmic scale) for three models: a distance-independent colonization and no extinction model (α), a distance-dependent colonization and no extinction model (α and β), a distance-independent colonization and patch area-independent extinction model (α and σ). α: colonization rate parameter, β: rate of colonization decrease with distance and σ: extinction rate parameter. Species occurrences were simulated in five virtual landscapes with various characteristics of connectivity and temporal turnover. *Int*: intermediate landscape, *LC*: low connectivity landscape, *HC*: high connectivity landscape, *LT*: low turnover landscape, *HT*: high turnover landscape. Boxplots represent the relative estimation error for the parameter indicated above.

Appendix C: Traits and variables of species sampled in Seine-et-Marne (A) and in Eure-et-Loir (B). If several values were reported by different sources for a pair trait/species, the median was retained. For nominal variables, classes with less than five species were deleted if merging with another neighboring class was not possible. Only the 76 species in the landscape (A) and the 62 species in the landscape (B) whose inferred dynamics ($\alpha\beta\sigma$ model) passed the model checking tests are taken into account. Releasing height and seed mass were log-transformed.

Trait / variable	Source	Description	Missing values (%) (A)	Missing values (%) (B)
Dispersal type	Kleyer et al. 2008	-dysochorous -endozoochorous -epizoochorous -hydrochorous	41	41
Dispersal vector	Kleyer et al. 2008	-small mammal in the wild -domestic animal -water -man -bird	51	46
Releasing height	Kleyer et al. 2008	m	22	10
Seed mass	Kleyer et al. 2008	mg	4	8
Specific leaf area	Kleyer et al. 2008	mm^2/mg	1	3
Terminal velocity	Kleyer et al. 2008	m/s^2	30	25
Light	Julve et al. 1998	ordinal (1-9)	4	8
Edaphic humidity	Julve et al. 1998	ordinal (1-9)	4	8
pH	Julve et al. 1998	ordinal (1-9)	4	8
Nitrogen	Julve et al. 1998	ordinal (1-9)	4	8

Appendix D: Relationship between (1) relative estimation error (logarithmic scale) and (2) estimation uncertainty (logarithmic scale) and simulated metapopulation dynamics. Each row corresponds to a model with a different set of parameters. α: colonization rate parameter, β: rate of colonization decrease with distance and σ: extinction rate parameter, *freq in RF*: frequency of occurrence in recent forest patches, *freq in AF*: frequency of occurrence in ancient forest patches. In each panel, each grey point represents the estimation error / uncertainty obtained with one virtual dataset, the green dotted line represents an arbitrary threshold equal to 0.25, and the red plain curve is the regression line fitted with local polynomial regressions.

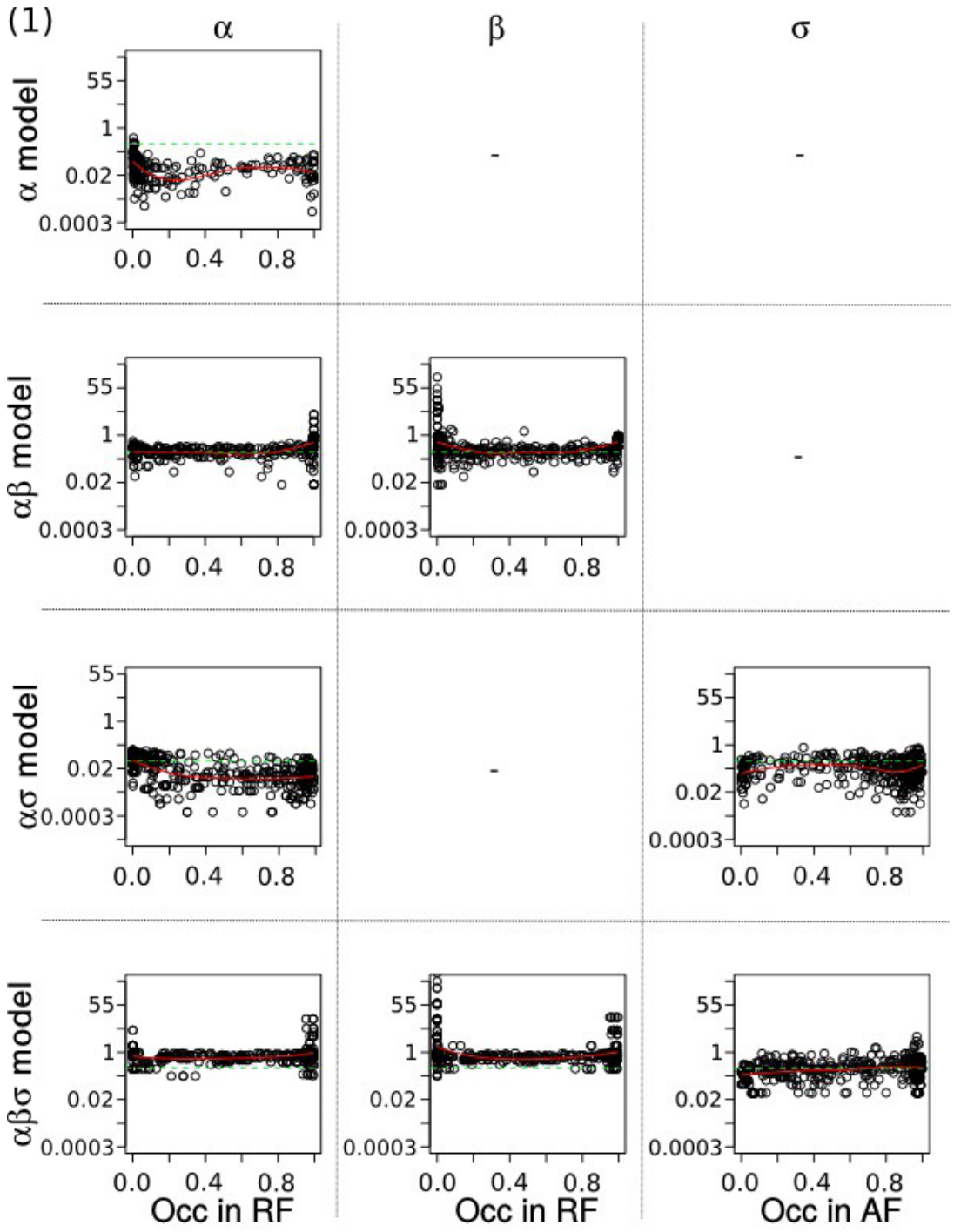

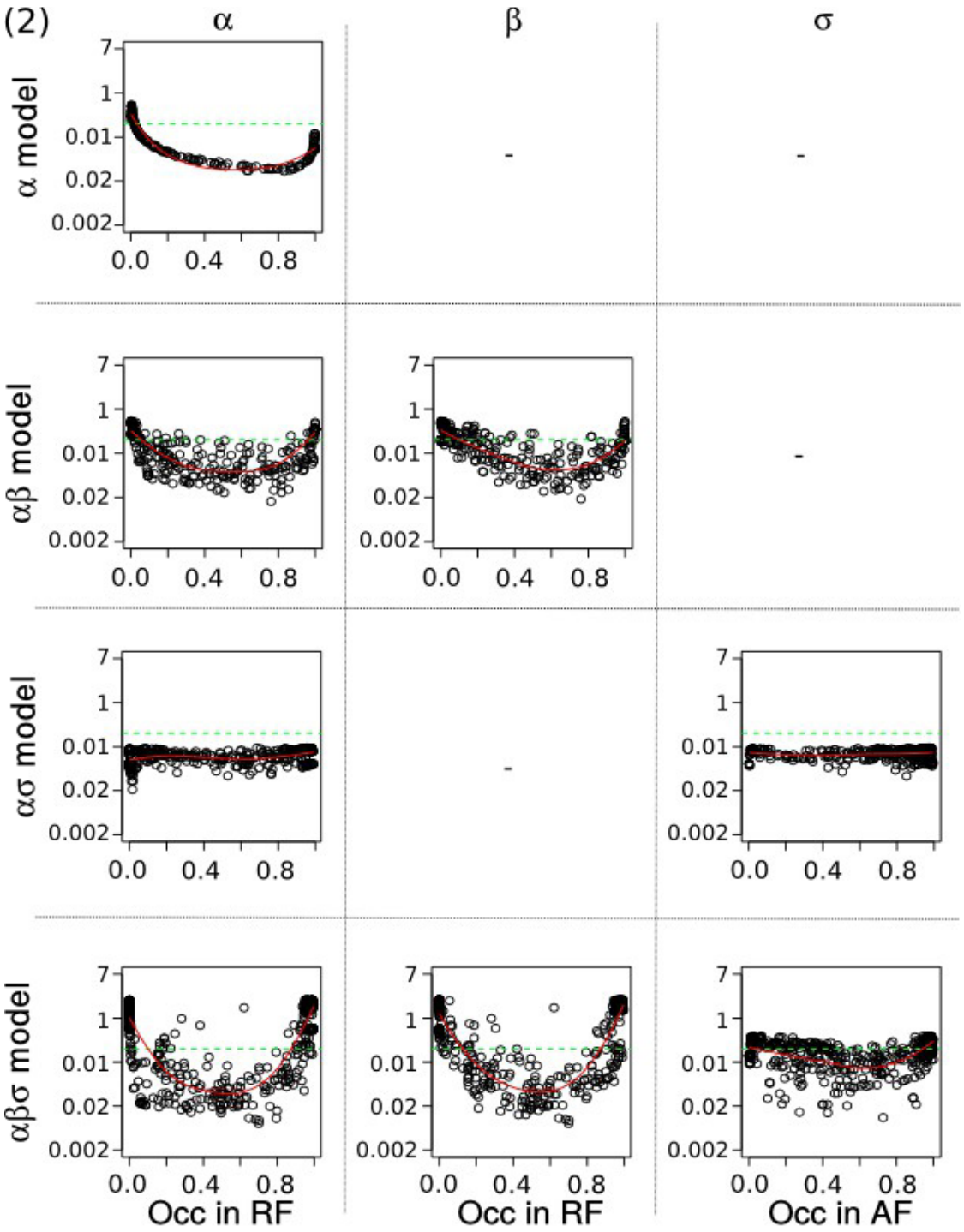
(2)
α
β
σ
α model
αβ model
ασ model
αβσ model
7
1
0.01
0.02
0.002
0.0
0.4
0.8
-
Occ in RF
Occ in RF
Occ in AF

Appendix E: Model checking tests for the species *Anemone nemorosa*. Histograms represent the simulated values of statistics from 100 simulations. Observed values are depicted by the vertical red lines. Dashed lines are the limits of the 95% of the range of the simulated values. (1) Distance-independent colonization with area-independent extinction model ($\alpha\sigma$); (2) Distance-dependent colonization with area-independent extinction model ($\alpha\beta\sigma$); *AF*: occurrence in ancient patches; *RF*: occurrence in recent patches, *p*: p-value. Distance to AF is the mean distance of occupied recent patches to nearest ancient forest patch. Parameters were inferred from eq. 6 with $F_i(t_{data})=0$.

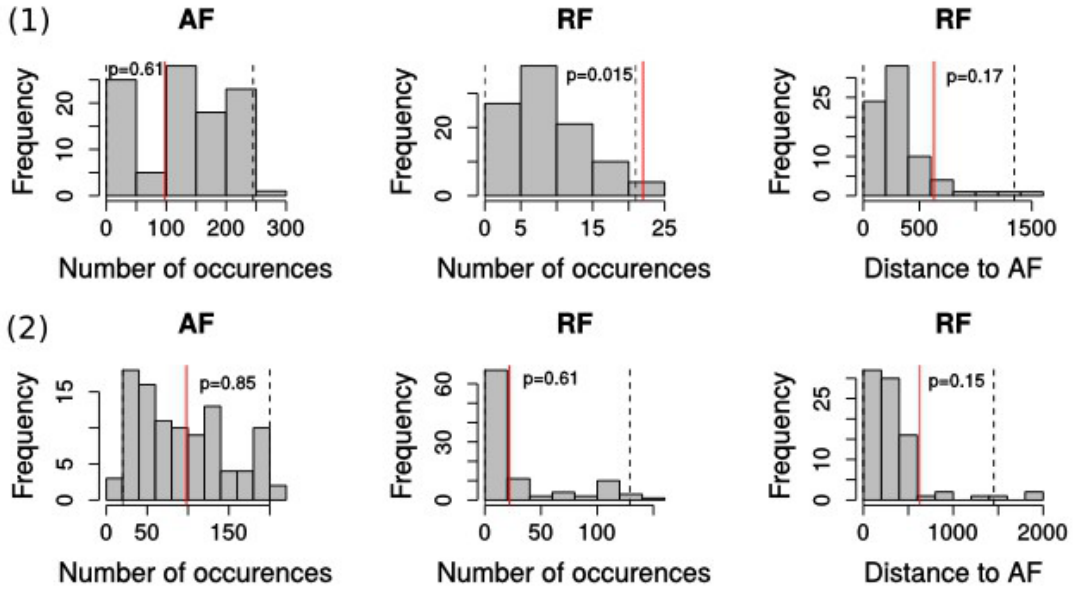

Appendix F: Affinity for ancient and recent forests, identified from sampling data and from literature, and inferred parameters with uncertainties for inferred colonization distance-dependent and extinction dynamic ($\alpha\beta\sigma$). Only 72% of the species in the Seine-et-Marne and 61% of the species in the Eure-et-Loir whose inferred dynamics ($\alpha\beta\sigma$ model) passed the model checking tests are displayed (but excluding two outliers in the first landscape and three outliers in the second). *Freq AF*: frequency in ancient forest, *Freq RF*: frequency in recent forest, *unc:* uncertainty, *AFS-RFS*: AFS and RFS identified from the literature (Hermy et al. 1999, Dupouey et al. 2002, Bergès et al. 2015), *a*: Seine-et-Marne, *b*: Eure-et-Loir, *NA:* species is not included in the dataset.

Species	*AFS-RFS*	Freq AF*a*	Freq RF*a*	AFS-RFS*a*	*αa*	*α* unc*a*	*σa*	*σ* unc*a*	*βa*	*β* unc*a*	Freq AF*b*	Freq RF*b*	AFS-RFS*b*	*αb*	*α* unc*b*	*σb*	*σ* unc*b*	*βb*	*β* unc*b*
Acer campestre	AFS	NA	NA	NA	NA	NA	NA	NA	NA	NA	0.09	0.28	RFS	-19.86	0.23	-1.81	0.31	-11	0.4
Acer pseudoplatanus	NA	NA	NA	NA	NA	NA	NA	NA	NA	NA	0.17	0.22	NA	-20.46	0.5	-1.91	0.38	-22.17	0.98
Agrimonia eupatoria	NA	0.1	0.21	RFS	-20.74	0.13	-1.8	0.14	-13.07	0.32	NA	NA	NA	NA	NA	NA	NA	NA	NA
Agrostis capillaris	NA	0.14	0.07	AFS	-20.88	0.13	-2.24	0.14	-11.96	0.24	0.11	0.09	NA	-20.4	0.17	-2.29	0.19	-11.77	0.28
Ajuga reptans	AFS	0.23	0.17	NA	-20.98	0.24	-2.11	0.4	-14.92	0.45	NA	NA	NA	NA	NA	NA	NA	NA	NA
Alliaria petiolata	NA	0.35	0.15	AFS	-21.52	0.16	-3.08	0.16	-17.88	0.75	NA	NA	NA	NA	NA	NA	NA	NA	NA
Alnus glutinosa	RFS	NA	NA	NA	NA	NA	NA	NA	NA	NA	0.09	0.31	RFS	-19.88	0.17	-2.07	0.23	-10.75	0.25
Anthoxanthum odoratum	NA	0.22	0.07	AFS	-21.16	0.16	-2.79	0.18	-11.78	0.46	NA	NA	NA	NA	NA	NA	NA	NA	NA
Arum maculatum	AFS	0.21	0.29	RFS	-20.84	0.1	-1.88	0.15	-14.63	0.18	NA	NA	NA	NA	NA	NA	NA	NA	NA
Athyrium filix-femina	AFS	NA	NA	NA	NA	NA	NA	NA	NA	NA	0.14	0.2	NA	-19.92	0.25	-1.97	0.52	-10.93	0.37
Betula pendula	NA	0.26	0.13	AFS	-21.3	0.6	-2.65	1	-16.81	1.23	0.21	0.32	RFS	-20.35	0.17	-1.8	0.18	-14.31	0.35
Brachypodium pinnatum	RFS	0.06	0.14	RFS	-20.86	0.07	-1.98	0.08	-13.19	0.14	NA	NA	NA	NA	NA	NA	NA	NA	NA
Calluna vulgaris	AFS	0.34	0.09	AFS	-21.54	0.35	-3.38	0.4	-12.1	0.9	0.29	0.21	AFS	-20.68	0.11	-2.43	0.19	-13.7	0.83
Carex flacca	NA	NA	NA	NA	NA	NA	NA	NA	NA	NA	0.23	0.15	AFS	-20.69	0.21	-2.31	0.26	-26.7	1.04
Carex pilulifera	AFS	NA	NA	NA	NA	NA	NA	NA	NA	NA	0.69	0.08	AFS	-22.02	0.62	-5.64	0.87	-18.17	1.08
Carex remota	AFS	NA	NA	NA	NA	NA	NA	NA	NA	NA	0.17	0.34	RFS	-20.29	0.18	-1.7	0.19	-14.39	0.39
Castanea sativa	NA	0.55	0.15	AFS	-21.6	0.63	-4.19	0.56	-11.29	1.15	0.4	0.37	NA	-20.5	0.38	-2.09	0.66	-14.07	1.05
Cirsium arvense	NA	0.18	0.19	NA	-21.29	0.25	-2.63	0.1	-20.2	1.14	NA	NA	NA	NA	NA	NA	NA	NA	NA
Cirsium palustre	NA	0.09	0.07	NA	-20.91	0.18	-2.03	0.21	-13.55	0.2	NA	NA	NA	NA	NA	NA	NA	NA	NA
Clematis vitalba	AFS	0.51	0.45	NA	-21.12	0.59	-2.41	1.01	-14.99	1.61	NA	NA	NA	NA	NA	NA	NA	NA	NA
Convallaria majalis	AFS	0.17	0.09	AFS	-20.99	0.13	-2.26	0.16	-12.76	0.28	NA	NA	NA	NA	NA	NA	NA	NA	NA
Cornus sanguinea	NA	NA	NA	NA	NA	NA	NA	NA	NA	NA	0.08	0.15	RFS	-20.48	0.16	-2.1	0.25	-13.25	0.3
Cytisus scoparius	NA	0.22	0.1	AFS	-21.12	0.28	-2.58	0.33	-12.3	0.61	0.35	0.28	NA	-20.6	0.17	-2.29	0.18	-13.68	0.4
Dactylis glomerata	NA	0.15	0.18	NA	-20.81	0.2	-1.91	0.21	-13.11	0.57	0.17	0.28	RFS	-20.31	0.2	-1.74	0.25	-14.25	0.35
Daphne laureola	AFS	0.29	0.07	AFS	-21.76	0.5	-3.43	0.75	-16.38	0.96	NA	NA	NA	NA	NA	NA	NA	NA	NA
Deschampsia cespitosa	AFS	NA	NA	NA	NA	NA	NA	NA	NA	NA	0.29	0.32	NA	-20.43	0.14	-1.97	0.2	-13.96	0.35
Deschampsia flexuosa	AFS	NA	NA	NA	NA	NA	NA	NA	NA	NA	0.46	0.26	AFS	-20.97	0.21	-3.01	0.28	-14.2	0.57
Digitalis purpurea	NA	NA	NA	NA	NA	NA	NA	NA	NA	NA	0.15	0.07	AFS	-20.56	0.22	-2.31	0.25	-12.6	0.35
Dryopteris carthusiana	AFS	NA	NA	NA	NA	NA	NA	NA	NA	NA	0.24	0.42	RFS	-20.3	0.53	-1.73	0.9	-14.12	1.33

Species	*AFS-RFS*	Freq AF*a*	Freq RF*a*	AFS-RFS*a*	*αa*	*α* unc*a*	*σa*	*σ* unca	*βa*	*β* unc*a*	Freq AF*b*	Freq RF*b*	AFS-RFS*b*	*αb*	*α* unc*b*	*σb*	*σ* unc*b*	*βb*	*β* unc*b*
Dryopteris dilatata	NA	NA	NA	NA	NA	NA	NA	NA	NA	NA	0.1	0.27	RFS	-20.4	0.61	-1.91	0.42	-14.16	1.13
Dryopteris filix-mas	AFS	0.54	0.21	AFS	-21.68	0.31	-3.82	0.45	-12.54	0.55	NA	NA	NA	NA	NA	NA	NA	NA	NA
Epilobium angustifolium	NA	NA	NA	NA	NA	NA	NA	NA	NA	NA	0.23	0.21	NA	-20.58	0.34	-2.17	0.56	-19.66	0.64
Epilobium montanum	AFS	NA	NA	NA	NA	NA	NA	NA	NA	NA	0.27	0.21	NA	-20.75	0.47	-2.58	0.79	-13.26	1.07
Epipactis helleborine	RFS	0.15	0.15	NA	-20.84	0.12	-1.98	0.13	-12.96	0.27	NA	NA	NA	NA	NA	NA	NA	NA	NA
Erica cinerea	RFS	0.07	0.07	NA	-21	0.17	-2.43	0.18	-12	0.19	NA	NA	NA	NA	NA	NA	NA	NA	NA
Euonymus europaeus	NA	NA	NA	NA	NA	NA	NA	NA	NA	NA	0.07	0.43	RFS	-20.3	0.2	-1.73	0.31	-14.01	0.49
Eupatorium cannabinum	NA	0.14	0.29	RFS	-20.84	0.2	-1.9	0.37	-14.01	0.4	0.17	0.16	NA	-20.54	0.27	-2.13	0.16	-14.28	0.55
Euphorbia dulcis	AFS	NA	NA	NA	NA	NA	NA	NA	NA	NA	0.21	0.27	RFS	-20.38	0.2	-1.86	0.22	-14.34	0.35
Fagus sylvatica	AFS	0.21	0.26	NA	-20.86	0.2	-1.91	0.31	-14.56	0.68	0.38	0.23	AFS	-20.82	0.15	-2.68	0.22	-13.86	0.32
Festuca heterophylla	AFS	0.2	0.06	AFS	-21.38	0.35	-2.89	0.41	-12.9	0.66	NA	NA	NA	NA	NA	NA	NA	NA	NA
Filipendula ulmaria	RFS	NA	NA	NA	NA	NA	NA	NA	NA	NA	0.15	0.27	RFS	-19.56	0.32	-1.99	0.42	-10.31	0.41
Fragaria vesca	NA	NA	NA	NA	NA	NA	NA	NA	NA	NA	0.4	0.29	AFS	-20.71	0.5	-2.56	0.21	-13.14	1.14
Galeopsis tetrahit	NA	0.23	0.06	AFS	-21.56	0.24	-3.12	0.25	-13.61	1.04	NA	NA	NA	NA	NA	NA	NA	NA	NA
Galium aparine	RFS	NA	NA	NA	NA	NA	NA	NA	NA	NA	0.2	0.42	RFS	-19.72	0.56	-1.96	0.38	-10.59	0.63
Galium palustre	NA	NA	NA	NA	NA	NA	NA	NA	NA	NA	0.09	0.27	RFS	-20.24	0.76	-2.81	0.75	-10.65	0.63
Geranium robertianum	RFS	0.16	0.25	RFS	-20.87	0.26	-1.98	0.45	-13.63	0.51	NA	NA	NA	NA	NA	NA	NA	NA	NA
Glechoma hederacea	NA	0.16	0.41	RFS	-20.95	0.22	-2.12	0.37	-13.65	0.57	NA	NA	NA	NA	NA	NA	NA	NA	NA
Heracleum sphondylium	NA	NA	NA	NA	NA	NA	NA	NA	NA	NA	0.06	0.23	RFS	-20.2	0.27	-1.62	0.33	-13.26	0.53
Holcus lanatus	NA	0.17	0.14	NA	-20.93	0.15	-2.11	0.18	-13.24	0.32	0.16	0.29	RFS	-20.24	0.19	-1.63	0.23	-14.24	0.34
Holcus mollis	NA	0.18	0.1	AFS	-21	0.14	-2.28	0.17	-12.75	0.3	0.27	0.15	AFS	-20.66	0.47	-2.66	0.2	-12.03	0.9
Humulus lupulus	NA	0.12	0.32	RFS	-20.88	0.1	-1.97	0.17	-13.83	0.2	NA	NA	NA	NA	NA	NA	NA	NA	NA
Hyacinthoides non-scripta	AFS	0.24	0.06	AFS	-21.6	0.25	-3.18	0.27	-13.98	0.83	0.12	0.42	RFS	-19.28	0.14	-1.62	0.14	-10.22	0.25
Hypericum maculatum	NA	NA	NA	NA	NA	NA	NA	NA	NA	NA	0.14	0.17	NA	-20.35	0.35	-1.87	0.36	-13.34	0.97
Hypericum perforatum	AFS	0.4	0.28	AFS	-21.24	0.12	-2.68	0.18	-13.34	0.25	NA	NA	NA	NA	NA	NA	NA	NA	NA
Hypericum pulchrum	AFS	NA	NA	NA	NA	NA	NA	NA	NA	NA	0.54	0.21	AFS	-21.32	0.5	-3.8	0.76	-15.47	1.43
Ilex aquifolium	AFS	0.07	0.13	RFS	-20.81	0.07	-1.9	0.08	-13.25	0.14	0.7	0.53	AFS	-21.02	0.78	-3.84	1.2	-18.06	1.6
Iris pseudacorus	NA	NA	NA	NA	NA	NA	NA	NA	NA	NA	0.09	0.27	RFS	-20.38	0.5	-1.86	0.22	-14.44	1.12
Juncus conglomeratus	AFS	NA	NA	NA	NA	NA	NA	NA	NA	NA	0.33	0.15	AFS	-21.01	0.17	-2.94	0.23	-18.06	0.31

Species	*AFS-RFS*	Freq AF*a*	Freq RF*a*	AFS-RFS*a*	*αa*	*α* unc*a*	*σa*	*σ* unca	*βa*	*β* unc*a*	Freq AF*b*	Freq RF*b*	AFS-RFS*b*	*αb*	*α* unc*b*	*σb*	*σ* unc*b*	*βb*	*β* unc*b*
Juncus effusus	NA	0.21	0.14	AFS	-21.04	0.17	-2.31	0.2	-13.02	0.43	NA	NA	NA	NA	NA	NA	NA	NA	NA
Juniperus communis	NA	0.2	0.11	AFS	-21.08	0.18	-2.41	0.22	-12.74	0.39	NA	NA	NA	NA	NA	NA	NA	NA	NA
Lamium galeobdolon	AFS	NA	NA	NA	NA	NA	NA	NA	NA	NA	0.06	0.27	RFS	-19.43	0.44	-1.75	0.33	-10.31	0.64
Lotus pedunculatus	NA	NA	NA	NA	NA	NA	NA	NA	NA	NA	0.29	0.12	AFS	-20.5	0.35	-3.05	0.25	-10.88	0.69
Lycopus europaeus	NA	NA	NA	NA	NA	NA	NA	NA	NA	NA	0.18	0.11	AFS	-20.49	0.31	-2.94	0.18	-10.94	0.51
Melampyrum pratense	AFS	0.11	0.07	AFS	-20.8	0.17	-1.99	0.19	-12.43	0.21	NA	NA	NA	NA	NA	NA	NA	NA	NA
Melica uniflora	AFS	NA	NA	NA	NA	NA	NA	NA	NA	NA	0.3	0.37	NA	-20.41	0.22	-1.91	0.37	-14.4	0.64
Mercurialis perennis	AFS	0.06	0.14	RFS	-20.77	0.06	-1.82	0.07	-13.29	0.13	NA	NA	NA	NA	NA	NA	NA	NA	NA
Mespilus germanica	AFS	NA	NA	NA	NA	NA	NA	NA	NA	NA	0.25	0.18	AFS	-20.61	0.42	-2.17	0.23	-23.28	0.78
Moehringia trinervia	NA	0.3	0.07	AFS	-21.69	0.52	-3.46	0.77	-12.76	1.32	NA	NA	NA	NA	NA	NA	NA	NA	NA
Mycelis muralis	NA	0.32	0.07	AFS	-21.76	0.52	-3.51	0.77	-13.32	1.51	NA	NA	NA	NA	NA	NA	NA	NA	NA
Narcissus pseudonarcissus	AFS	0.25	0.08	AFS	-21.26	0.54	-2.86	0.57	-12.07	1.42	NA	NA	NA	NA	NA	NA	NA	NA	NA
Pinus sylvestris	RFS	0.33	0.36	NA	-20.86	0.2	-1.96	0.32	-13.62	0.47	NA	NA	NA	NA	NA	NA	NA	NA	NA
Plantago lanceolata	NA	0.08	0.05	NA	-20.94	0.11	-2.49	0.1	-11.53	0.26	NA	NA	NA	NA	NA	NA	NA	NA	NA
Platanthera chlorantha	AFS	0.16	0.06	AFS	-21.17	0.18	-2.59	0.21	-12.56	0.31	NA	NA	NA	NA	NA	NA	NA	NA	NA
Poa nemoralis	AFS	0.37	0.1	AFS	-21.74	0.24	-3.54	0.29	-13.41	0.49	0.25	0.28	NA	-20.5	0.15	-2.07	0.2	-14.29	0.27
Polygonatum multiflorum	AFS	0.5	0.22	AFS	-21.68	0.37	-3.53	0.56	-15.91	0.37	NA	NA	NA	NA	NA	NA	NA	NA	NA
Polypodium interjectum	NA	0.14	0.12	NA	-20.82	0.1	-1.92	0.11	-13.26	0.22	NA	NA	NA	NA	NA	NA	NA	NA	NA
Polypodium vulgare	NA	0.18	0.07	AFS	-21.16	0.19	-2.57	0.23	-12.64	0.38	0.1	0.12	NA	-20.3	0.12	-1.77	0.13	-13.43	0.27
Populus tremula	AFS	0.35	0.09	AFS	-21.75	0.34	-3.47	0.34	-14.86	0.89	0.49	0.55	NA	-19.38	0.32	-0.79	0.44	-33.17	1.14
Potentilla sterilis	AFS	NA	NA	NA	NA	NA	NA	NA	NA	NA	0.2	0.18	NA	-20.24	0.29	-2.45	0.26	-11.03	0.54
Primula veris	NA	0.29	0.12	AFS	-21.45	0.21	-2.93	0.34	-15.26	0.47	NA	NA	NA	NA	NA	NA	NA	NA	NA
Prunella vulgaris	NA	0.28	0.09	AFS	-21.56	0.39	-3.11	0.63	-15.54	0.76	NA	NA	NA	NA	NA	NA	NA	NA	NA
Prunus mahaleb	NA	0.16	0.21	NA	-20.84	0.27	-1.95	0.28	-13.21	0.46	NA	NA	NA	NA	NA	NA	NA	NA	NA
Pteridium aquilinum	AFS	0.31	0.1	AFS	-21.6	0.45	-3.28	0.42	-13.14	1.19	NA	NA	NA	NA	NA	NA	NA	NA	NA
Ranunculus ficaria	NA	0.08	0.12	RFS	-20.66	0.07	-1.66	0.08	-13.05	0.14	NA	NA	NA	NA	NA	NA	NA	NA	NA
Ribes rubrum	RFS	0.25	0.34	RFS	-20.87	0.12	-1.95	0.2	-13.98	0.28	NA	NA	NA	NA	NA	NA	NA	NA	NA
Robinia pseudacacia	NA	NA	NA	NA	NA	NA	NA	NA	NA	NA	0.14	0.05	AFS	-20.56	0.71	-2.43	0.91	-12.13	1.01
Rosa arvensis	NA	0.41	0.29	AFS	-21.25	0.12	-2.71	0.19	-13.36	0.27	NA	NA	NA	NA	NA	NA	NA	NA	NA

Species	*AFS-RFS*	Freq AF*a*	Freq RF*a*	AFS-RFS*a*	*αa*	*α* unc*a*	*σa*	*σ* unc*a*	*βa*	*β* unc*a*	Freq AF*b*	Freq RF*b*	AFS-RFS*b*	*αb*	*α* unc*b*	*σb*	*σ* unc*b*	*βb*	*β* unc*b*
Rubus caesius	RFS	0.12	0.27	RFS	-20.77	0.17	-1.78	0.26	-13.92	0.85	NA	NA	NA	NA	NA	NA	NA	NA	NA
Rumex acetosa	NA	0.13	0.07	AFS	-21.2	0.12	-2.63	0.15	-12.64	0.23	NA	NA	NA	NA	NA	NA	NA	NA	NA
Rumex acetosella	NA	0.14	0.07	AFS	-20.93	0.17	-2.25	0.2	-12.2	0.25	NA	NA	NA	NA	NA	NA	NA	NA	NA
Salix caprea	RFS	NA	NA	NA	NA	NA	NA	NA	NA	NA	0.21	0.19	NA	-20.55	0.47	-2.47	0.25	-12.03	0.89
Sanguisorba minor	NA	0.1	0.08	NA	-20.87	0.1	-2.22	0.11	-11.99	0.17	NA	NA	NA	NA	NA	NA	NA	NA	NA
Scrophularia nodosa	AFS	0.06	0.12	RFS	-20.76	0.06	-1.8	0.07	-13.31	0.12	0.23	0.12	AFS	-20.3	0.23	-2.72	0.28	-10.82	0.42
Solanum dulcamara	NA	0.19	0.32	RFS	-20.95	0.1	-2.09	0.16	-13.97	0.21	0.1	0.38	RFS	-20.22	0.36	-1.6	0.2	-14.32	0.77
Solidago virgaurea	AFS	0.14	0.07	AFS	-20.93	0.17	-2.26	0.2	-12.2	0.25	NA	NA	NA	NA	NA	NA	NA	NA	NA
Sorbus torminalis	AFS	0.26	0.19	AFS	-20.79	0.44	-2.29	0.19	-11.46	0.79	0.45	0.29	AFS	-20.91	0.24	-2.87	0.28	-14.23	0.65
Stachys officinalis	NA	NA	NA	NA	NA	NA	NA	NA	NA	NA	0.27	0.15	AFS	-20.82	0.16	-2.59	0.2	-17.24	0.53
Stachys sylvatica	AFS	0.26	0.27	NA	-20.89	0.1	-1.98	0.15	-14.2	0.18	NA	NA	NA	NA	NA	NA	NA	NA	NA
Stellaria holostea	AFS	0.31	0.08	AFS	-21.7	0.34	-3.35	0.52	-15.74	0.61	0.21	0.27	NA	-20.38	0.47	-1.86	0.23	-14.34	0.94
Tamus communis	NA	0.31	0.38	RFS	-20.83	0.32	-1.9	0.53	-13.67	0.75	0.15	0.42	RFS	-20.24	0.25	-1.64	0.42	-13.94	0.63
Teucrium chamaedrys	NA	0.18	0.07	AFS	-21.18	0.21	-2.6	0.23	-12.57	0.4	NA	NA	NA	NA	NA	NA	NA	NA	NA
Teucrium scorodonia	NA	0.37	0.11	AFS	-21.35	0.24	-3.46	0.23	-11.24	0.44	NA	NA	NA	NA	NA	NA	NA	NA	NA
Tilia cordata	AFS	0.37	0.15	AFS	-21.6	0.54	-3.23	0.18	-16.11	1.05	NA	NA	NA	NA	NA	NA	NA	NA	NA
Ulex europaeus	NA	NA	NA	NA	NA	NA	NA	NA	NA	NA	0.15	0.16	NA	-20.31	0.4	-1.77	0.5	-13.61	0.8
Urtica dioica	RFS	0.32	0.34	NA	-20.97	0.13	-2.16	0.21	-13.6	0.3	0.17	0.44	RFS	-20.32	0.51	-1.76	0.86	-14.39	1.26
Veronica chamaedrys	NA	NA	NA	NA	NA	NA	NA	NA	NA	NA	0.22	0.43	RFS	-19.68	0.53	-1.99	0.45	-10.5	0.53
Veronica officinalis	AFS	NA	NA	NA	NA	NA	NA	NA	NA	NA	0.28	0.15	AFS	-20.87	0.18	-2.69	0.2	-16	0.46
Viburnum opulus	AFS	0.14	0.1	NA	-20.82	0.11	-1.93	0.13	-13.01	0.22	NA	NA	NA	NA	NA	NA	NA	NA	NA
Viola hirta	NA	0.25	0.07	AFS	-21.48	0.23	-3.1	0.2	-12.69	0.65	NA	NA	NA	NA	NA	NA	NA	NA	NA
Viola odorata	NA	0.14	0.23	RFS	-21.16	0.25	-2.42	0.18	-15.49	0.66	NA	NA	NA	NA	NA	NA	NA	NA	NA
Viola reichenbachiana	AFS	0.1	0.09	NA	-20.89	0.08	-2.22	0.1	-12.09	0.16	NA	NA	NA	NA	NA	NA	NA	NA	NA
Viola riviniana	AFS	0.23	0.1	AFS	-21.26	0.36	-2.75	0.45	-12.58	0.7	NA	NA	NA	NA	NA	NA	NA	NA	NA

Chapitre III : Effet du turnover des habitats sur le processus de relaxation des métapopulations

Manuscrit correspondant :

Lalechère E., Jabot F., Archaux F., Deffuant D. (in review). Effects of habitat turnover on time-delayed metapopulation dynamics. *Theoretical Ecology.*

Effects of habitat turnover on time-delayed metapopulation dynamics.

Étienne Lalechère [a1] , Franck Jabot [a] , Frédéric Archaux [b] , Guillaume Deffuant [a]

[a] UR LISC, Irstea, 9 avenue Blaise Pascal, F-63178 Aubière, France

[b] UR EFNO, Irstea, Domaine des Barres, F-45290 Nogent-sur-Vernisson, France

Corresponding author:

[1] E-mail address: lalechereetienne@gmail.com

Current address: UR LISC, Irstea, 9 avenue Blaise Pascal, F-63178 Aubière, France

Abstract

Habitat turnover concomitantly causes destruction and creation of habitat patches. Following such a perturbation, metapopulations harbor either an extinction debt or an immigration credit, that is the future future decrease or increase in population numbers due to this disturbance. Time-delayed metapopulation dynamics are likely to depend both on the spatial configuration of the habitat turnover and on species dispersal ability. The effect of these characteristics on the magnitude of the extinction debt or immigration credit and on the relaxation time (time to new equilibrium) is poorly known. In this contribution, we provide a theoretical investigation on metapopulation dynamics following habitat turnover, based on simulations in virtual landscapes. We consider two virtual species (a short-distance and a long-distance disperser) and four scenarios of habitat turnover. Two scenarios simulate either a net habitat loss or a net habitat gain. The other two scenarios simulate a fragmentation or an aggregation of the habitat patches, with no net loss or gain of total habitat area. Our analyses reveal that (i) the main determinant of time-delayed metapopulation dynamics is the net change in total habitat area; (ii) when there is no net loss or gain of habitat area, metapopulation dynamics is positively affected by the species dispersal distance and the habitat aggregation post turnover; (iv) relaxation time weakly depends on the magnitude of the immigration credit or the extinction debt, (v) the initial metapopulation spatial structure also influences the magnitude of the extinction debt and the immigration credit. These results shed light on the interplay between species dispersal ability and habitat turnover spatial structure in metapopulation dynamics.

Keywords: Forcing events - Spatially correlated disturbances - Time-lags - Time-delayed metapopulation dynamics - Landscape dynamics

1. Introduction

Habitat loss is among the main drivers of biodiversity loss (Sala et al. 2000). It can trigger immediate species loss, but also time-delayed losses that are commonly coined by the term “extinction debt” (Tilman et al. 1994). Such historical legacies have received theoretical explanations (Tilman et al. 1994, Hanski and Ovaskainen 2002) and have been documented for many taxa and in many biomes (Kuussaari et al. 2009).

Most research on time-delayed biodiversity dynamics focus on habitat loss and extinction debt, while habitat gain and more generally habitat turnover are non-negligible parts of habitat dynamics globally (Sala et al. 2000). Habitat gain can be due for instance to natural recovery and to habitat creation or restoration for conservation purposes (Bedward et al. 2009, Baeten et al. 2010, Ruete et al. 2017). It can trigger a gain in species richness that is likely to increase over time due to an “immigration credit” (Nagelkerke et al. 2002, Jackson and Sax 2010). More generally, habitat turnover concomitantly causes destruction and creation of habitat patches (*e.g.* Bergès et al. 2015). The effects on biodiversity of these two processes of patch destruction and creation are likely to interact (Piqueray et al. 2011, Bagaria et al. 2015, Naaf and Kolk 2015). However, quantitative theoretical expectations on the effects of habitat turnover on biodiversity are still in their infancy (Jackson and Sax 2010).

In particular, the effect of habitat turnover on biodiversity dynamics is likely to be influenced by both the spatial structure of habitat turnover and species dispersal ability. Indeed, previous research on the effect of habitat loss on biodiversity shows an effect of the spatial aggregation of perturbations on species extinction. In particular, when disturbed areas are spatially aggregated, the effects on biodiversity have been shown to depend on species dispersal ability, with local dispersers being more prone to extinction than global dispersers (Liao et al. 2015, Liao et al. 2016). Besides, the interaction between the spatial structure of perturbations and species distribution has been shown to matter (Keil et al. 2015, Kitzes and Harte 2015). For example, Kitzes and Harte (2015) evidenced that after habitat loss, extinction debt decreases as the spatial aggregation of individuals increases due to the persistence of large populations. Fewer results are available in cases of habitat turnover. Notably, the theoretical study of Hiebeler et al. (2016) shows that large-scale habitat turnover has a stronger negative effect on survival of local dispersers than on of global dispersers.

Beyond the limited research focus on the effect of habitat turnover on biodiversity, a second limitation of most studies is that they rarely disentangle the magnitude of the extinction debt or immigration credit and the time needed to reach a novel equilibrium

following perturbations (relaxation time; Diamond 1972, Hylander and Ehrlén 2013). A stronger focus on relaxation time is particularly important in a context of habitat turnover. Indeed, habitat turnover is likely to constantly perturb biodiversity dynamics from its way towards equilibrium, so that an important component of biodiversity dynamics is the rate at which extinction debt and immigration credit are used.

We here study the time-delayed responses of metapopulations to habitat turnover with a special focus on the effect of (i) the spatial configuration of the habitat turnover and (ii) the mean dispersal distance on both the relaxation time and the magnitude of extinction debt and immigration credit. In doing so, we follow Hylander and Ehrlén (2013) in defining extinction debt and immigration credit at the species scale with reference to the number of living populations of the metapopulation. This approach is practical to accurately disentangle the interplay of dispersal ability and habitat spatial structure on biodiversity responses. We specifically address how the metapopulation response is influenced by (i) net change in total habitat area and (ii) the change in spatial aggregation of patches following habitat turnover. Then we investigate (iii) how relaxation time is influenced by these habitat characteristics and, finally, (iv) whether previous findings are similar for the two dispersal scenarios.

2. Materials and methods

We used projections of metapopulation dynamics in virtual binary landscapes constituted of habitat patches and of an unviable surrounding matrix. We focused on the metapopulation dynamics following a sudden instantaneous modification of the landscape. We considered four scenarios of habitat turnover (Fig. 1): (i) a scenario of habitat gain (HG), (ii) one of habitat loss (HL), and two scenarios of habitat turnover with no net habitat loss or gain and with either (iii) habitat aggregation (AG) or (iv) habitat fragmentation (FR). Additional details about the effect of habitat turnover *per se* is illustrated from an intermediate scenario, with no net habitat loss nor gain and and an intermediate fragmentation degree, in Appendix S1. We below describe in turn the procedure of landscape generation (section 2.1), the metapopulation model (section 2.2) and the statistical analyses performed on predictions (section 2.3).

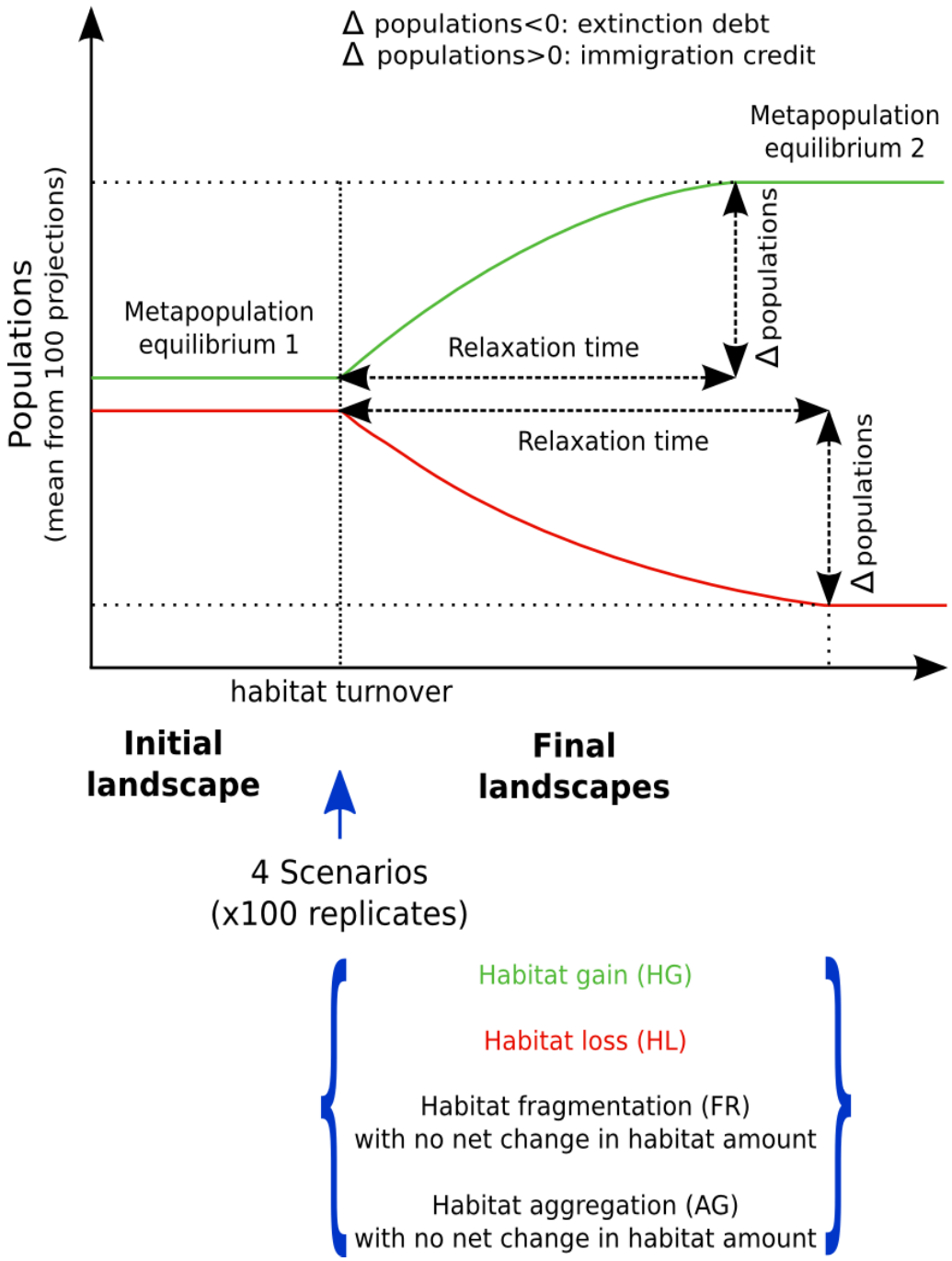

Figure 1: Schematic representation of projected metapopulation dynamics. Four scenarios of habitat turnover are considered. For each one, the time-delayed dynamics of a short-distance disperser and a long-distance disperser are considered. The initial landscape is the same for each final landscapes that vary according to habitat turnover scenario. A positive or a negative change in population number, just after perturbation until the metapopulation is at equilibrium 2, are respectively an immigration credit and an extinction debt. As a consequence, the extinction debt and the immigration credit excludes immediate events of extinction and colonization that occur respectively with the complete destruction and the fragmentation of occupied patches.

2.1 Landscape dynamics

Generation of landscape grids are performed in the language Python using the pakage 'nlmpy' (Etherington et al. 2015), in which continuous grid values can be generated and range from 0 to 1 according to an autocorrelation parameter a_i. We first simulate a set of 100 initial landscapes on a square grid of 100 × 100 cells (with a_i set to 0 corresponding to a spatially random assignment of grid values). For each of these 100 replicates, we simulate four "perturbation" landscapes of the same size (100 × 100 cells) with various autocorrelation levels a_p ($0<a_p<1$) that correspond to the four scenarios of habitat turnover (Fig. 1). Grid values of the "perturbation" landscapes are rescaled between -1 and 1. These perturbation landscapes are then summed to the initial landscape to obtain the landscapes after habitat turnover. This procedure leads to 100 sets of paired landscapes (before and after perturbation) for each of the four scenarios of habitat turnover. These continuous landscapes are subsequently transformed into binary values (0/1), differentiating habitat patches created (a patch can be a single isolated pixel or a set of contiguous pixels) from the surrounding matrix, using two thresholds t_i and t_f for the initial and final landscapes. Ranges of simulated parameters a_i, a_p, t_i and t_f for the different scenarios are provided in Table S2, and a more detailed description of the landscape simulation procedure is provided in Appendix S2.

The arbitrary choice of landscape parameter values are performed with two goals in mind. First, we target an amount of occupied habitat around 20% of habitat patches in the landscape prior to perturbation. This target is chosen so that the habitat already experienced a sizeable level of fragmentation. Second, we target a random spatial autocorrelation of habitat patches (a_i~0) of the initial landscape to test the effect of perturbations that fragment (a_i~-1) or aggregate (a_i~1) habitat patches. The parameters used to simulate perturbations are much variable than the values reported in this section in order to investigate a wide range of situations across replicates and scenarios (Table S2).

2.2 Metapopulation model

Metapopulation dynamics follows the patch occupancy model of Hanski (1994) that simulates events of local extinction and colonization in the network of habitat patches. The occupancy dynamics of the network of habitat patches is modelled as a discrete time process, with events of local extinction and colonization, and events of patch destruction and creation. At each time step t, each patch i is either occupied by a population of the focal species ($OCC_i(t)=1$) or not ($OCC_i(t)=0$). If a patch is unoccupied, it is colonized between step t and step $t+1$ by the focal species with

probability $C_i(t)$. If it is occupied, the local population of the focal species can go extinct between step t and $t+1$ with probability $E_i(t)$.

The extinction probability $E_i(t)$ is:

$$E_i(t) = min\left(\frac{\sigma}{(A_i/A_{min})^{\theta}}, 1\right) \quad (1)$$

where σ is the extinction rate parameter, A_{min} is the minimum patch area and θ regulates the decay of this rate with the area A_i of patch i.

The colonization probability $C_i(t)$ is given by:

$$C_i(t) = \frac{CON_i(t)^2}{CON_i(t)^2 + 1} \quad (2)$$

where $CON_i(t)$ measures the level of connectivity between patch i and the other patches that are occupied at time t. It is calculated as:

$$CON_i(t) = \alpha \cdot \sum_{j \neq i} \left(A_j \times OCC_j(t) \times \exp^{-\beta d_{ij}}\right) \quad (3)$$

where d_{ij} is the Euclidean distance between patches i and j from edge to edge (whatever the area between the patches i and j consists of matrix or habitat), α is a colonization parameter and β is a parameter assuming a decay of colonization with distance.

The dynamics of $OCC_i(t)$ is stochastic. At each time step t and for each patch i, a random variable $u_i(t)$ is drawn between 0 and 1 from a uniform distribution and the next state of the patch i $OCC_i(t+1)$ is given by:

$$OCC_i(t+1) = 1 - OCC_i(t) \ \ if \ \ u_i(t) < OCC_i(t) \times E_i(t) + \left(1 - OCC_i(t)\right) \times C_i(t) \quad (4)$$

and

$$OCC_i(t+1) = OCC_i(t) \quad (5)$$

otherwise.

Finally the landscape is dynamical itself, with events of patch destruction and creation. When a patch *i* is newly created at time step *t*, it is considered to be unoccupied ($OCC_i(t)=0$), until a first colonization event takes place. In the case of an increase in patch area the additional area is a new empty (recent) patch. Therefore in the final landscapes, some patches are contiguous (but not in the initial landscapes).

To ensure that the metapopulation is at dynamical equilibrium just before habitat turnover takes place, we run the metapopulation dynamics on the initial landscapes during 500 time steps, starting from a "full" occupancy of all habitat patches (Etienne et al. 2004). This number of steps proved to be sufficient to reach the metapopulation equilibrium as it led to a constant mean trajectory of the number of populations. Metapopulation dynamics then goes on for 1000 additional time steps after habitat turnover (Fig. 1).

We study the dynamics of two contrasted virtual species: a short-distance disperser (hereafter called *SD*) and a long-distance disperser (hereafter called *LD*). The metapopulation model parameter β is fixed at $3x10^{-4}$ and $1x10^{-4}$ for the SD and the LD species respectively, so that the mean dispersal distance (hereafter called "dispersal distance" for simplicity) of SD equals 19% of map width and 58% for LD. Other model parameters are fixed: $\alpha=exp(-18)$, $\sigma=exp(-0.1)$ and $\theta=0.7$. These parameter combinations ensure that (i) the metapopulation occupies close to 20% of the habitat patches of the initial landscapes and (ii) extinction rates are lower than 0.001 for "source" patches of more than 50 cells.

We run 100 projections of metapopulation dynamics for the two species types (SD and LD) for each one of the 100 simulated pairs of landscapes (before and after perturbation).

2.3 Statistical analyses

To compare the different final landscapes across scenarios of habitat turnover, we calculate for each simulation (100 simulations x 4 scenarios) the mean patch connectivity (with $\alpha=1$, $\beta=2x10^{-4}$ and $OCC_i(t)=1$ in eq. 3), the mean between-patch distance as a proxy for patch aggregation at the landscape level, the number of patches, the number of source patches, the distance to nearest neighboring patch, the total area of patches and the total area gain and loss (relatively to the total area of the initial landscapes). These variables are standardized to perform a principal component analysis

(PCA) and to discriminate the different scenarios using the R package ade4 1.7-5 (Thioulouse et al. 1997).

We compute relaxation time t_r based on the mean temporal trajectory of the number of populations. This mean trajectory is computed based on the 100 replicates of projected metapopulation dynamics for each species x scenarios x landscape replicates. More precisely, we fit a linear model from moving windows of 10 values and calculate the regression slope. We then consider that the relaxation time t_r is reached when the absolute value of the slope is less than 0.01.

We then calculate the difference in the number of inhabited patches (hereafter called *Δpopulations*) between time t_r and time *1* (just after perturbation). The term extinction debt refers to cases for which *Δpopulations* is negative and the term immigration credit for those for which *Δpopulations* is positive. The extinction debt and the immigration credit are computed in a way that excludes immediate events of extinction and colonization that are directly caused by habitat turnover (between time 0 and 1). We henceforth only consider events that are time-delayed *i.e.* for patches that are present after habitat turnover. In doing so, we consider that the complete destruction of a patch does not contribute to the extinction debt as the patch is not present anymore after habitat turnover. We similarly consider that the fragmentation of a source population into several populations does not contribute to the immigration credit, because the initial number of populations is computed after this event of habitat fragmentation.

Finally, we compute a number of covariates, immediately after habitat turnover and at equilibrium, to understand the influence of initial conditions and the consequences of landscape dynamics: the mean populations connectivity (eq. 3), the mean area of occupied patches and the mean between-population distance.

3. Results

The four scenarios of habitat turnover are clearly discriminated by the principal component analysis (PCA). The first two axes of the PCA explain 76.4% of the variance (Fig. 2). The first axis explains 51.8% of the variance and discriminates the habitat gain (HG) and the habitat loss (HL) scenarios. It is mainly associated with variation in mean distance to the nearest neighboring patch, number of patches, mean patch connectivity and total area of patches (Table 1, Fig. 2). The second axis is associated with variation in mean between-patch distance and number of source patches. It discriminates the habitat aggregation (AG) or habitat fragmentation (FR) scenarios.

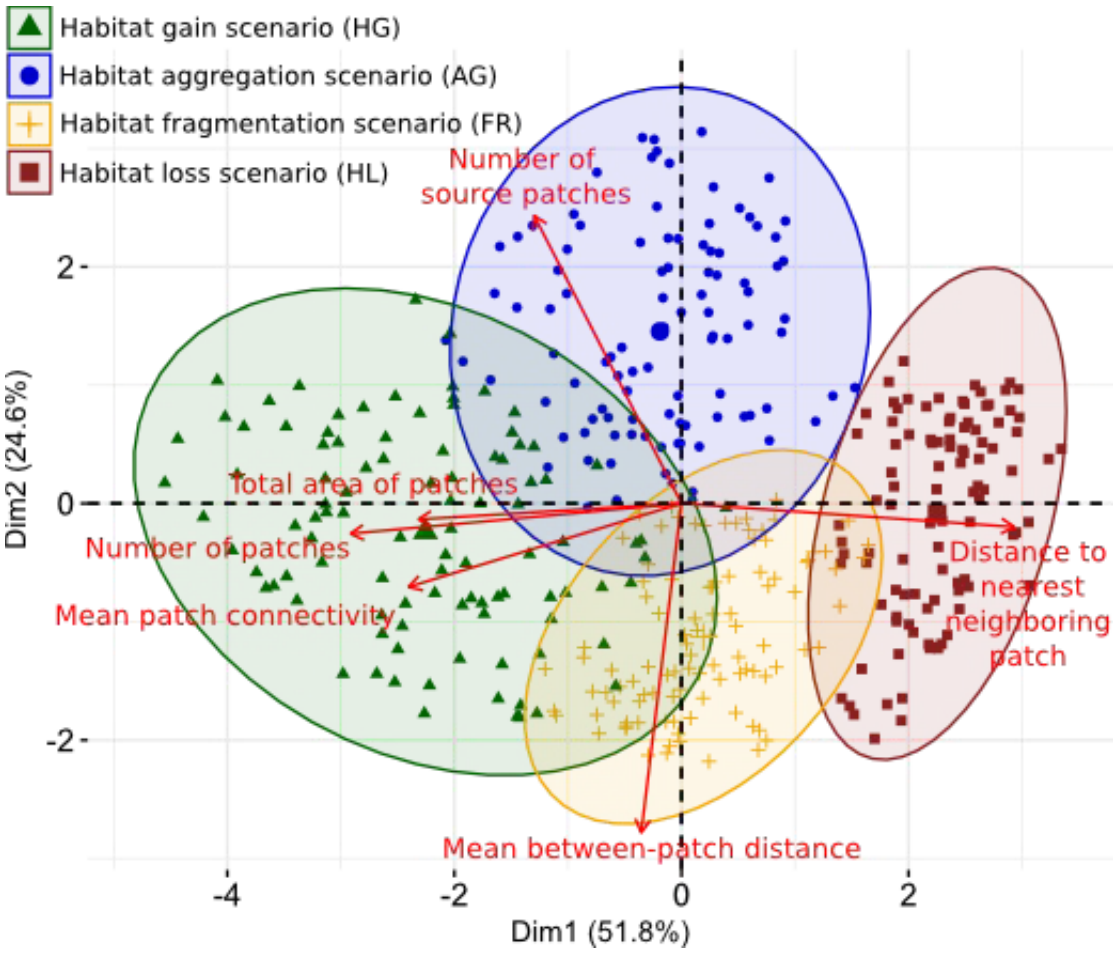

Figure 2: Principal component analysis (PCA) of the structural characteristics of final landscapes.

Table 1: Mean structural characteristics of final landscapes in the four scenarios of habitat turnover. Distances are expressed in cells.

	HL: habitat loss	HG: habitat gain	FR: increased fragmentation	AG : increased aggregation
Mean patch connectivity	117.3 (min=83.1; max=173.3)	180.4 (min=124.7; max=240.8)	133.1 (min=93.43 ; max=178.5)	148.6 (min=107.7 ; max=191.8)
Total area of patches (%)	18 (min=13 ; max=24)	26 (min=20 ; max=34)	21 (min=16 ; max=26)	21 (min=16 ; max=26)
Total area gain (%)	3.9 (min=1.5 ; max=7.0)	29.0 (min=12.0 ; max=47.5)	13.8 (min=6.0 ; max=20.5)	18.0 (min=10.0 ; max=30.2)
Total area loss (%)	19.4 (min=8.9 ; max=28.8)	2.9 (min=0.8 ; max=5.4)	14.7 (min=6.4 ; max=22.3)	17.8 (min=10.2 ; max=29.2)
Mean between-patch distance	46.9 (min=44.9 ; max=49.8)	47.6 (min=46.2; max=49.2)	48.8 (min=47.7 ; max=50.0)	43.9 (min=41.2 ; max=45.9)
Distance to nearest neighboring patch	0.65 (min=0.56 ; max=0.75)	0.31 (min=0.23 ; max=0.39)	0.45 (min=0.35 ; max=0.61)	0.41 (min=0.30 ; max=0.57)
Number of patches	416 (min=330 ; max=528)	761 (min=552 ; max=911)	624 (min=456 ; max=820)	585 (min=462 ; max=693)
Number of source patches	41 (min=30 ; max=51)	49 (min=30 ; max=72)	38 (min=30 ; max=50)	50 (min=39 ; max=67)

3.1 Final effects of habitat turnover on metapopulations

Regardless of species dispersal distance, we observe an extinction debt when the total patch area decreases (HL, Fig. 3A, Fig. 4) and an immigration credit when it increases (HG, Fig. 3A, Fig. 4). In these scenarios, extinction debt and immigration credit are respectively associated to a decrease and an increase in the total area of occupied patches (Fig. 3C). The short-distance disperser (SD) species consistently has lower final number of populations than the long-distance disperser (LD) species in these two scenarios of habitat turnover (Fig. 3A, Fig. 4). Scenarios of habitat aggregation or fragmentation lead to intermediate responses in magnitude, with the short-distance disperser (SD) species suffering mainly from an extinction debt in the fragmentation scenario (Fig. 3A, Fig. 4A). In the habitat aggregation scenario, the SD species also mainly present an extinction debt (Fig. 3A, Fig. 4A) that is nevertheless associated to an increase in the total area of occupied patches (Fig. 3C), *i.e.* fewer populations in larger patches. In both scenarios, the long-distance disperser (LD) species mainly present an

immigration credit (Fig. 3A, Fig. 4B). The scenario of habitat fragmentation (FR) leads to lower final population numbers than under the scenario of habitat aggregation (AG; Fig. 3A, Fig. 4). Note that the results reported here are not mainly driven by variations in patch number or total area between scenarios, since we obtain qualitatively similar results when documenting changes in the proportion of patches that are occupied instead of the total number of occupied patches (Fig. 3B) and when documenting changes in the proportion of area that is occupied instead of the total area occupied (Fig. 3D). Instead, our results are mostly due to variations among scenarios in the spatial configuration of habitats (Fig. 2). Additional details about the effect of habitat turnover, with no net habitat loss nor gain and no habitat fragmentation nor aggregation, are given in Appendix S1. In this scenario, the SD species mainly present an extinction debt and the LD species mainly present an immigration credit.

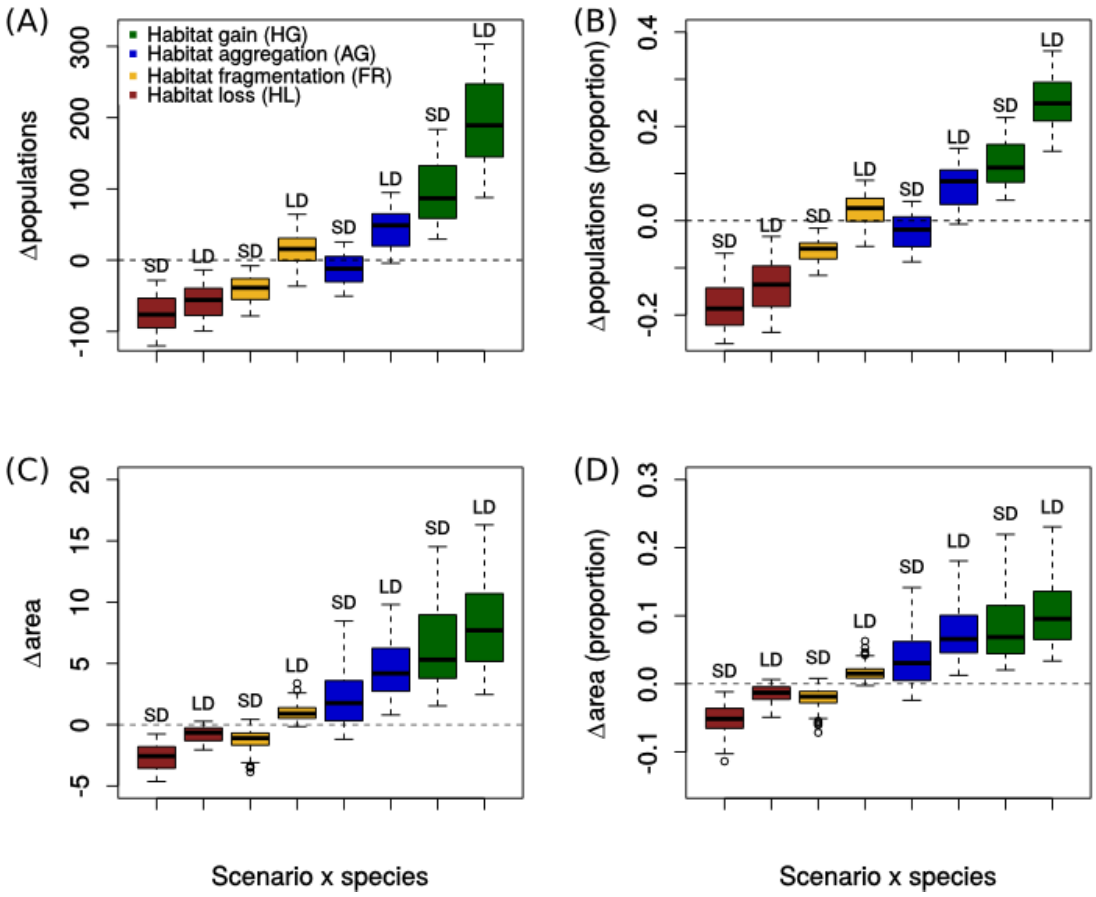

Figure 3: Difference between several metapopulation characteristics at the relaxation time (t_r) and those just after perturbation (*t=1)* in the four landscape scenarios and for the two species types. *(A)*: extinction debt (negative change in population number) and immigration credit (positive change in population number); *(B)*: extinction debt and immigration credit in proportion of the total number of patches; (C): change in the total area of occupied patches and (D) change in the total area of occupied patches in proportion of the total area. *SD*: short-distance disperser; *LD*: long-distance disperser. The graphs use the box-and-whisker representation where boxes encompass values between the 25th and 75th percentiles, horizontal lines represent median values, and 'whiskers' give the 95% range of the values. A box is composed of 100 values from landscape replicates. One value is a mean computed from 100 replicates of projected metapopulation dynamics.

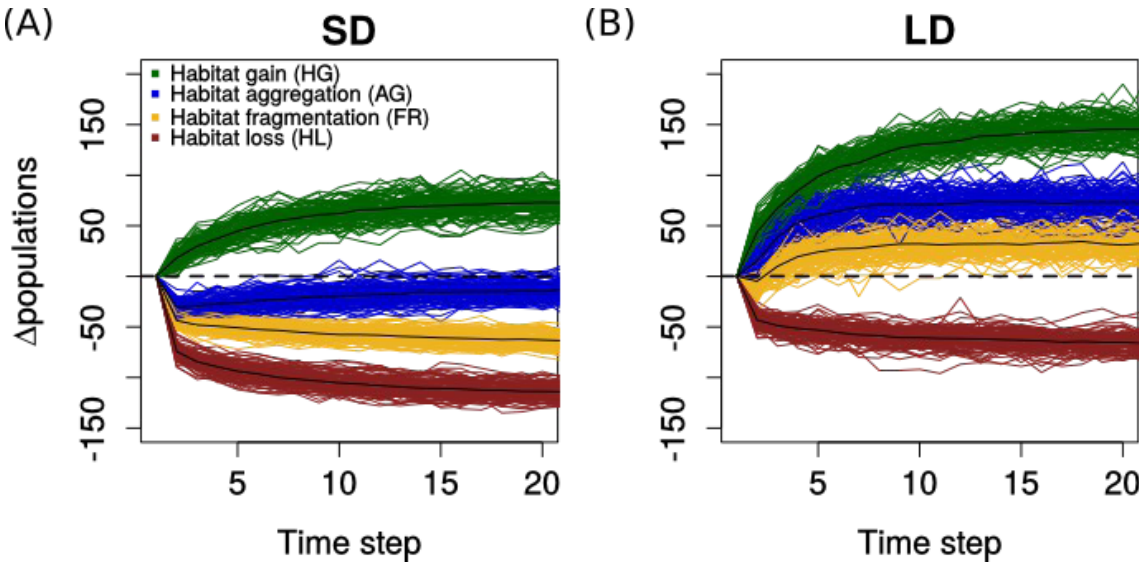

Figure 4: Example of stochastic metapopulation dynamics after habitat turnover for a short-distance disperser (A) and a long-distance disperser (B) in one set of final landscapes. Black lines are means computed from 100 projections of species dynamics. *SD*: short-distance disperser; *LD*: long-distance disperser.

3.2 Effects of species and habitat turnover characteristics on relaxation times

Computed relaxation times vary from 6 to 141 time steps (41.3 time steps on average). They are smaller for the long-distance (LD) than the short-distance disperser (SD) species in the HL and the HG scenarios (Fig. 5). Relaxation times are more variable among scenarios for the SD than for the LD species (the median relaxation time vary between 35.5 and 48.5 time steps for the SD species and between 27.5 and 35.0 time steps for the LD species, Fig. 5). Surprisingly, relaxation times are poorly correlated with the magnitude of the extinction debt or immigration credit both within and among scenarios of habitat turnover (Pearson correlation coefficient is 0.32 for the SD species and is 0.12 for the LD species, Fig. 6).

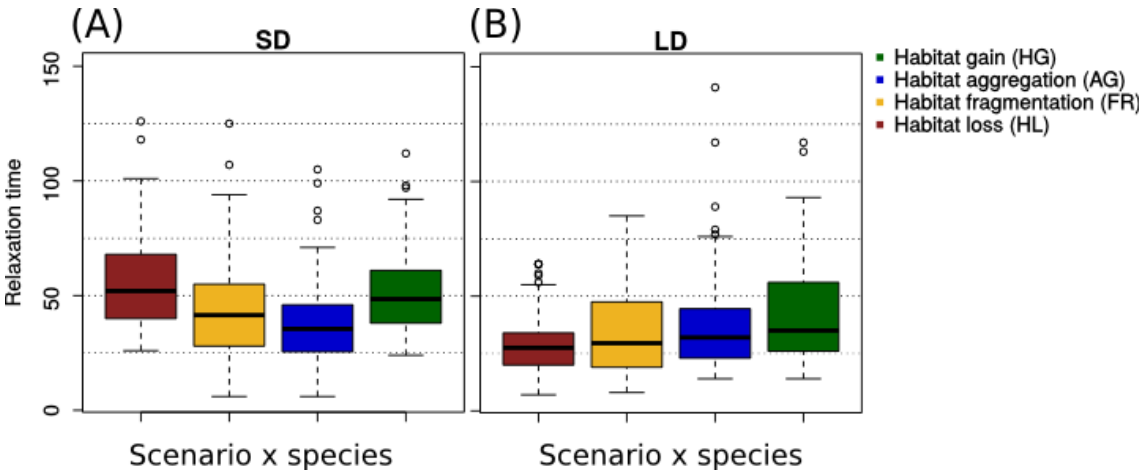

Figure 5: Relaxation time in the four landscape scenarios for a short-distance (A) and a long-distance (B) disperser. The graphs use the same box-and-whisker representation as in Fig.3.

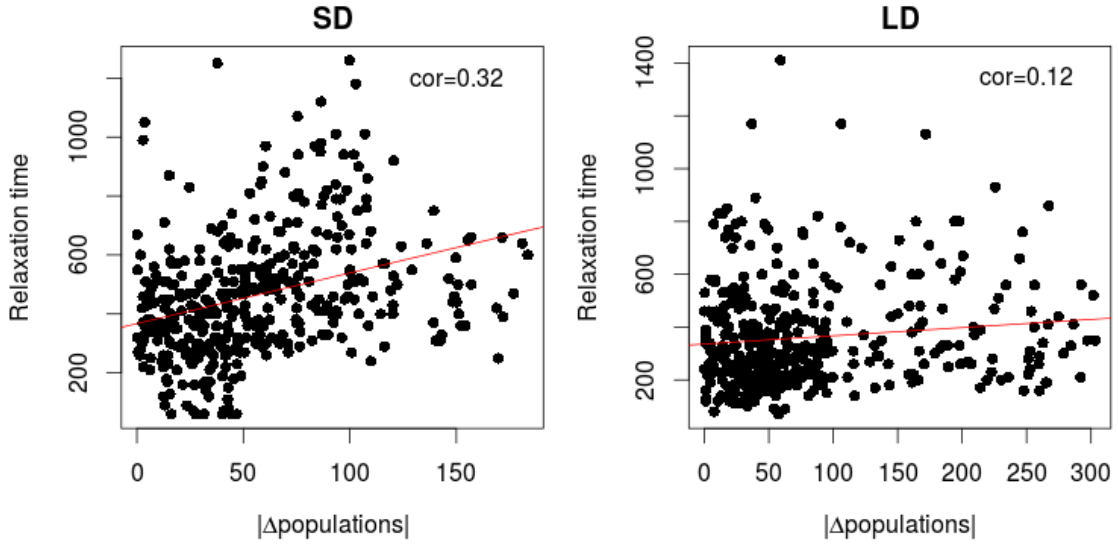

Figure 6: Relationship between the relaxation time and the magnitude of the extinction debt or the immigration credit (*Δpopulations*). *SD*: short distance disperser, *LD*: long-distance disperser. Linear regression lines are in red. Pearson correlation coefficients are reported.

3.3 Explaining the variability in metapopulation responses between and within scenarios

Between scenario variability explains 61.37% of the variability among landscape replicates and within scenario variability 38.6%. When comparing predictions among the various scenarios, the variation in population number (extinction debt or immigration credit) is globally explained by the mean distance to the nearest

neighboring patch after habitat turnover (Fig. 7A) that is strongly correlated with the number of patches (Pearson correlation coefficient=-0.91). This correlation is not systematically recovered within scenarios but explains among-scenarios variability (Fig. 7A). When comparing predictions within scenarios, the variation in population number is overall better explained by the mean populations connectivity immediately after habitat turnover (Table 2, Fig. 7B). The importance of the mean occupied area and of the mean between-population distance (at *t=1*) is more variable among scenarios and species (Table 2). For the species and the scenarios that lead to an extinction debt (Fig. 3A), the variation in population number is strongly positively related with the mean area of occupied patches (Pearson correlation coefficients range from 0.61 to 0.97, Table 2). For the species and the scenarios that lead to an immigration credit (Fig. 3A), the variation in population number is strongly positively related with the mean between-population distance (Pearson correlation coefficients range from 0.65 to 0.81, Table 2).

Table 2: Pearson correlation coefficient between the extinction debt or the immigration credit (*Δpopulations*) and mean metapopulation characteristics (expressed in cells) immediately after habitat turnover. Total area gain and loss are given relatively to the total area of the initial landscapes. *SD*: short-distance disperser; *LD*: long-distance disperser.

	Habitat loss (HL)	Habitat gain (HG)	Habitat fragmentation (FR)	Habitat aggregation (AG)
Mean populations connectivity	*SD*: 0.55 *LD*: 0.75	*SD*: 0.76 *LD*: 0.58	*SD*: 0.68 *LD*: 0.87	*SD*: 0.93 *LD*: 0.80
Mean area of occupied patches	*SD*: 0.95 *LD*: 0.91	*SD*: 0.07 *LD*: 0.03	*SD*: 0.97 *LD*: 0.62	*SD*: 0.61 *LD*: 0.43
Mean between-population distance	*SD*: -0.04 *LD*: 0.48	*SD*: 0.65 *LD*: 0.81	*SD*: 0.11 *LD*: 0.77	*SD*: 0.48 *LD*: 0.70

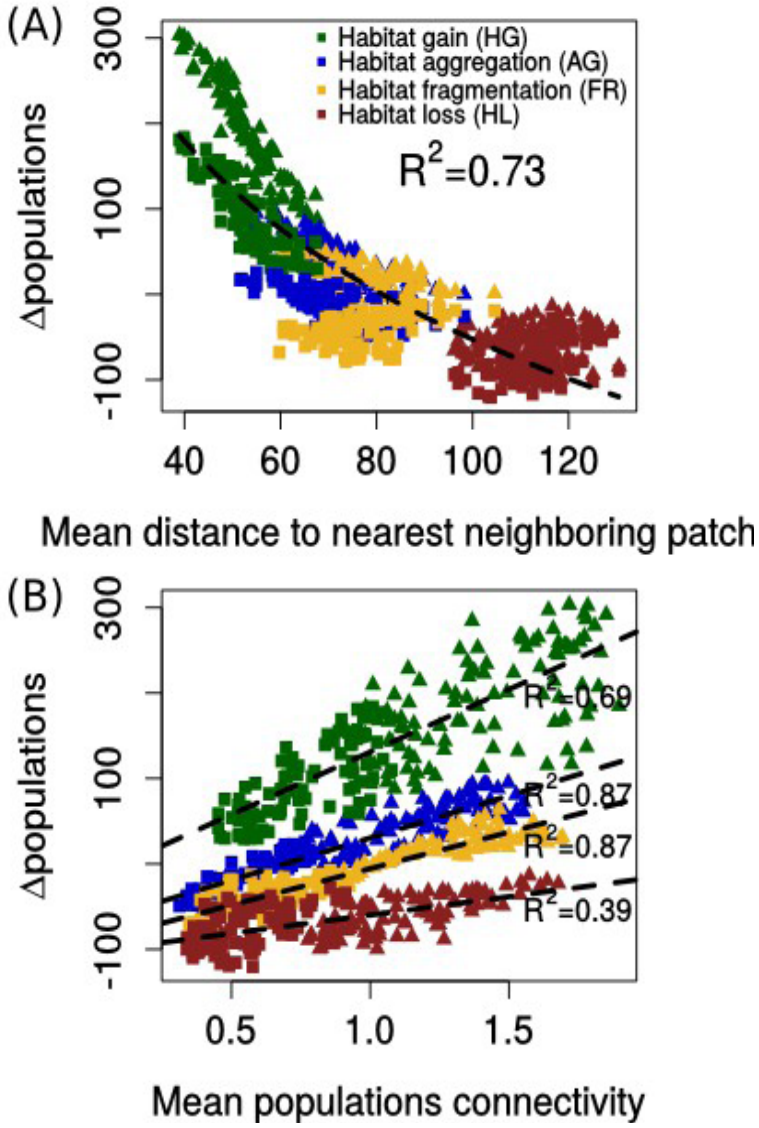

Figure 7: Explanatory factors of the extinction debt and immigration credit between (A) or within (B) habitat turnover scenarios. Squares represent the short-distance disperser and triangles represent the long-distance disperser. Dotted lines are log-linear regression line (A) and linear regression lines (B).

3.4 Spatial metapopulation structure in response to habitat turnover.

For the habitat loss scenario (HL), the mean area of occupied patches increases with habitat loss (Fig. 8AC), and the mean between-population distance decreases (Fig. 8AC) due to the loss of populations. This metapopulation confinement to large and aggregated patches is more pronounced in cases of large extinction debts (see the displacement of the surfaces and the shift of the orientation of the colour gradient between *t=1* and *t=1000* in Fig. 8AC).

For the habitat gain scenario (HG), the mean area of occupied patches decreases with habitat gain (Fig. 8BD) and the final populations are less distant than before habitat gain (Fig. 8BD) due to the gain in population number. This metapopulation expansion in small habitat patches is more pronounced in cases of large immigration credit (see the displacement of the surfaces and the orientation of the colour gradient between *t=1* and *t=1000* in Fig. 8BD).

For the habitat aggregation scenario (AG), the mean between-population distance decreases with habitat aggregation (Fig. 8EF). For the long-distance disperser, the immigration credit is associated with a decrease in the mean area of occupied patches (Fig. 8F). For the short-distance disperser, the extinction debt is associated with an increase in the mean area of occupied patches (Fig. 8E). Nevertheless, an immigration credit is observed for this species when the mean area of occupied patches and the mean between-population distance are initially large (see the orientation of the colour gradient at *t=1* in Fig. 8E).

For the habitat fragmentation scenario (FR), the mean between-population distance slightly decreases following habitat fragmentation (Fig. 8GHIJ). For the short-distance disperser, the extinction debt is associated with an increase in the mean area of occupied patches (Fig. 8GI). For the long-distance disperser, the immigration credit is associated with a decrease in the mean area of occupied patches (Fig. 8HJ). Nevertheless, an extinction debt is observed for this species when the mean area of occupied patches and the mean between-population distance are small initially (see the orientation of the colour gradient at *t=1* in Fig. 8H).

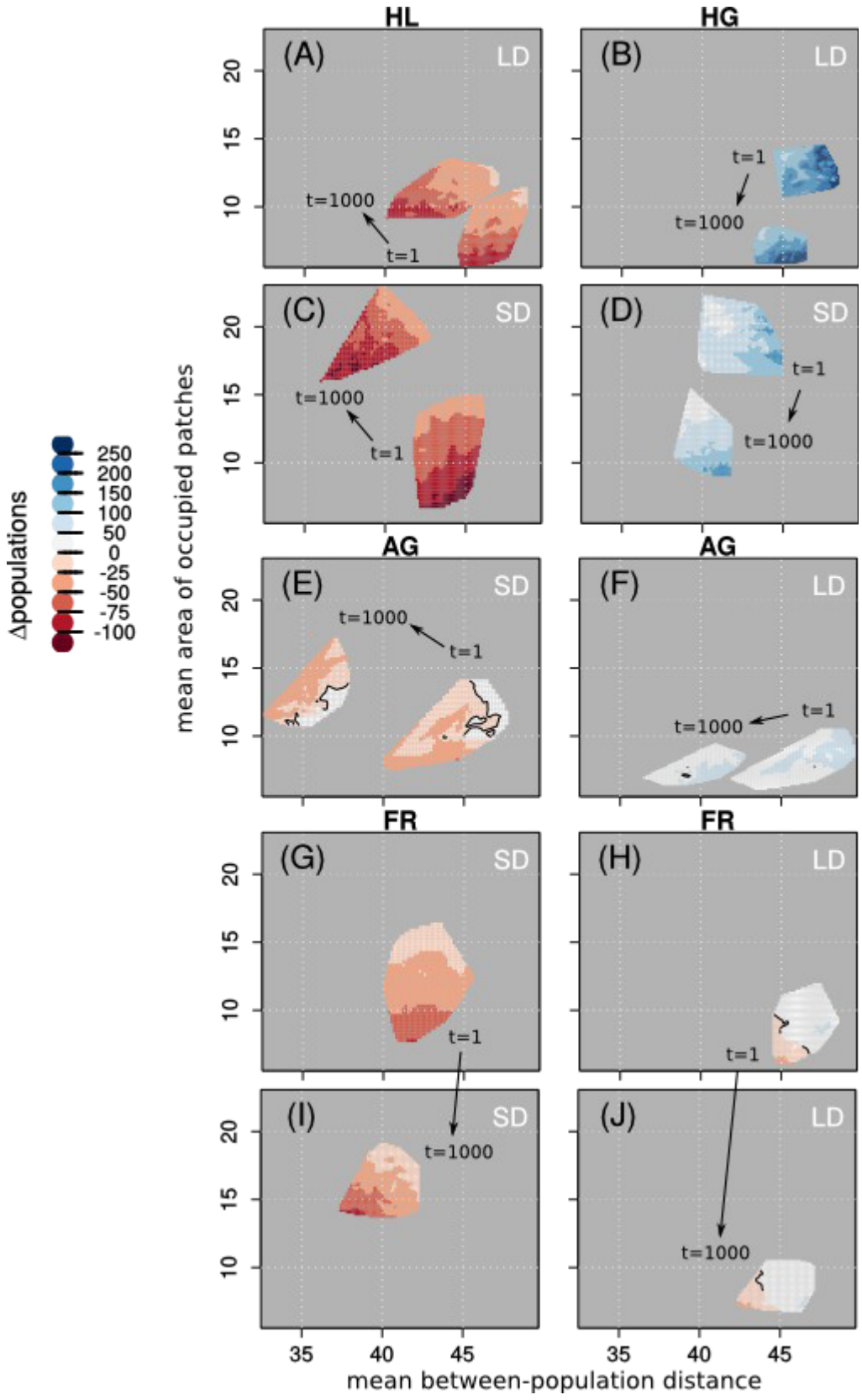

Figure 8: Relationship between time-delayed metapopulation dynamics and changes in two metapopulation characteristics (x and y axes) following habitat turnover (between *t=1* and *t=1000)*. Each panel correspond to a combination of scenarios of habitat turnover x species. The panels G and H are duplicated to avoid overlap. *SD*: short-

distance disperser; *LD*: long-distance disperser; *HL*: habitat loss scenario; *HG*: habitat gain scenario, *FR*: habitat fragmentation scenario; *AG*: habitat aggregation scenario. Δ*populations* is the difference in the number of inhabited patches between t_r and *t=1* (just after perturbation). Extinction debt (Δ*populations<0*) is reported in red-like colors and immigration credit (Δ*populations<0*) is reported in blue-like colors. Extinction debt and immigration credit depends on metapopulation structural characteristics (expressed in cells) immediately after habitat turnover (*t=1*). Metapopulation structural characteristics at the end of the dynamics (*t=1000*) are also represented. We use raw results of 100 landscape replicates to create colored surfaces with a linear interpolation of the variable Δ*populations* from x (mean area of occupied patches) and y (mean between-population distance) coordinates. For each raw result metapopulation structural characteristics is a mean computed from 100 replicates of projected metapopulation dynamics in one landscape.

4. Discussion

4.1 Effects of habitat gain or loss

First, we evidenced that the net change in total habitat area is the main determinant of metapopulation time-delayed dynamics compared to the effect of species dispersal distance (HL and HG scenarios, Fig. 3A). We logically found that an increase or a decrease in habitat area respectively create an immigration credit or an extinction debt (HL and HG scenarios, Fig. 3A). However, we could expect less intuitive results, depending on the balance between habitat creation and destruction (*e.g.* Johst et al. 2011). The short-distance disperser (SD) species had lower final number of populations than the long-distance disperser (LD) species in these two scenarios of habitat change consistently with the theoretical study of Johst et al. (2002) on habitat turnover.

Second, we found that the amplitude of the immigration credit and of the extinction debt depends on the initial metapopulation spatial structure. In the habitat loss scenario (HL), the extinction debt was stronger when species occur initially in smaller patches on average and ultimately leads to metapopulation confinement in large and aggregated patches (Table 2, Fig. 8). In the habitat gain scenario (HG), the immigration credit was stronger when populations are initially widespread in the landscape and ultimately leads to metapopulations expansion in small patches (Table 2, Fig. 8). In other words, the increase in population number allows to support the presence of populations in smaller patches.

4.2 Effects of habitat fragmentation or aggregation

When there was no net change in habitat area (FR and HA scenarios, Fig. 3A), dispersal distance was found to be the main determinant of the extinction debt or the immigration credit whereas spatial configuration of habitat turnover (fragmentation or aggregation) was more related to their magnitudes (Fig. 3A). These credits or debts were of lower magnitude than those observed in the habitat gain and habitat loss scenarios. Time delayed-metapopulation dynamics were positively affected by the species dispersal distance and the habitat aggregation post turnover. This latter result is in accordance with Van Teefelen et al. (2012) who reviewed theoretical and empirical works on habitat dynamics and related that networks with few large patches are better for species viability compared to networks with many small patches (Table 2).

Habitat fragmentation (FR) mainly brought to an extinction debt when species dispersal distance was small. When dispersal distance was large, the simulated fragmentation mainly led to the colonization of new habitat patches and thus to an immigration credit notably because of the persistence of some source patches (Table 1). However, we found that habitat fragmentation brought to an immigration credit only when populations were initially larges (Fig. 8H). When populations occupied small patches (Fig. 8H), we evidenced that habitat fragmentation led to an extinction debt. These theoretical findings are consistent with the recent work of Fahrig (2017) who reviewed empirical studies and gave clear evidences of variable effects of fragmentation while controlling for habitat loss, as we did. For instance, fragmentation could implies a larger number of smaller patches with smaller distances between them and therefore an increase in functional connectivity (Fahrig 2017). In this study we compared time-delayed metapopulation dynamics among the final landscapes (*i.e.* the scenarios) but we did not compare the initial and the four final landscapes (Fig. 1). Favorable changes in the spatial configuration of patches between the initial and the final landscapes may explain the positive effect of fragmentation observed for the LD species (Appendix S1).

We also evidenced that habitat aggregation (AG) mainly brought to an immigration credit for a long-distance disperser but mainly to an extinction debt for a short-distance disperser (Fig. 3A). However, we showed that habitat aggregation led to an extinction debt only when populations were initially spatially aggregated and occupied small patches (Fig. 8EF). Even in that case, habitat aggregation could be view as favorable because the total area of occupied patches often increased (Fig. 3C). Actually, patch aggregation was sometimes concomitant to the creation of small fragments so that some populations went extinct rapidly and the subsequent increase in population number was then not sufficient to compensate for these extinctions (HA scenario, Fig. 4A). Possible negative effects of habitat aggregation, for species that have limited dispersal distance,

are related to habitat turnover in previous studies. Johst et al. (2011) found from a theoretical study that increasing landscape connectivity may not increase short-distance species viability in dynamical landscapes. In the same vein, Hodgson et al. (2009) demonstrated that patch occupancy does not increase with increasing connectivity in situations of patch turnover. They conclude that the negative effect of patch turnover can mask the positive effect of connectivity.

4.3 Determinants of the relaxation time

For both species we found a modest correlation between the relaxation time and the magnitude of the immigration credit or the extinction debt (Fig. 5A). This finding corroborates the hypothesis of Hylander and Ehrlén (2013) which postulates that other factors than the variation in population number explain relaxation time value. Therefore, relaxation time is a parameter of interest in itself that needs to be studied to improve our understanding of time-delayed biodiversity dynamics. We evidenced that it depended on the interaction between species dispersal distance and landscape structure (Fig. 5). Indeed, the relaxation time of the SD species could be larger (in the HG and HL scenarios) than for the LD species and was more influenced by landscape spatial structure (Fig. 5A vs. Fig. 5B). This findings is consistent with studies that related relaxation time to species intrinsic and extrinsic properties (Essl et al. 2015). For instance, some observations related a positive correlation between the payment of the extinction debt and patch area but also a negative correlation between these payment and fragmentation degree (Ferraz et al. 2003, Halley et al. 2013b). Fast turnover rates can also explained that long-distance dispersers have small relaxation times (Cronk 2016). Turnover rates are related with colonisation and extinction parameters that were fixed in our study and can also affect species dispersal abilities (Ruete et al. 2014, Ruete et al. 2017).

4.4 Perspectives of the study

In the present study, we simulated instantaneous habitat turnover while assuming gradual habitat changes is certainly more realistic. Indeed, some perturbations are not instantaneous such as fires or periodic climatic events (Jackson and Sax 2010). Temporal patterns of perturbations are known to be at least as important as their spatial patterns (Hodgson et al. 2009, Johst et al. 2011, Jackson and Sax 2010, Liao et al. 2015, Essl et al. 2015). Some studies have put forward the need to investigate the effect of rapid vs. gradual perturbations (Jackson and Sax 2010, Wearn et al. 2012, Essl et al. 2015). Our study therefore should be viewed as a first investigation on the impact of habitat turnover on metapopulation dynamics, stressing that our approach can be easily

extended to any temporal pattern of habitat turnover. In the context of ecosystem management and conservation offsets, other studies highlighted the importance of the delay between a perturbation and the intervention which aimed at recovering the original state (Hughes et al. 2013, Bull et al. 2015). Our approach could be used to investigate these points theoretically.

Acknowledgements

This work was supported by the French National research institute of science and technology for environment and agriculture (IRSTEA). EL was supported by the Regional Council of Auvergne-Rhône-Alpes.

Appendix

Appendix S1: Effect of habitat turnover on metapopulation dynamics including an intermediate scenario with neither habitat gain or loss and an intermediate fragmentation degree

The five scenarios of habitat turnover are generated following the procedure described in Appendix S2. These scenarios are clearly discriminated by the principal component analysis (PCA). The first two axes of the PCA explain 69.8% of the variance (Fig. S1.A). The first axis explains 49.1% of the variance and discriminated the habitat gain (HG) and habitat loss (HL) scenarios. It is mainly associated with variation in mean distance to the nearest neighboring patch, number of patches, mean connectivity and total area (Fig. S1.A). The second axis is associated with variation in mean distance between patches and number of large patches. It discriminates the final habitats of the habitat aggregation (AG) or habitat fragmentation (FR) scenarios. The intermediate scenario have an intermediate position among the two PCA axis (Fig. S1.A). It is used to asses the effects of habitat turnover with neither net habitat loss or gain and an intermediate fragmentation degree.

For the intermediate scenario of habitat turnover, on average 14.6% (min=6.2, max=23.4) and 15.0% (min=6.3, max=24.4) of the total area are respectively destroyed and created relatively to the area of the initial landscapes. The median relaxation time is 28 time steps for the short-dispersal species and 30 time steps for the long-dispersal species. This scenario mainly lead to and extinction debt for the short-distance disperser (Fig. S1.Ba). However, the total area is on average quite stable so the effect of habitat turnover could be considered neutral for this species (Fig. S1.Bb). For the long-distance disperser we mainly observe an immigration credit that is associated to an increase in total area (Fig. S1). This result is explained by the increase in patch number relatively to the initial landscapes (from 1.0 to 2.4 times). In all the scenario we mainly observe such an increase (from 0.83 times to 3.0 times, with an average of 1.7 times). It is due to our choice to consider that in the case of an increase in patch area the additional area is a new empty (recent) patch until a first colonization takes place. Therefore in the final landscapes, some patches are contiguous that contribute to increase the number of patch. This approach is particularly appropriate for species, such as forest plants, that are frequent in core zone of patches and take times to colonize peripheral zone (Bergès et al. 2015). By contrast, this approach is not adequate for very mobile species such as large mammals.

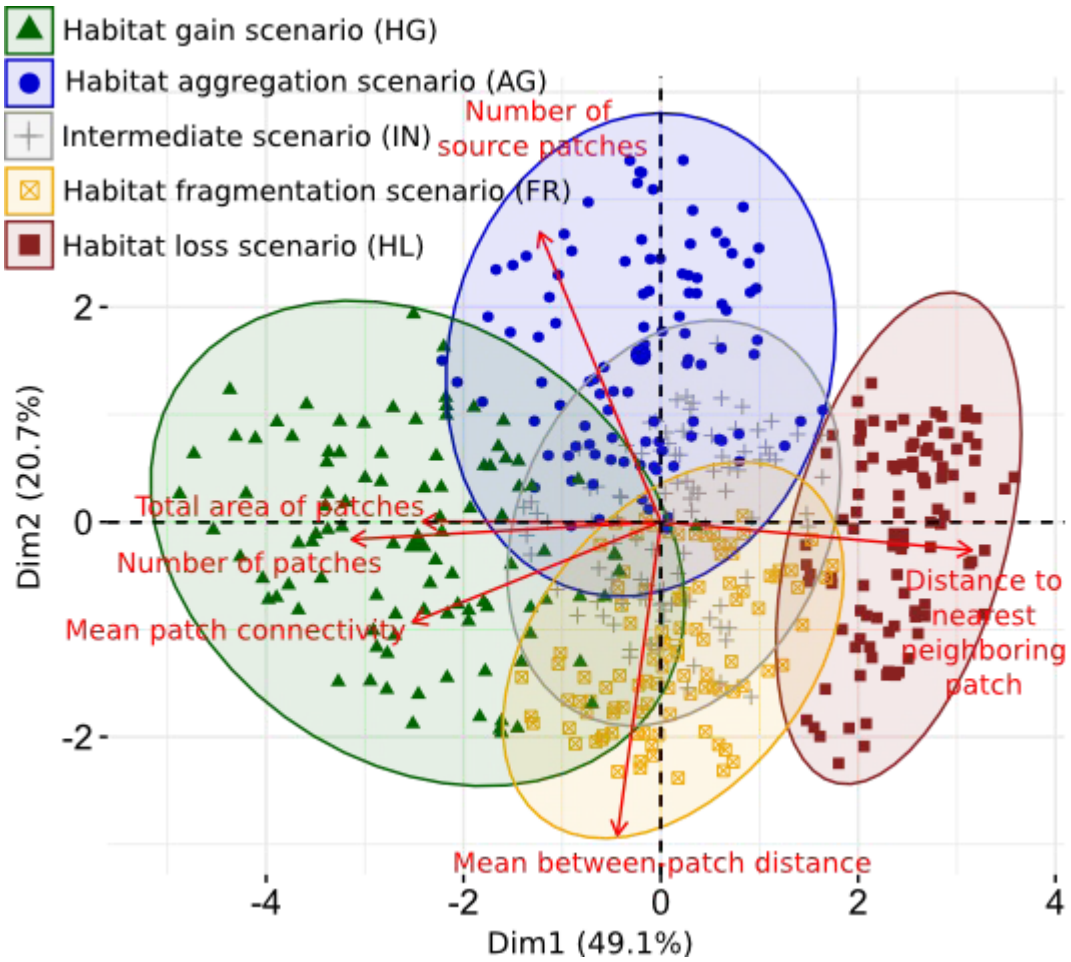

Figure S1.A: Principal component analysis (PCA) of the structural characteristics of final landscapes.

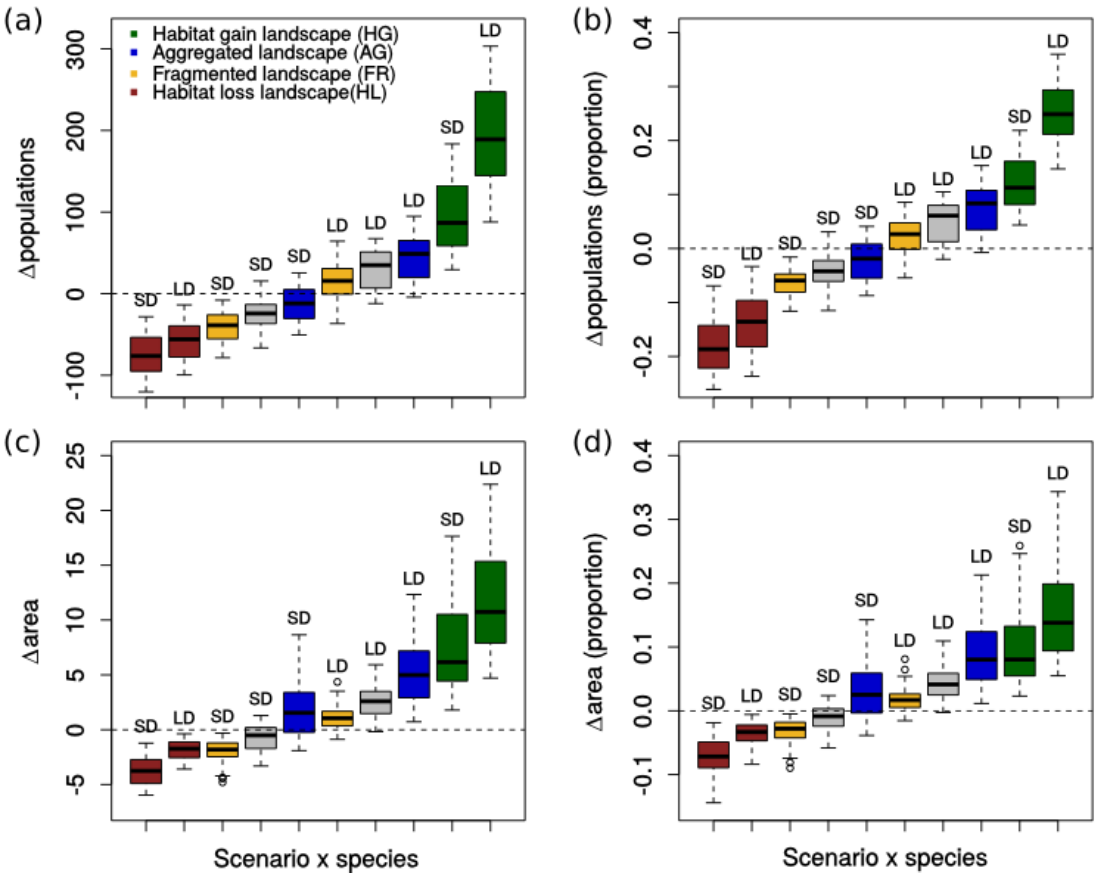

Figure S1.B: Difference between several metapopulation characteristics at the relaxation time (t_r) and those just after perturbation (*t=1)* in the five landscape scenarios and for the two species types. *(a)*: extinction debt (negative change in population number) and immigration credit (positive change in population number); *(b)*: extinction debt and immigration credit in proportion of the total number of patches; (c): change in the total area of occupied patches and (d) change in the total area of occupied patches in proportion of the total area. *SD*: short-distance disperser; *LD*: long-distance disperser. The graphs use the same box-and-whisker representation as in Fig.3. One value is a mean computed from 100 replicates of projected metapopulation dynamics.

Appendix S2: Procedure of landscape generation

A dynamical landscape is simulated in 3 steps (Fig. S2): (1) a square raster of 100×100 pixels is created corresponding to an old map $\left(m_{cont}^{old}\right)$. Pixels values are randomly generated between 0 and 1 with an autocorrelation parameter a_i. Pixels are classified as habitat when the pixel value is above a chosen threshold t_i, in order to transform this map into a binary map $\left(m_{bin}^{old}\right)$. differentiating habitat pixels from matrix pixels (unsuitable habitat). The threshold t_i is fixed as the *np* percentile of the distribution of pixel values, which allow us to control the proportion of habitat in the landscape. (2) A transition map that represents the perturbation $\left(m_{cont}^{pert}\right)$ is then simulated with pixels

values that are randomly generated between 0 and 1 according to an autocorrelation parameter a_p. The $m_{expanded}^{pert}$ map corresponds to the m_{cont}^{pert} map rescaled between r_1 ($r_1<0$) and r_2 ($r_2>0$) to control the quantity of area gain respectively to area loss. (3) A recent map (m_{cont}^{rec}) is simulated following the following equation:

$$m_{cont}^{rec} = m_{cont}^{old} + \varphi \times m_{expanded}^{pert} \quad (1)$$

where the parameter φ controls the pixel turnover rate. A binary (habitat/matrix) recent map (m_{bin}^{rec}) is then produced from the m_{cont}^{rec} map following the same procedure as for the old map. The threshold t_f is fixed either as (i) the *np* percentile of the distribution of pixel values of the m_{cont}^{old} map to mimic an increase or decrease the total habitat area according to r_1 and r_2; or (ii) as the *np* percentile of the distribution of pixel values of the m_{cont}^{rec} map to keep the total habitat area constant (but with habitat turnover).

The old (m_{bin}^{old}) and the recent (m_{bin}^{rec}) binary maps are then vectorized, to delineate patches from pixels, and exported as shapefile using the Python package 'rgdal'. We use R v.3.0.2 (R Core Team 2013) with the packages maptools v.0.8-39 (Bivand and Lewin-Koh 2013) and rgdal v.1.1-10 (Bivand et al. 2013) for vector GIS manipulations. The projection 'Lambert 93' is assigned to shapefiles. Patches erosion (fixed to -0.1) is done to avoid invalid geometry due to point intersection between two diagonal patches. Therefore, species dynamics are simulated from vector maps. Finally, these maps are intersected to differentiate patches present in the old map but not in the recent map, patches present in both the old and the recent maps and patches present in the recent map only. This step was necessary to identify patches that were occupied in the old map to report their state of occupancy in the recent map. In the case of an increase in patch area, the additional area was considered as an new empty (recent) patch until a first colonization takes place. In the case of a decrease in patch area, the patch is considered as ancient.

We simulate five landscape types. The old landscape is the same for each one and the five recent landscapes vary according to the characteristics of perturbations. This choice is made to compare species dynamics in recent landscapes without bias due to old landscapes. The old landscape and the five recent landscapes are replicated 100 times from parameters randomly sampled from interval of values. Sampled values followed an uniform distribution law. Each landscape type is defined by a specific combination of these intervals (Table S2).

Firstly, two landscape types are simulated from perturbation that induce a biased habitat turnover that favors high habitat area gain (hereafter called ‘habitat gain’ or ‘HG’ landscape) when $|r_1<r_2|$ or high habitat area loss (hereafter called ‘habitat loss’ or ‘HL’ landscape) when $|r_1>r_2|$. For these landscape types, the pixel values of the intermediate maps (that represent the perturbation) are spatially randomly distributed ($a_p \approx 0$, Table S1).

Secondly, two other landscape types are simulated from perturbations that have a low spatial aggregation (hereafter called ‘habitat fragmentation’ or ‘FR’ landscape) or high aggregation (hereafter called ‘habitat aggregation’ or ‘AG’ landscape). Pixel values are respectively highly fragmented ($a_p \approx -1$, Table S2) or highly aggregated ($a_p \approx 1$, Table S2) and the total habitat area is kept constant.

Finally, one landscape type is simulated from perturbations that have an intermediate spatial aggregation (hereafter called ‘intermediate’ or ‘IN’ landscape). Pixel values have an intermediate degree of fragmentation ($a_p \approx 0$, Table S2) and the total habitat area is kept constant.

We do not test the effect of np, a_i and φ that are fixed. Nonetheless, the interval of values enable to get variable landscapes according to these parameters. The parameter np range from 0.7 to 0.8 so that the total habitat area is close to 20% for the old landscape of the fragmented and the aggregated landscape types. The spatial autocorrelation of the pixels of the old map is random and range from -0.05 to 0.05. The parameter φ range from 0.05 to 0.15 to limit the maximal habitat gain and loss to a maximum of 30% of the total habitat area of the fragmented and the aggregated landscape types.

Table S2: Parameters used to simulate five landscape types. Each landscape type is replicated 100 times, with random sampling of parameters into interval values from an uniform distribution law. *HL*: habitat loss landscape, *HG*: habitat gain landscape, *FR*: habitat fragmentation landscape, *AG*: habitat aggregation landscape.

	HL	HG	FR	AG	IN
a_f	-0.05; 0.05	-0.05; 0.05	-1; -0.9	0.9; 1	-0,1; 0,1
r_1	-1; -0.9	-0.5; -0.4	-1; -0.9	-1; -0.9	-1; -0.9
r_2	0.4; 0.5	0.9; 1	0.9; 1	0.9; 1	0.9; 1

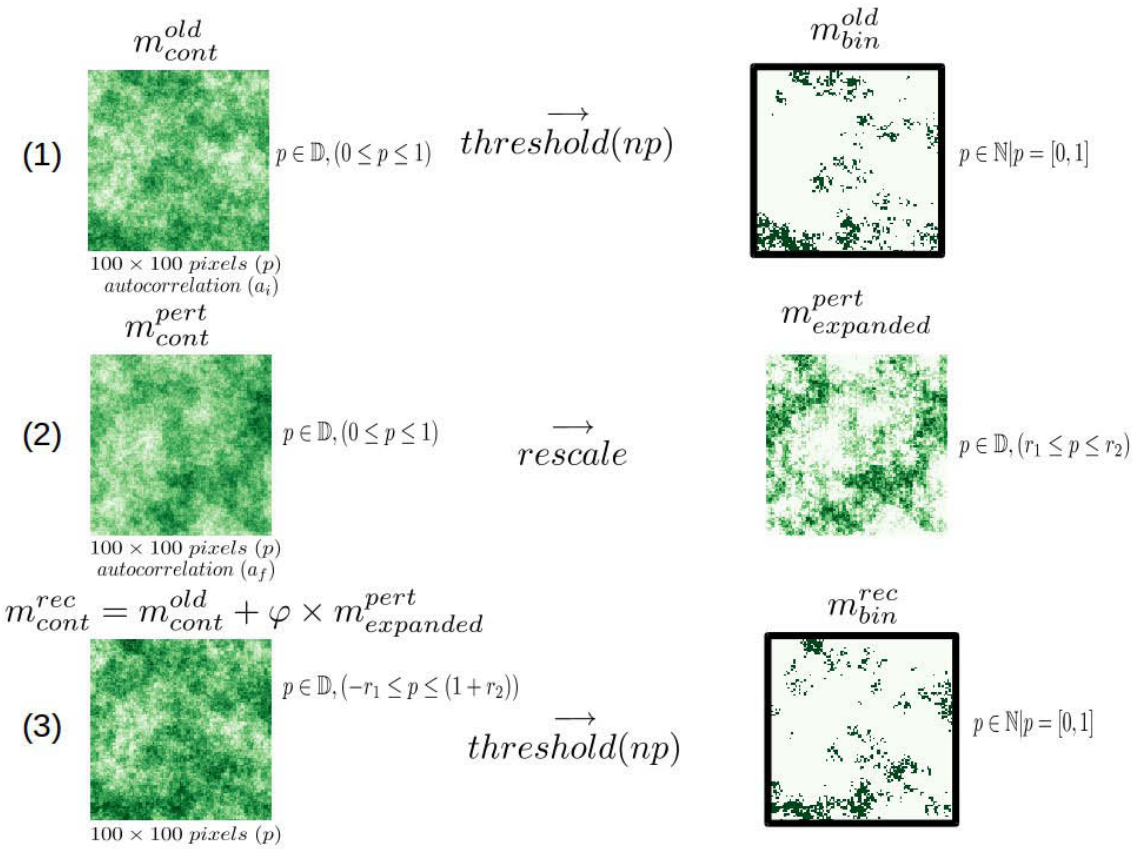

Figure S2: Overall view of the approach used to simulate habitat turnover. The two binary maps with the black frame represent the landscapes before (above) and after (below) habitat turnover occurs.

Chapitre IV : Analyse des projections de la dynamique des plantes forestières suite au turnover des habitats : la Seine-et-Marne comme cas d'étude

Manuscrit correspondant :

Lalechère E., Jabot F., Archaux F., Deffuant D. (in review). Projected regional forest plant community dynamics following habitat turnover: a case study in the Seine-et-Marne area, France. *Journal of Vegetation Science.*

Projected regional forest plant community dynamics following habitat turnover: a case study in the Seine-et-Marne area, France.

Étienne Lalechère [a1] , Franck Jabot [a] , Frédéric Archaux [b] , Guillaume Deffuant [a]

[a] UR LISC, Irstea, 9 avenue Blaise Pascal, F-63178 Aubière, France

[b] UR EFNO, Irstea, Domaine des Barres, F-45290 Nogent-sur-Vernisson, France

Corresponding author:

[1] E-mail address: lalechereetienne@gmail.com

Current address: UR LISC, Irstea, 9 avenue Blaise Pascal, F-63178 Aubière, France

Abstract

Many Western European and North American countries are experiencing a strong reforestation since two centuries due to agricultural abandonment. Other land use changes, such as urbanization, can simultaneously trigger forest erosion. In this context of habitat turnover, forest understorey plant dynamics depend on the balance between immigration credit in post-agricultural forest and extinction debt in ancient forest. The transient and final community properties following concomitant habitat creation and destruction are poorly known. In this contribution, we study the projected transient regional forest plant dynamics and identify the determinants of the relaxation time at both the landscape and patch-scales. Species incidences are projected in 9208 patches of the Seine-et-Marne region (France) that has been characterized by a strong development of post-agricultural forests and a moderate erosion of ancient forests for the period 1840-2000. We use metapopulation parameters calibrated in the same study area from static biodiversity data and landscape history to project forest plant dynamics. We focus on 33 generalist forest species that are able to colonize both ancient and post-agricultural forests. Our analyses reveal that (i) extinction in ancient forests slows down the colonization process that lasts between 250 and 990 years after habitat turnover, depending on species characteristics, (ii) the species incidence in post-agricultural forests converges towards the one in ancient forests long before the overall species incidence stabilizes at the landscape scale (*i.e.* long before the relaxation time), (iii) landscape- and patch-scale relaxation times depend on species colonization ability and patch functional connectivity, (iv) the colonization process is rather slow for ancient forest species and (v) the incidence of ancient forest species becomes larger than the incidence of other species at the end of the colonization dynamics thanks to a strong persistence. Ancient forest species may potentially benefit from a large immigration credit but they need centuries to use it. On such time scale, many perturbations are

likely to question the realization of this potential credit.

Keywords: Land-use history legacy - Long-term change - Landscape dynamics - Time lags - Delayed dynamics

1. Introduction

Land use conversion is among the main drivers of biodiversity changes (Sala et al. 2000, Newbold et al. 2015). Species responses to this driver are often not immediate due to delayed extinction and colonization processes (Jackson and Sax 2010). Such time lags have been estimated to extend over decades to centuries for forest plant species (Paltto et al. 2006, Vellend et al. 2006, Cronk 2016). Such historical legacies are coined by the terms "extinction debt" (Tilman et al. 1994) and "immigration credit" (Hanski 2000, Nagelkerke et al. 2002, Jackson and Sax 2010) that are respectively measured as a future negative or a positive change in population or species numbers (Tilman 1994, Hanski 2000, Hanski and Ovaskainen 2002, Hylander and Ehrlén 2013).

In Western Europe and eastern North America, a strong reforestation is occurring since two centuries due to agricultural abandonment (Flinn and Vellend 2005, Hermy and Verheyen 2007). Post-agricultural forests harbour an immigration credit since they are progressively colonized by propagules of nearby plant populations located in ancient forests (Naaf and Kolk 2015). Ongoing reforestation is associated with clearance of ancient forest although at lower rate than creation of recent forests, a phenomenon that can trigger an extinction debt (Hahs et al. 2009, Rogers et al. 2009). Several studies point out a risk of decline of ancient forest source populations even in a reforestation context (Baeten et al. 2010, De Frenne et al. 2011). It remains finally unclear how the extinction debt could balance the immigration credit when ancient forests are partially eroded in a context of post-agricultural reforestation.

In these forests, various dynamics have been observed in the recent past thanks to resurvey data and analyses of present flora distributions. For example, using a 50-year resurvey in the German region of Prignitz, Kolk et al. (2017) observed a significant increase in ancient forest plant species richness in post-agricultural forests but not in ancient forests. They found that this increase occurs only in post-agricultural forests for ancient forest specialists. These findings evinced the colonization of post-agricultural forests from ancient forests. In contrast, the study of Baeten et al. (2010) showed that, in a context of forest development, the overall forest plant diversity decreased over 30 years. At the species scale, they found that local species frequencies strongly diverged between ancient and post-agricultural forests. They attribute these dynamics to the

increase of common competitive species associated to the depletion of source populations in ancient forests.

These contrasted dynamics might be explained by different environmental constraints. Indeed, species recruitment in post-agricultural forests is limited by dispersal and species ability to pass through local environmental filters (Verheyen et al. 2003b, Vellend et al. 2007, Brunet et al. 2012). First, some species (ancient forest species, hereafter called AFS) are more confined to ancient forests notably due to a low seed dispersal distance (Hermy et al., 1999). Then, abiotic conditions which are known to influence plant recruitment could be different in ancient and post-agricultural forests (Flinn and Vellend 2005, Hermy and Verheyen 2007). Thus, generalist species, with large ecological amplitude, are more likely to colonize post-agricultural forests from nearby populations located in ancient forests.

These contrasted dynamics might also be explained by different stages of payment of extinction debts and use of immigration credit. The extinction debts due to strong pre-industrial forest clearance has not always been paid depending on the region (Vellend et al. 2006, Naaf and Kolk. 2015). For exemple, Naaf and Kolk (2015) found that the extinction debt due to forest loss and fragmentation that occurred more than a century ago, was certainly already paid on the contrary to Vellend et al. (2006) who studied forest plants in Belgium (Vlaams-Brabant region). Regarding immigration credit, Naaf & Kolk (2015) found that the colonization process of recent forests was still ongoing more than a century after landscape change. In contrast, Basnou et al. (2016) found that the colonization is fast enough to exhaust most colonization credit in recent Mediterranean forests after 40 years, except for vertebrate-dispersed species.

Previous studies have detected the presence of an extinction debt or an immigration credit but their magnitude has not been disentangled from the time needed to reach a novel equilibrium following perturbations (relaxation time; Diamond 1972, Hylander and Ehrlén 2013). However, the rate at which extinction debt and immigration credit are paid/used is particularly important in a context of habitat turnover that constantly perturb biodiversity dynamics from its way towards equilibrium (Hylander and Ehrlén 2013). In addition, relaxation times can be largely independent of the magnitude of the extinction debts and the immigration credits and might be better explained by species dispersal abilities and landscape configuration (Lalechère et al. in review).

Here we study projected plant dynamics in ancient and post-agricultural forests in a patchy landscape (Seine-et-Marne region, France) characterized by a strong development of post-agricultural forests and a moderate erosion of ancient forests

during the same period (1840-2000). We use metapopulation parameters calibrated in the same study area from static biodiversity data and landscape history in Lalechère et al. (2017) and focus on generalist species (*i.e.* with large ecological amplitude). This model can be calibrated independently for different species, although it does not integrate interspecific interactions. The immigration credit and the extinction debt are defined at the species level with reference to species incidence as a proxy for the number of populations in a metapopulation (Hylander and Ehrlén 2013). In this study, we answer the following main questions: (i) How the balance between immigration credit in post-agricultural forests and extinction debt in ancient forests affects species dynamics? (ii) How does the patch scale and the landscape scale relaxation times vary with species characteristics and patch functionnal connectivity? (iii) Is there a risk of decline of ancient forest species despite a strong overall reforestation?

2. Materials and methods

2.1 Study area

The study area is the French administrative unit of Seine-et-Marne (7144km^2). To assess past land use change legacy, we use historical forest shapefiles from 1840 digitized maps (military maps) and 2000 forest shapefiles from the French geographical national institute (IGN BD TOPO). We consider that the landscape turnover occurred in 1920. Hedgerows and small forests are mapped in agricultural and riparian areas in the 2000 forest map but not in the 1840 forest map: to avoid an overestimation of the increase of connectivity in the recent map, we remove patches smaller than 1 ha on both maps. This threshold has a weak effect on the overall structure of the patch network (Lalechère et al. 2017). Forest areas increased between 1840 and 2000 from 99920ha to 151237ha in Seine-et-Marne (+51%) whereas 21650ha (22%) of the 1840 forest were cleared. Post-agricultural forest patches are often small and contiguous to ancient forests and represent 48.2% (7083 patches) of the forest areas in 2000 (9208 patches). The mean area of ancient and post-agricultural forest patches are respectively 36.8ha (min=1ha, max=16500ha) and 10.3 ha (min=1ha, max=1095ha) and their mean distance to nearest neighbor patch are respectively 12.0m (min=0m, max=863.3m) and 71.5m (min=0m, max= 3292.0m).

2.2 Species data

We make use of presence / absence plant data collected by the French national forest inventory (IFN: Inventaire Forestier National) and the national botanic conservatory (CBNBP: Conservatoire Botanique National du Bassin Parisien). IFN sampling occured

in 2004 and was based on random selection of locations where flora is inventoried in 700m^2 quadrats. CBNBP data were collected between 2000 and 2010 and sampling area was not fixed: it was on average 2.2 ± 5.3 ha. Between 2000 and 2010 10.6% of patches were sampled. Among the 76 species for which the metapopulation model was calibrated in Etienne et al. (2017), we exclude the ones with low ecological amplitude, since are less likely to colonize post-agricultural forests. Indeed environmental conditions, not accounted for in our modelling, are possibly different between the two types of forests. This selection step leads to a subset of 45 species, based on an expert's opinion about species ecological amplitude, and plants' affinity for acidity, humidity, light and nitrogen. In addition, we exclude eight tree species whose distribution may primarily reflect the actions of foresters, the species *Melampyrum pratense* that went extinct in the projections, and the three outlier species *Anthoxanthum odoratum*, *Cirsium palustre* and *Teucrium scorodonia* (metapopulation parameters were five times lower than the 1st quartile or five times upper than the 3rd quartile of the parameters of the other species). Finally, analyses are performed for 33 species. The list of the studied species and of their calibrated dynamical characteristics is reported in Table S1.

2.3 The metapopulation model

The metapopulation model is close to the one proposed by Verheyen et al. (2004). The occupancy dynamics of the network of patches is modelled as a deterministic process. At each time step t ($t=10$ years), each patch i has an incidence $J_i(t)$ (probability of occupancy) that depends on a colonization rate $C_i(t)$, an extinction rate $E_i(t)$ and its incidence $J_i(t-1)$ at the previous time step. More precisely, the dynamics of $J_i(t)$ is approximated by the following difference equation:

$$J_i(t+1) = J_i(t) \times \left(1 - E_i(t)\right) + \left(1 - J_i(t)\right) \times C_i(t) \quad (1)$$

The extinction rate $E_i(t)$ is assumed constant and equals σ. The colonization rate $C_i(t)$ is given by:

$$C_i(t) = \frac{CON_i(t)^2}{CON_i(t)^2 + 1} \quad (2)$$

where $CON_i(t)$ measures the level of connectivity between patch i and the other patches at time t. It is given by:

$$CON_i(t) = \alpha \cdot \sum_{j \neq i} \left\{ A_j \times J_j(t) \times \exp^{-\beta d_{ij}} \right\} \quad (3)$$

where d_{ij} is the geographical distance between patches i and j, α is a colonization parameter and β is a parameter assuming a decay of colonization with distance. Geographical distances between patches are Euclidean distances computed from patch edge-to-edge.

The modelled landscape is dynamical itself, with events of patch destruction and creation. When a patch is newly created at time step t, it is considered to be unoccupied ($J_i(t)=0$).

Finally, the dynamics of patch incidence $J_i(t)$ is computed from 1840 until year 3840 (*i.e.*, 200 time steps). Such a duration was found to be sufficient to reach a novel equilibrium after habitat turnover.

Equations 1, 2, 3 are also used to compute equilibrium patch incidences in 1840. To do this, we follow Etienne et al. (2004), and (i) initialize the incidence of all patches at one (*i.e.* all patches are occupied) τ time steps in the past $J_i(-\tau)=1$, (ii) compute the dynamics of $J_i(t)$ from $t=-\tau$ to $t=0$ using equations 1, 2, 3. Using a large value for τ, ensures that we get initial conditions $J_i(0)$ that are close to the metapopulation dynamic equilibrium. In the following, we use a τ value equal to 100.

The parameters α, β and σ described above were inferred in Lalechère et al. (2017) based on the combined use of two types of data: (i) historical maps of landscape patches that inform on past landscape dynamics and (ii) present occupancy data collected in a subset of the landscape patches. The inference procedure accounts for imperfect detection. More details can be find in Lalechère et al. (2017).

2.4 Analyses of projected forest plant dynamics

We analyse the mean temporal trajectory of patch incidences (from $t=1$ to $t=200$) that is a proxy of the proportion of occupied patches (Fig. S1). For all the species, mean patch incidences initially decrease and then strongly increase until a new metapopulation equilibrium is reached (Fig. 1). In ancient forest, we quantify the extinction debt as the initial decline of the mean incidence. It is measured as the difference of the mean incidence at time t_{debt}, just before the mean incidence in ancient forest increases and time $t=1$ just after habitat turnover. Then, we define the convergence time t_{conv} as the number

of time steps (from $t=1$) necessary so that the mean incidence in ancient forests equals the mean incidence in post-agricultural forests (with an accuracy of 10^{-2}). Finally, we calculate the immigration credit as the variation in the mean incidence of patches (post-agricultural forests) between $t=1$ and the relaxation time t_r at which mean patch incidences reach an equilibrium.

More precisely, for each time step t, from $t=6$ to $t=196$, we extract 10 successive estimated mean patch incidences values on moving windows (from $t-5$ to $t+4$). We fit a linear model to calculate a local regression slope between the estimated incidence and t. We then consider that the relaxation time is reached when the absolute value of the slope is less than 0.0001 (results are qualitatively similar with a threshold of 0.001 or 0.00005). We then calculate the immigration credit as the difference of the mean incidence at time t_r, and time $t=1$ just after habitat turnover. We also compute the relaxation time Pt_r at the patch scale, based on the temporal trajectory of patch incidence with the same method, to assess how patch characteristics impact species dynamics.

We relate landscape- or patch-scale relaxation times with species metapopulation parameters, mean functional connectivity or patch functional connectivity (eq. 2) using Spearman correlation coefficients and linear regression analyses that are weighted with parameters uncertainties. We also use a connectivity metric that do not account for species dynamical characteristics to compare patches according to landscape configuration only (α, β and J_j are respectively fixed to 1, 0.001 and 1 in eq. 3). To gain a more detailed understanding of these links, we calculate the mean area of patches, the mean distance of post-agricultural patches to nearest ancient forest patch and the mean functional connectivity of patches (eq. 3) from $t=1$ to $t=100$. These quantities are calculated to assess the changes in the spatial pattern of patches that have a large probability of occupancy. For this purpose, we include only 50% of the patches that have the largest incidences at each time step.

Finally, species are classified according to their preference for ancient forests with Fisher exact test for frequency comparison. Ancient forest species being those species statistically more frequent in ancient forest and non-AFS the others. In order to compare between-species incidences, we calculate the relative mean temporal trajectory of patch incidences that is the mean incidence of the focal species divided by the sum of the mean incidence of all the species. Similarly, we also calculate the relative incidence at the patch scale.

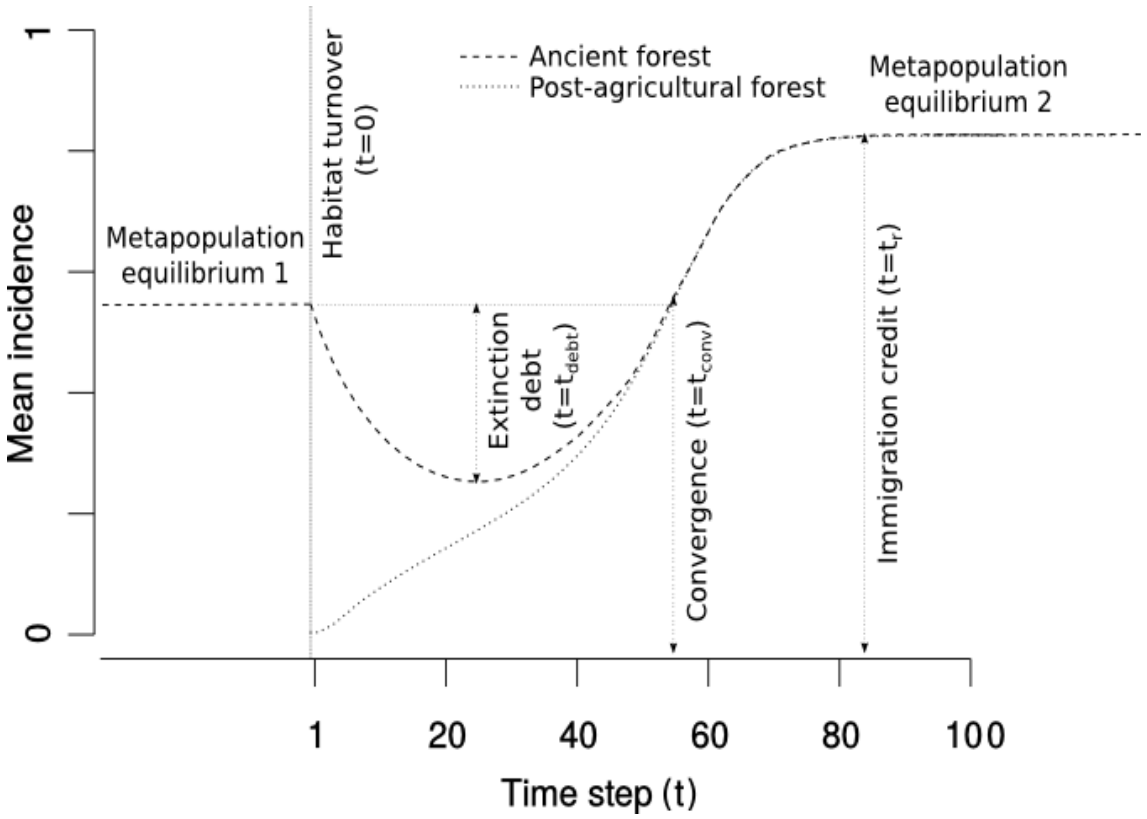

Figure 1: Schematic representation of the mean trajectories of observed incidences, in ancient and post-agricultural forests. First, ancient forest erosion triggers an extinction debt until the time t_{debt} when it is counterbalanced by the immigration credit in post-agricultural forest. Then, the mean incidence in ancient and post-agricultural forest converges at time t_{conv}. Finally, the immigration credit is used at the time t_r when a new metapopulation equilibrium is reached.

3. Results

Due to patch erosion, a moderate extinction debt was observed in ancient forest for all species (Fig. 2A). Its magnitude ranged from 0.02 to 0.08 (i.e. species disappeared on average from 2 to 8% of patches) depending on species characteristics. This initial debt was counterbalanced by colonization events from post-agricultural forests, 40 to 250 years after habitat turnover, depending on plant species (t_{debt}, Fig. 2A). Then, a convergence of the mean incidence between ancient and post-agricultural forests was reached 130 to 600 years after habitat turnover (t_{conv}, Fig. 2B). Finally, a strong immigration credit (from 0.69 to 0.75) was obtained for both forest types. The relaxation time was reached 250 to 990 years after habitat turnover (t_r, Fig. 2B). It was strongly correlated with the convergence time (t_{conv}, Spearman's rho=0.98). Interestingly, mean incidence at t_{conv} largely underestimated the mean incidence at equilibrium (mean underestimation of 73%).

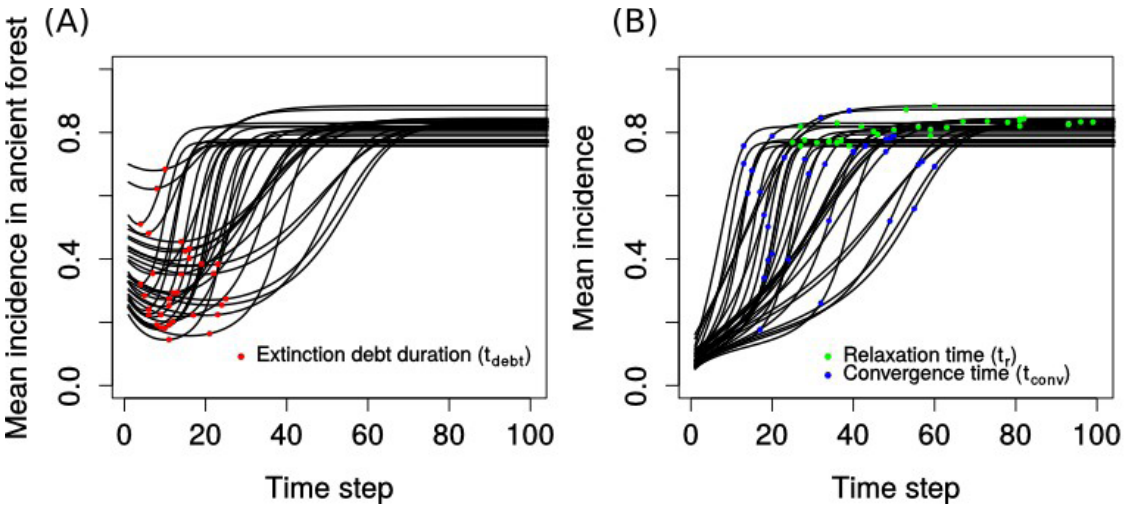

Figure 2: Projected mean incidence in ancient forest (A) or in ancient and post-agricultural forest (B) for 33 species.

At the landscape scale, the relaxation time was positively correlated with the magnitude of the immigration credit (Fig. 3A) and with species colonization ability (characterized as the ratio α/σ, Fig. 3B). The relaxation time was also negatively correlated with mean functional connectivity (Fig. 3C) but not with species parameter of dispersal distance β.

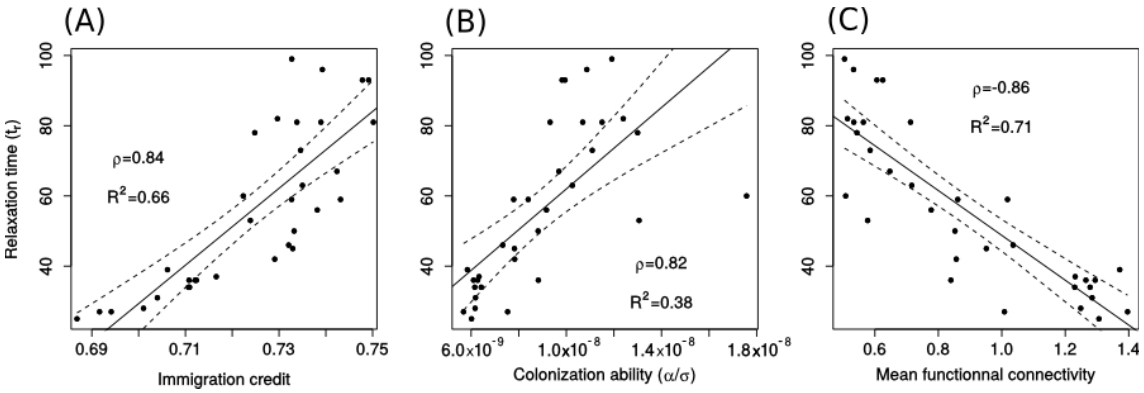

Figure 3: Relationship between species relaxation time (t_r) and the magnitude of the immigration credit (A), species colonization ability (α/σ, B) and mean functional connectivity (C). Regression lines are represented with 95% credible interval (plain and dotted lines respectively).

At the patch scale, the relaxation time (Pt_r) ranged from 250 to 1000 years regardless of species. The differences between the maximum and minimum Pt_r value, for a given species, ranged from 0 to 60 years. Incidence increased first in the most connected patches (large post-agricultural patches adjacent to ancient forests) and then in the least connected patches (Fig. 4). As a consequence, patch-scale relaxation time was negatively correlated with patch functional connectivity (Spearman correlation test $p<0.001$ for 22 species including both AFS and non-AFS, Fig. 5A). This correlation was

larger for species that have a low dispersal distance (Fig. 5B) such as *Narcissus pseudonarcissus*. This species was the most impacted by between-patch distances. For this species for instance, the extinction debt in ancient forest was larger in the least connected patches (Fig. 6A) and the immigration credit was larger in the most connected patches (Fig. 6B).

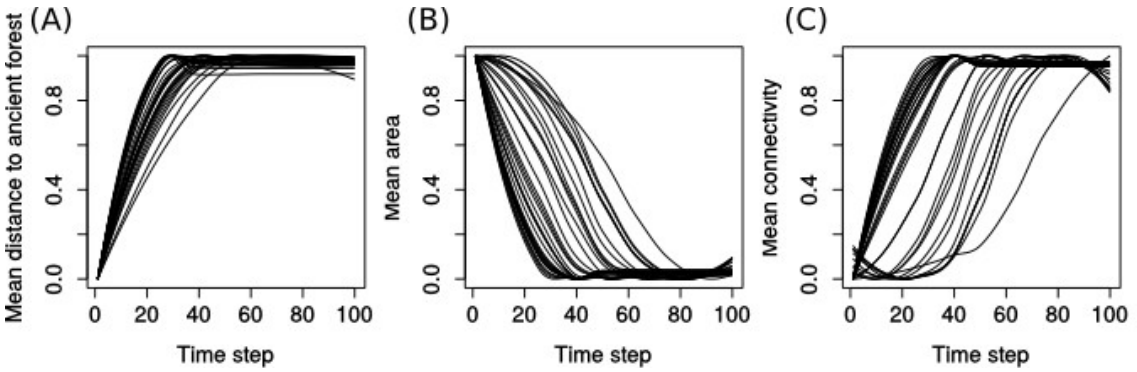

Figure 4: Temporal dynamics of the mean distance to ancient forest of the post-agricultural patches with high incidence (A), of the mean area of patches with high incidence (ancient and post-agricultural, B) and of the mean connectivity of patches with high incidence (ancient and post-agricultural, C) following habitat. High incidence patches are the 50% of the patches that have the largest incidences. High incidence patches are redefined at each time step t. Lines are smoothed with the loess R function. Means are rescaled between 0 and 1 for clarity purpose.

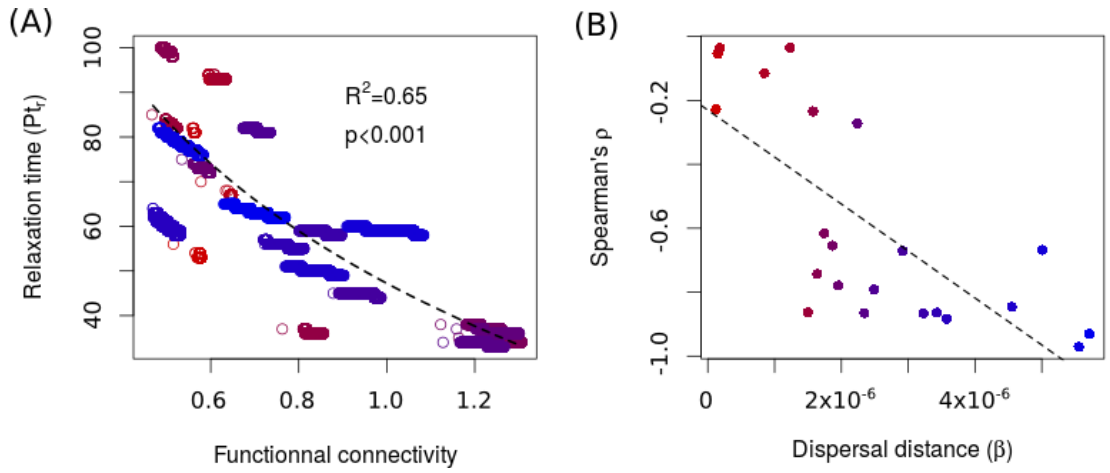

Figure 5: Relationship between patch-scale relaxation times (Pt_r) and their functional connectivity for 22 species (panel A, each species is color coded). This relashionship is larger (Spearman's rho coefficient ρ) for species that have a low dispersal distance (panel B, blue color). Dotted line represents logarithmic regression line in panel (A) and linear regression line in panel (B).

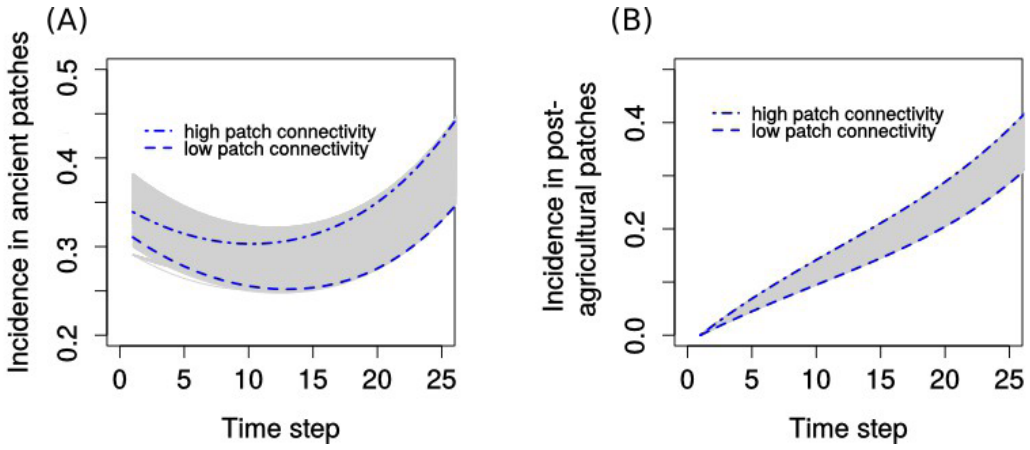

Figure 6: Incidence in ancient (A) and post-agricultural (B) patches for the species *Narcissus pseudonarcissus* that is the most impacted by between-patches distance.

Among the 33 species studied, 21 were classified as ancient forest species (Table S1). All had smaller α parameter values than other species (Wilcoxon one-tailed test $p<0.001$, Fig. 7B). This result explains that the relative incidence was smaller for AFS during the first time steps (Fig. 7A). AFS also had a larger α/σ ratio than other species (Wilcoxon one-tailed test $p<0.001$, Fig. 7C) meaning that they had a larger long-term persistence. Consequently, ancient forest species were able to colonize more patches at the end of the dynamics than other species, despite the very slow use of their immigration credit (except for *Clematis vitalba*, Fig. 7A). At the patch scale, relative incidences were generally larger in the least connected patches for non-AFS, such as *Dactylis glomerata*, because fewer species are able to thrive in these patches (Fig. 8). On the contrary, relative incidences were generally larger in the most connected patches for AFS, such as *Narcissus pseudonarcissus*, because fewer species are able to persist in these patches (Fig. 8). The variability of the relative incidences between these two species was larger in the least connected patches compared to the most connected ones (Fig. 8). Finally, relative incidence of AFS became larger than relative incidence of non-AFS earlier in the most connected patches (Fig. 8).

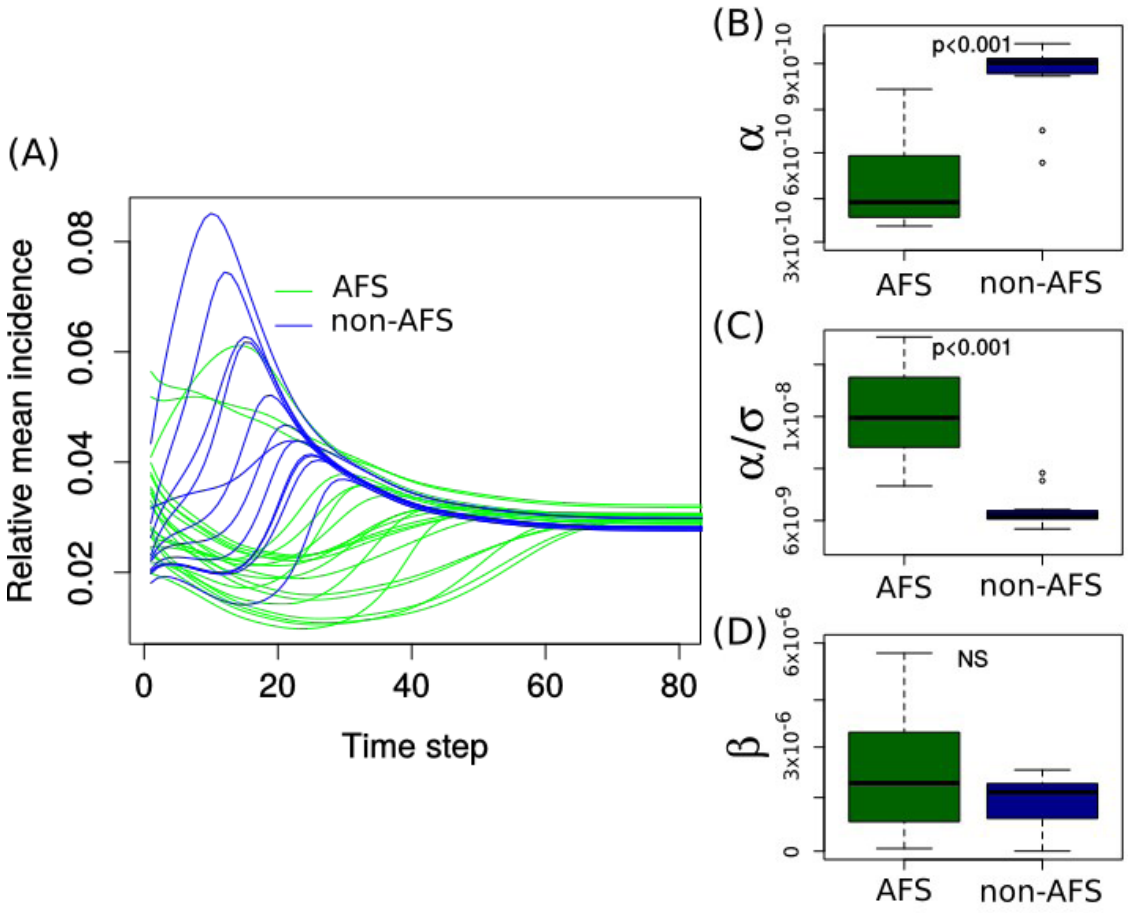

Figure 7: Relative mean incidence and dynamical parameters of ancient forest species (AFS, 21 species) and other species (non-AFS, 12 species). Relative mean incidence is the mean incidence of the focal species divided by the sum of the mean incidence of all the species. *NS*: not significant. At the end of the dynamics AFS have larger relative mean incidences than other species (excepted *Clematis vitalba*).

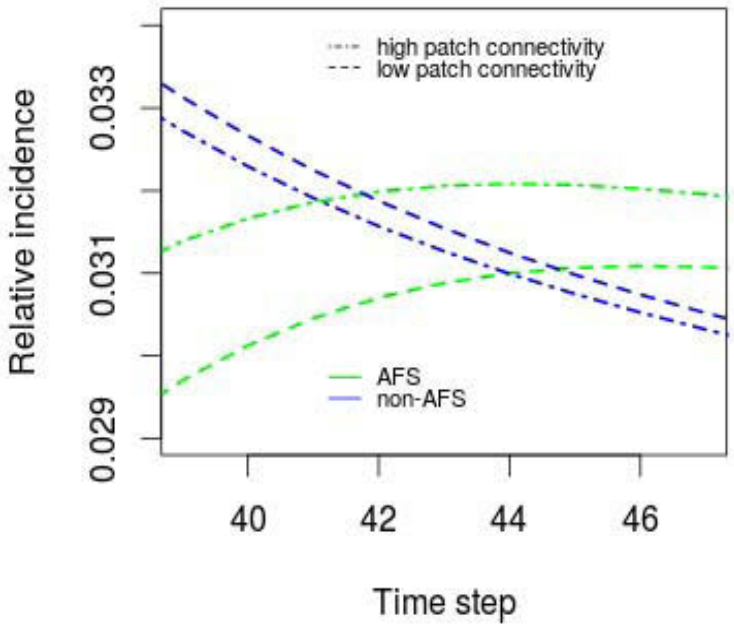

Figure 8: Relative incidence for the ancient forest species *Narcissus pseudonarcissus* (AFS, in green) and *Ilex aquifolium* (non-AFS, in blue) in the most and the least connected patches. Relative incidence is the patch incidence of the focal species divided by the sum of the patch incidence of all the species.

4. Discussion

4.1 Extinction debt slows down the use of the immigration credit and convergence between ancient and post-agricultural forests.

Projected plant dynamics indicate that the order of magnitude of relaxation times ranges from several centuries to near to a millenary (Fig. 2A). Previous studies about immigration credit reported smaller time lags, mainly decades or several centuries (Bagaria et al. 2015, Naaf and Kolk 2015, Hautekèete et al. 2015). First, these differences could be explained by the extinction debt that slows down the immigration credit in our study area in comparison to Naaf and Kolk (2015) who concluded that the extinction debt was already paid. Then, these differences could be explained by the mechanistic approach used in this study while previous studies mainly used resurvey data, space-for-time substitution or correlative statistical approaches and thus are rather detecting time lags (Kuussaari et al. 2009, Bagaria et al. 2015, Hautekèete et al. 2015) without regard to the time needed to reach a novel equilibrium (*i.e* the relaxation time).

In our study area, we could expect a strong immigration credit fostered by post-agricultural forests that increased the total forest area by 51% during the 1840-2000 period. Nevertheless, the erosion of ancient forests (22%) triggers a moderate extinction debt that can persist for 40 to 250 years and that temporarily overshadows the immigration credit. The extinction debt in ancient forests is then counterbalanced by the immigration credit thanks to a rescue effect from nearby post-agricultural forest populations (Brown and Kodric-Brown 1977, Hanski 1999).

Our findings bring a meaningful complement to the resurvey study of Kolk et al. (2017) who have demonstrated that ancient forest species richness could increase in post-agricultural forests, in absence of an extinction debt. At the species scale, we found that the extinction debt slows down but does not prevent the immigration credit for both AFS and non-AFS species (Fig. 2B). We also point out that the convergence of the mean incidence trajectories in ancient forests and in post-agricultural forests does not indicate that a novel equilibrium has been reached (Fig. 2B). After convergence, the majority of post-agricultural patches are still to be colonized (on average 75% depending on the species). These patches have large relaxation times because they are far from ancient forest patches and weakly connected to the bulk of the patch network (Fig. 4,5).

4.2 The relaxation time depends on species characteristics and patch functional connectivity.

A rapid payment of the extinction debt is generally thought to be related with small patch area and large fragmentation degree (Diamond 1972, Halley et al. 2013b, Cronk 2016). However, the determinants of the relaxation time in a context of immigration credit are poorly known while habitat gain, and more generally habitat turnover, are non-negligible parts of habitat dynamics globally (Newbold et al. 2015). In this contribution, we demonstrate that the relaxation time is mostly explained by the mean functional connectivity of patches and then by the magnitude of the immigration credit at the landscape scale (Fig. 3). This result means that the number of patches colonized at the relaxation time, that depends on species colonization ability, partially explains the duration of the relaxation process but is not its main determinant. These results are consistent with previous studies that found that the relaxation time depends on the interplay between species traits and landscape characteristics (Essl et al. 2015, Lalechère et al. in review). In addition, our findings corroborate the hypothesis of Hylander and Ehrlén (2013) who postulated that the magnitude of the relaxation time is not only due to the number of populations that appear or that go extinct, and the results

of Lalechère et al. (in review) from a theoretical study of metapopulation dynamics following habitat turnover. At the patch scale, the variability of relaxation times is logically small for a given species because patch incidence is related to the incidence of neighboring patches (eq. 3, Fig. 5). However, we found that relaxation times decrease with increasing patch functional connectivity and that dispersal distance mediates the strength of these relationships (Fig. 5). This is due to the spatial pattern of colonization: the colonization occurs first in the most connected patches (larger post-agricultural patches that are adjacent to ancient forests) and then in the least connected ones (Fig. 4).

4.3 Immigration credit can be stronger but payed rather slowly for ancient forest species.

Investigating relative incidences, we observed that the rate at which the immigration credit is used is strongly different between AFS and non-AFS (Fig. 7). Non-AFS have a high turnover rate in which large colonization capacity is associated with large propensity to extinction and AFS have a low turnover rate in which limited colonization capacity is associated with limited propensity to extinction (Lalechère et al. 2017). As a consequence, colonization of post-agricultural forests by non-AFS is fast during the first part of the dynamics, contrary to AFS that have small turnover rates. These results are consistent with the literature that relates the turnover rates to the speed of the relaxation process (Verheyen et al. 2004, Auffret et al. 2016, Cronk 2016). During the last part of the dynamics (Fig. 7), AFS colonize more patches than non-AFS due to a strong long-term persistence (Fig. 7C). This ability to persist migth be related to species demographic strategies (sensu Grime et al. 1988) as AFS are more often stress-tolerant species (Hermy et al. 1999, Honnay et al. 2002). The inversion of the dominance between AFS and other species occurs first in the most connected patches and then in the least connected patches that are colonized later by AFS (Fig. 8). Finally, our results points out that ancient forest species could have a large potential of colonization.

4.4 Perspectives of the study

First, we focused on the metapopulation dynamics following a sudden instantaneous modification of the landscape because we do not have intermediate maps between 1840 and 2000 that could allow to understand the trajectory of these modifications. Some theoretical studies showed that the temporal patterns of habitat turnover could matter (Johst et al. 2011, Liao et al. 2015). Davis et al. (2017) demonstrated empirically that the diversity of forest herbs was better explained by the net change in forest cover than by forest change trajectories. Our approach could be used in order to assess the importance of the temporal structure of habitat turnover to understand time-delayed

metapopulation dynamics.

Second, we focused on generalist understorey species with large ecological amplitude for which the frequencies in post-agricultural forests and in ancient forests are more likely to converge, despite the fact that environmental filtering is not accounted for in our modelling. Our findings could be extrapolated to a large number of regions where environmental filtering is a poor determinant of plant distributions or where environmental conditions do not differ between recent and ancient forests (Verheyen et al. 2003a, Verheyen et al. 2006, Vellend et al. 2007, De Frenne et al. 2011, Brunet et al. 2012). For species that are strongly limited by abiotic filtering, we could hypothesize that (i) the convergence never occurs due to strong differences in abiotic conditions between ancient or post-agricultural forests (Jacquemyn et al. 2003, Vellend 2005, Rogers et al. 2009), or (ii) the convergence arises due to an homogenization of abiotic conditions over time (Matlack 2009, Naaf and Kolk 2016, Baeten and Verheyen 2017). Investigating these hypotheses remains challenging. One possibility would be to explicitly model the quality of the different patches (*e.g.* Verheyen et al. 2004) and the temporal dynamics of environmental conditions (*e.g.* Keith et al. 2008, Mestre et al. 2017).

Acknowledgements

This work was supported by the French National research institute of science and technology for environment and agriculture (IRSTEA). EL was supported by the Regional Council of Auvergne-Rhône-Alpes. We are grateful to the French national forest inventory (IFN: Inventaire Forestier National) and the national botanic conservatory (CBNBP: Conservatoire Botanique National du Bassin Parisien) for providing us with floristic inventory data. Ancient forest map was made available from research project “Distrafor” funded by the French Ministry of Environment through GIP Ecofor. We also thank Yann Dumas and Richard Chevalier for their expertise about species ecological amplitude.

Appendix

Table S1: List of the studied species and their characteristics. Parameters (α, β and σ) are mentioned with uncertainties. AFS are those species statistically more frequent in ancient forest and non-AFS the others (tested with Fisher exact test for frequency comparison). *Freq AF*: frequency in ancient forest, *Freq RF*: frequency in recent forest, *unc:* uncertainty.

Species	Freq AF	Freq RF	AFS	α	α unc	σ	σ unc	β	β unc
Brachypodium pinnatum	0.06	0.14	non-AFS	-20.86	0.07	-1.98	0.08	-13.19	0.14
Calluna vulgaris	0.34	0.09	AFS	-21.54	0.35	-3.38	0.4	-12.1	0.9
Cirsium arvense	0.18	0.19	non-AFS	-21.29	0.25	-2.63	0.1	-20.2	1.14
Clematis vitalba	0.51	0.45	non-AFS	-21.12	0.59	-2.41	1.01	-14.99	1.61
Convallaria majalis	0.17	0.09	AFS	-20.99	0.13	-2.26	0.16	-12.76	0.28
Cytisus scoparius	0.22	0.1	AFS	-21.12	0.28	-2.58	0.33	-12.3	0.61
Dactylis glomerata	0.15	0.18	non-AFS	-20.81	0.2	-1.91	0.21	-13.11	0.57
Daphne laureola	0.29	0.07	AFS	-21.76	0.5	-3.43	0.75	-16.38	0.96
Dryopteris filix-mas	0.54	0.21	AFS	-21.68	0.31	-3.82	0.45	-12.54	0.55
Epipactis helleborine	0.15	0.15	non-AFS	-20.84	0.12	-1.98	0.13	-12.96	0.27
Festuca heterophylla	0.2	0.06	AFS	-21.38	0.35	-2.89	0.41	-12.9	0.66
Galeopsis tetrahit	0.23	0.06	AFS	-21.56	0.24	-3.12	0.25	-13.61	1.04
Humulus lupulus	0.12	0.32	non-AFS	-20.88	0.1	-1.97	0.17	-13.83	0.2
Hyacinthoides non-scripta	0.24	0.06	AFS	-21.6	0.25	-3.18	0.27	-13.98	0.83
Ilex aquifolium	0.07	0.13	non-AFS	-20.81	0.07	-1.9	0.08	-13.25	0.14
Juniperus communis	0.2	0.11	AFS	-21.08	0.18	-2.41	0.22	-12.74	0.39
Mycelis muralis	0.32	0.07	AFS	-21.76	0.52	-3.51	0.77	-13.32	1.51
Narcissus pseudonarcissus	0.25	0.08	AFS	-21.26	0.54	-2.86	0.57	-12.07	1.42
Poa nemoralis	0.37	0.1	AFS	-21.74	0.24	-3.54	0.29	-13.41	0.49
Polygonatum multiflorum	0.5	0.22	AFS	-21.68	0.37	-3.53	0.56	-15.91	0.37
Polypodium interjectum	0.14	0.12	non-AFS	-20.82	0.1	-1.92	0.11	-13.26	0.22
Polypodium vulgare	0.18	0.07	AFS	-21.16	0.19	-2.57	0.23	-12.64	0.38
Populus tremula	0.35	0.09	AFS	-21.75	0.34	-3.47	0.34	-14.86	0.89
Prunella vulgaris	0.28	0.09	AFS	-21.56	0.39	-3.11	0.63	-15.54	0.76
Pteridium aquilinum	0.31	0.1	AFS	-21.6	0.45	-3.28	0.42	-13.14	1.19
Rosa arvensis	0.41	0.29	AFS	-21.25	0.12	-2.71	0.19	-13.36	0.27
Rubus caesius	0.12	0.27	non-AFS	-20.77	0.17	-1.78	0.26	-13.92	0.85
Scrophularia nodosa	0.06	0.12	non-AFS	-20.76	0.06	-1.8	0.07	-13.31	0.12
Solidago virgaurea	0.14	0.07	AFS	-20.93	0.17	-2.26	0.2	-12.2	0.25
Stellaria holostea	0.31	0.08	AFS	-21.7	0.34	-3.35	0.52	-15.74	0.61
Tamus communis	0.31	0.38	non-AFS	-20.83	0.32	-1.9	0.53	-13.67	0.75
Viburnum opulus	0.14	0.1	non-AFS	-20.82	0.11	-1.93	0.13	-13.01	0.22
Viola riviniana	0.23	0.1	AFS	-21.26	0.36	-2.75	0.45	-12.58	0.7

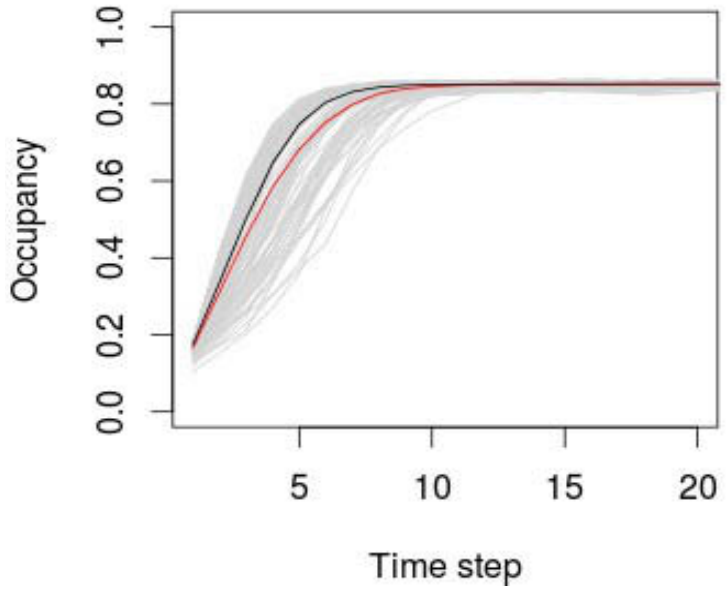

Figure S1: Occupancy defined from the mean temporal trajectory of patch incidences (in black) or from the mean proportion of occupied patches (in red) calculated from 100 simulations (in grey). In the latter case, patch occupancy (0 or 1) is derived from patch incidence (that ranges from 0 to 1) using a random trial following an uniform distribution law. For each patch, occupancy changes (from 0 to 1 or from 1 to 0) when random trial is less than incidence. The mean incidence is used as a proxy of the proportion of occupied patches.

Chapitre V : Discussion générale

V.1 Bilan

L'objectif des travaux présentés dans ce manuscrit est d'évaluer l'apport des modèles de métapopulation hors équilibre pour comprendre les dynamiques qui font suite au turnover des habitats à partir d'une approche théorique ou d'inventaires incomplets actuels de biodiversité et de deux cartographies de paysages, l'une historique, l'autre contemporaine des inventaires de biodiversité (1840 et 2000). Nous avons évalué la robustesse de la méthode d'inférence utilisée en estimant les incertitudes et les erreurs d'estimations associées aux paramètres. Les prédictions des modèles ont ensuite été confrontées aux données en évaluant la capacité des modèles à reproduire les patrons de répartition des plantes forestières en forêts anciennes et récentes. Puis, nous avons établi des corrélations entre les traits des espèces et les paramètres des modèles afin d'identifier les filtres qui peuvent limiter le recrutement. Ensuite, nous avons comparé des scénarios virtuels de turnover d'habitat en discriminant l'effet d'un changement de la quantité totale d'habitat de l'effet d'une modification de l'agrégation spatiale des habitats. Ces scénarios ont été simulés afin de comprendre l'effet relatif du turnover des habitats et de la dispersion des espèces sur la dette d'extinction, le crédit d'immigration et le temps de relaxation. Finalement, nous avons projeté les dynamiques de métapopulation à long terme, à partir des données empiriques, afin d'évaluer l'interaction entre le crédit d'immigration et la dette d'extinction dus à la reforestation qui est à l’œuvre en parallèle de l'érosion partielle des forêts anciennes. À partir de ces projections, nous avons estimé le temps de relaxation à l'échelle du patch et du paysage pour en identifier les déterminants.

Nous avons démontré (chapitre II) qu'à partir d'inventaires de biodiversité incomplets (~10% des patchs échantillonnés) et de cartographies de paysages, il est possible d'inférer les propriétés de dynamique des espèces et de reproduire les patrons de répartition actuels d'une majorité d'entre elles avec des modèles simples. Le nombre de processus écologiques qui peuvent être modélisés est cependant limité étant donné l'augmentation rapide des erreurs d'estimation avec le nombre de paramètres. Les modèles utilisés se focalisent sur la dispersion des espèces suite à un changement de la connectivité alors que les changements de la qualité de l'habitat ou les interactions interspécifiques ne sont pas formalisés. Ces modèles se sont révélés suffisants pour reproduire les patrons spatiaux observés pour une majorité d'espèces, ce qui suggère que la dispersion est un déterminant majeur de la répartition des plantes forestières et que l'hypothèse que les espèces sont à l'équilibre avec le paysage actuel est à rejeter pour la

plupart d'entre elles. Ces résultats concordent avec des travaux antérieurs qui portent sur l'importance de la dispersion et les dynamiques hors équilibre (Verheyen et al. 2003b, Vellend 2007, De Frenne et al. 2011). Les espèces pour lesquelles les modèles n'ont pas permis de reproduire les données observées sont celles qui ont les dynamiques de colonisation les plus rapides d'après les projections d'incidence réalisées. Il est donc probable que les cartes d'Etats-Major de 1840 soient trop anciennes pour expliquer la répartition actuelle de ces espèces. Une autre explication est que d'autres processus écologiques doivent être formalisés pour rendre compte de leurs dynamiques (Dupré et Ehrlén 2002, Jacquemyn et al. 2003, Kimberley et al. 2014, Hermy et Verheyen 2007). Finalement, cette approche s'avère particulièrement adaptée pour l'étude des dynamiques de métapopulations hors équilibre pour d'autres organismes ou d'autres écosystèmes (Pereira et al. 2013) du fait de (i) la possibilité d'inférer des paramètres de dynamique même en l'absence de suivi temporel de biodiversité et même si les inventaires ne portent que sur une fraction seulement des fragments d'habitats ; et de (ii) la robustesse de la méthode et sa capacité à reproduire des dynamiques d'espèces à l'échelle régionale (~10000 patchs).

D'un point de vu thématique, les résultats du chapitre II indiquent que les plantes forestières se positionnent sur un continuum caractérisant leurs vitesses de dynamique, en accord avec des travaux antérieurs (Verheyen et al. 2004). Nous avons montré que ce continuum explique la présence préférentielle des espèces en forêts récentes ou en forêts anciennes. Ainsi, il permet de caractériser les espèces en allant au-delà d'une simple dichotomie entre les communautés d'espèces de forêts anciennes et celles des forêts récentes. La position le long de ce continuum dépend des traits de dispersion des espèces et de leur affinité pour certaines conditions environnementales. De plus, les paramètres de dynamiques des espèces ne sont pas identiques entre les deux zones d'études. Ces résultats suggèrent qu'un filtrage environnemental est à l’œuvre, en sus d'un filtrage lié à la dispersion.

A partir de projections des dynamiques d'espèces, nous avons établi le potentiel de colonisation des espèces de forêts anciennes à long terme (chapitre IV) qui fait suite à une dynamique très lente à plus court terme, également mise en évidence dans de précédents travaux (Verheyen et al. 2003a, Verheyen et al. 2004, De Frenne et al. 2011, Brunet et al. 2012). L'expression de ce potentiel reste incertain vu l'amplitude du temps de relaxation (250 à 990 ans). En effet, aux modifications passées des paysages, s'ajouteront de nouvelles qui à leur tour modifieront le retour à l'équilibre des métapopulations sur des périodes de l'ordre de plusieurs siècles. L'amplitude du temps de relaxation est à imputer en partie à la dette d'extinction, en forêts anciennes, qui contrebalance temporairement le processus d'immigration en début de dynamique. Finalement, l'approche utilisée permet de modéliser le processus de relaxation et ainsi

de mettre en évidence des dynamiques contrastées, pour une même espèce, en fonction de l'horizon temporel considéré.

D'un point de vue théorique, les travaux présentés dans le chapitre III permettent de mettre en lumière l'importance respective de la dispersion des espèces et de la configuration spatiale du turnover des habitats pour expliquer des dynamiques de métapopulations hors équilibre. Ainsi, nous avons montré que la distance de dispersion est le déterminant principal de ces dynamiques lorsque le turnover des habitats modifie le degré de fragmentation du paysage. Au contraire, la distance de dispersion des espèces a un rôle secondaire lorsque la surface totale d'habitat est modifée. Ensuite, nous avons établi que la corrélation entre le temps de relaxation et l'amplitude du crédit d'immigration ou de la dette d'extinction est modeste. Ce résultat corrobore l'hypothèse d'Hylander et Ehrlén (2013) qui stipule que le temps de relaxation ne s'explique pas uniquement par le nombre de populations amenées à se former ou à s'éteindre. Nous avons finalement mis en évidence que ce temps de relaxation dépend de l'interaction entre la dispersion des espèces et le scénario de turnover des patchs.

Il a été possible d'identifier plus précisément les déterminants du temps de relaxation à partir des données empiriques (chapitre IV). Dans un contexte de reforestation, le temps de relaxation s'explique en partie par le nombre de populations qui sont amenées à se former à l'échelle du paysage et donc par la capacité de colonisation des espèces. Cependant, nous avons aussi montré que le temps de relaxation est corrélé positivement à la connectivité fonctionnelle, la distance de dispersion des espèces ayant un rôle de médiateur sur l'intensité de cette relation.

V.2 Limites et perspectives

Afin d'approfondir notre compréhension des interactions entre dynamique de paysage et dynamique de biodiversité plusieurs perspectives sont à considérer. Les travaux présentés dans ce manuscrit sont focalisés sur des dynamiques de métapopulations décalées dans le temps suite à une perturbation initiale (*e.g.* le turnover des habitats). Ces dynamiques de métapopulations ne sont donc pas comparées à celles qui pré-existent avant que la perturbation intervienne, ni aux réponses immédiates des métapopulations. Par exemple, Kitzes et Harte (2015) ont réalisé une comparaison des extinctions immédiates et décalées dans le temps, dans un contexte de destruction des habitats pour montrer, que leur importance réciproque dépend du taxon considéré. Il reste à mettre en perspective ces résultats dans un contexte où la dette d'extinction et le crédit d'immigration se contrebalance.

L'approche proposée dans ce manuscrit peut être utilisée pour étudier l'effet de l'évolution du turnover des patchs au cours du temps sur les dynamiques de biodiversité. Cet aspect a été négligé dans ce manuscrit où le turnover des patchs est considéré comme instantané. L'effet de perturbations plus graduelles et du délai entre la perturbation et la restauration ou la création des habitats restent à évaluer comme le soulignent certains travaux (Jackson and Sax 2010, Hughes et al. 2013, Bull et al. 2015, Essl et al. 2015). Appliqué au turnover des habitats, il s'agit de désynchroniser la création et la destruction de patchs pour tester l'importance de ce délai. Il reste également à déterminer pour quelles espèces les trajectoires temporelles précises de ce turnover apportent ou non une information supplémentaire utile (Davis et al. 2017). Finalement, l'effet des patrons spatiaux et temporels des perturbations peuvent être aussi importants l'un que l'autre et sont donc à mettre en perspective (Liao et al. 2015).

La représentation du paysage adoptée ici, qui oppose patchs d'habitat et matrice inhospitalière, est relativement simple et comporte certaines hypothèses simplificatrices. Tout d'abord il est peu probable que la matrice freine la dispersion des espèces de la même façon en fonction des éléments qui la composent (Prugh et al. 2008). Les modèles stochastiques d'occupation des patchs doivent donc permettre de s'affranchir de cette hypothèse en sus de l'hypothèse d'équilibre. Pour cela, il est possible de calculer les distances inter-patchs relativement à la nature de la matrice en attribuant différent coûts de dispersion à différents usages du sol. Ensuite, la variabilité inter-patch doit être prise en compte de façon plus réaliste c'est-à-dire en fonction des conditions environnementales et pas uniquement de la surface et de l'isolement géographique des patchs. Pour modéliser les conditions environnementales, les approches qui couplent un modèle de dispersion à un modèle de niche semblent particulièrement prometteuses (Mestre et al. 2017). L'intérêt d'un modèle de niche serait d'estimer la qualité des patchs à partir d'une information spatialement explicite sur les conditions environnementales. Cette information peut être issue de cartographies des propriétés du sol dont la résolution doit être cohérente avec l'échelle à laquelle les processus modélisés sont à l’œuvre. Ensuite, l'intégration de paramètres supplémentaires dans le modèle permettrait de définir la dépendance de la colonisation et de l'extinction à la qualité du patch (*e.g.* Verheyen et al. 2004). Le champ d'application des approches qui couplent un modèle de niche à un modèle de dispersion reste cependant à élargir aux espèces hors équilibre. D'autre part, la modélisation des conditions environnementales pourrait permettre d'ajouter une dimension au continuum identifié dans le chapitre II et d'y positionner les espèces de façon absolue, c'est-à-dire indépendamment de la région. Corroborer cette hypothèse permettrait d'expliquer pourquoi les listes d'espèces de forêts anciennes et récentes ne sont pas concordantes en fonction des régions (Hermy et al. 2007, Matuszkiewicz et al. 2013) et aussi de proposer un système de classification alternatif.

Outre ces hypothèses simplificatrices, la vision d'un patch comme une entité homogène pose problème puisqu'elle s'affranchie de la variabilité intra-patch qui peut exister. Premièrement, une réflexion est à mener pour savoir s'il faut diviser les patchs hétérogènes en autant de patchs homogènes et comment faire ces ruptures le long de gradients environnementaux le plus souvent continus. Deuxièmement, cette représentation du patch ne rend pas compte de la dispersion qui peut se produire au sein des patchs de grandes surfaces. La distribution des plantes forestières peut pourtant être particulièrement hétérogène au sein d'une forêt (Bergès et al. 2015). Dans ce manuscrit nous avons considéré que lorsque la surface d'un patch s'accroît au cours du temps, la surface créée est un patch distinct. Des patchs dont l'âge est différent peuvent donc être contigus. Cette distinction est particulièrement appropriée pour étudier la répartition des plantes forestières qui répondent à l'âge des patchs et qui ont des dynamiques de colonisation très lentes au cours du temps. Notre approche permet donc de répondre à ce problème. Cependant, une solution qui semble être particulièrement appropriée pour prendre en compte les deux aspects de la variabilité intra-patch (gradients environnementaux et dispersion) est de combiner des modèles d'abondance et des modèles d'occupation des patchs pour modéliser la dynamique des individus à l'échelle d'une population (Sutherland et al. 2014).

La calibration de modèles plus complexes est cependant limitée par la qualité des données utilisées. Les résultats du chapitre II suggèrent que l'exhaustivité d'un inventaire n'est pas forcément déterminante. Approfondir l'analyse de robustesse réalisée permettrait de vérifier cette hypothèse. De cette façon, il serait possible de faire le lien entre le biais d'estimation et l'exhaustivité d'un inventaire et aussi d'identifier des solutions potentielles pour optimiser l'échantillonnage. En effet, on peut faire l'hypothèse qu'un inventaire partiel mais réalisé dans des patchs aux caractéristiques contrastées (selon leur connectivité par exemple) soit suffisamment informatif. L'exhaustivité d'un inventaire dépend aussi de la surface échantillonnée dans chaque patch. À partir des données empiriques utilisées dans ce manuscrit il a été possible de calculer la détectabilité d'une espèce à l'échelle du patch en fonction de cette surface. Cette méthode s'est révélée être moins efficace en comparaison de l'approche adoptée dans le chapitre II (détectabilité fixe). Ce résultat peut être imputé à une corrélation faible entre le nombre d'espèces inventoriées et la surface échantillonnée. La surface ne serait donc pas un bon proxy du nombre d'espèce. Ce résultat souligne une limite majeure des inventaires de biodiversité utilisés qui n'ont pas eu pour objectif premier l'exhaustivité. Ces éléments mettent en avant l'importance d'identifier les verrous à lever pour maximiser la qualité des inventaires en fonction du plan d'échantillonnage, de la détectabilité des espèces et des biais observationnels.

Pour conclure, le présent manuscrit s'inscrit dans la lignée des travaux qui étudient les dynamiques de biodiversité hors-équilibre à partir d'approches mécanistes. L'intérêt de ces approches est de modéliser le processus de relaxation pour calculer des métriques qui synthétisent l'évolution de la biodiversité à long-terme suite à une perturbation initiale. Les délais temporels des réponses de la biodiversité sont susceptibles de s'accumuler aux niveaux d'organisation supérieurs (Essl et al. 2015). Il convient donc de transposer ces approches et les concepts de dette d'extinction et de crédit d'immigration à l'échelle des populations et des individus pour comprendre les mécanismes qui sous-tendent ces délais aux niveaux d'organisation supérieurs pris en compte dans ce manuscrit.

Bibliographie

Adriaens, D., Honnay, O., & Hermy, M. (2006). No evidence of a plant extinction debt in highly fragmented calcareous grasslands in Belgium. *Biological Conservation*, *133*(2), 212-224.

Archaux, F., Camaret, S., Dupouey, J. L., Ulrich, E., Corcket, E., Bourjot, L., ... & Dumé, G. (2009). Can we reliably estimate species richness with large plots? An assessment through calibration training. *Plant Ecology*, *203*(2), 303.

Archaux, F., Henry, P. Y., & Gimenez, O. (2012). When can we ignore the problem of imperfect detection in comparative studies?. *Methods in Ecology and Evolution*, *3*(1), 188-194.

Auffret, A. G., Aggemyr, E., Plue, J., & Cousins, S. A. (2017). Spatial scale and specialization affect how biogeography and functional traits predict long‐term patterns of community turnover. *Functional Ecology*, *31*(2), 436-443.

Baeten, L., Hermy, M., Van Daele, S., & Verheyen, K. (2010). Unexpected understorey community development after 30 years in ancient and post‐agricultural forests. *Journal of Ecology*, *98*(6), 1447-1453.

Baeten, L., Verheyen, K. (2017). Changes in the nature of environmental limitation in two forest herbs during two decades of forest succession. *Journal of Vegetation Science*.

Bagaria, G., Helm, A., Rodà, F., & Pino, J. (2015). Assessing coexisting plant extinction debt and colonization credit in a grassland–forest change gradient. *Oecologia*, *179*(3), 823-834.

Basnou, C., Vicente, P., Espelta, J. M., & Pino, J. (2016). Of niche differentiation, dispersal ability and historical legacies: what drives woody community assembly in recent Mediterranean forests?. *Oikos*, *125*(1), 107-116.

Bedward, M., Ellis, M. V., & Simpson, C. C. (2009). Simple modelling to assess if offsets schemes can prevent biodiversity loss, using examples from Australian woodlands. *Biological conservation*, *142*(11), 2732-2742.

Bergès, L., Avon, C., Arnaudet, L., Archaux, F., Chauchard, S., & Dupouey, J.-L. (2015). Past landscape explains forest periphery-to-core gradient of understorey plant communities in a reforestation context. *Diversity and Distributions*, *22*(1), 3-16.

Bertrand, C., Burel, F., & Baudry, J. (2016). Spatial and temporal heterogeneity of the crop mosaic influences carabid beetles in agricultural landscapes. *Landscape Ecology*, *31*(2), 451-466.

Bivand, R., & Lewin-Koh, N. (2013). maptools: Tools for reading and handling spatial objects. *R package version 0.8*, *27*.

Bivand, R., Keitt, T., & Rowlingson, B. (2014). rgdal: Bindings for the geospatial data abstraction library. *R package version 0.8-16*.

Boitani, L., Falcucci, A., Maiorano, L., & Rondinini, C. (2007). Ecological networks as conceptual frameworks or operational tools in conservation. *Conservation Biology*, *21*(6), 1414-1422.

Boorman, S. A., & Levitt, P. R. (1973). Group selection on the boundary of a stable population. *Theoretical Population Biology*, *4*(1), 85-128.

Brown, J. H., & Kodric-Brown, A. (1977). Turnover rates in insular biogeography: effect of immigration on extinction. *Ecology*, *58*(2), 445-449.

Brunet, J., De Frenne, P., Holmström, E., & Mayr, M. L. (2012). Life-history traits explain rapid colonization of young post-agricultural forests by understory herbs. *Forest Ecology and Management*, *278*, 55-62.

Bull, J. W., Hardy, M. J., Moilanen, A., & Gordon, A. (2015). Categories of flexibility in biodiversity offsetting, and their implications for conservation. *Biological Conservation*, *192*, 522-532.

Burel, F., & Baudry, J. (1999). Ecologie du paysage. Concepts, méthodes et applications, *TEC & DOC Paris*.

Ceballos, G., Ehrlich, P. R., & Dirzo, R. (2017). Biological annihilation via the ongoing sixth mass extinction signaled by vertebrate population losses and declines. *Proceedings of the National Academy of Sciences*, *114*(30), E6089-E6096.

Chipperfield, J. D., Dytham, C., & Hovestadt, T. (2011). An updated algorithm for the generation of neutral landscapes by spectral synthesis. *PLoS One*, *6*(2), e17040.

Connor, E. F., & McCoy, E. D. (1979). The statistics and biology of the species-area relationship. *The American Naturalist*, *113*(6), 791-833.

Crist, E., Mora, C., & Engelman, R. (2017). The interaction of human population, food production, and biodiversity protection. *Science*, *356*(6335), 260-264.

Cronk, Q. (2016). Plant extinctions take time. *Science*, *353*(6298), 446-447.

Dambrine, E., Dupouey, J. L., Laüt, L., Humbert, L., Thinon, M., Beaufils, T., & Richard, H. (2007). Present forest biodiversity patterns in France related to former Roman agriculture. *Ecology*, *88*(6), 1430-1439.

Datry, T., Pella, H., Leigh, C., Bonada, N., & Hugueny, B. (2016). A landscape approach to advance intermittent river ecology. *Freshwater Biology*, *61*(8), 1200-1213.

Davis, A. J., Thill, J. C., & Meentemeyer, R. K. (2017). Multi-temporal trajectories of landscape change explain forest biodiversity in urbanizing ecosystems. *Landscape Ecology*, 1-15.

Decocq, G., Andrieu, E., Brunet, J., Chabrerie, O., De Frenne, P., De Smedt, P., ... & Mifsud, E. G. (2016). Ecosystem services from small forest patches in agricultural landscapes. *Current Forestry Reports*, *2*(1), 30-44.

De Frenne, P., Baeten, L., Graae, B. J., Brunet, J., Wulf, M., Orczewska, A., ... & Hermy, M. (2011). Interregional variation in the floristic recovery of post-agricultural

forests. *Journal of Ecology*, *99*(2), 600-609.

Diamond, J. M. (1972). Biogeographic kinetics: estimation of relaxation times for avifaunas of southwest Pacific islands. *Proceedings of the National Academy of Sciences*, *69*(11), 3199-3203.

Driscoll, D. A. (2007). How to find a metapopulation. *Canadian Journal of Zoology*, *85*(10), 1031-1048.

Dupouey, J.-L., Dambrine, E., Laffite, J. D., & Moares, C. (2002). Irreversible impact of past land use on forest soils and biodiversity. *Ecology*, *83*(11), 2978-2984.

Dupré, C., & Ehrlén, J. (2002). Habitat configuration, species traits and plant distributions. *Journal of Ecology*, *90*(5), 796-805.

Economo, E. P., & Keitt, T. H. (2008). Species diversity in neutral metacommunities: a network approach. *Ecology letters*, *11*(1), 52-62.

Ehrlén, J., & Eriksson, O. (2000). Dispersal limitation and patch occupancy in forest herbs. *Ecology*, *81*(6), 1667-1674.

Ellenberg, H., Weber, H. E., Düll, R., Wirth, V., Werner, W., & Paulißen, D. (1992). Zeigerwerte von pflanzen in Mitteleuropa. *Scripta Geobotanica*, *18*(1), 1-258.

Essl, F., Dullinger, S., Rabitsch, W., Hulme, P. E., Pyšek, P., Wilson, J. R., & Richardson, D. M. (2015). Historical legacies accumulate to shape future biodiversity in an era of rapid global change. *Diversity and Distributions*, *21*(5), 534-547.

Etherington, T. R., Holland, E. P., & O'Sullivan, D. (2015). NLMpy: a python software package for the creation of neutral landscape models within a general numerical framework. *Methods in Ecology and Evolution*, *6*(2), 164-168.

Etienne, R. S., ter Braak, C. J. F., & Vos, C. C. (2004). Application of stochastic patch occupancy model to real metapopulations. In: Ecology, genetics, and evolution of metapopulations, *Elsevier Burlington*, 105-132.

Fahrig, L. (2017). Ecological responses to habitat fragmentation per se. *Annual Review of Ecology, Evolution, and Systematics*, *48*(1).

Ferraz, G., Russell, G. J., Stouffer, P. C., Bierregaard, R. O., Pimm, S. L., & Lovejoy, T. E. (2003). Rates of species loss from Amazonian forest fragments. *Proceedings of the National Academy of Sciences*, *100*(24), 14069-14073.

Flemons, P., Guralnick, R., Krieger, J., Ranipeta, A., & Neufeld, D. (2007). A web-based GIS tool for exploring the world's biodiversity: The Global Biodiversity Information Facility Mapping and Analysis Portal Application (GBIF-MAPA). *Ecological Informatics*, *2*(1), 49-60.

Flinn, K. M., & Vellend, M. (2005). Recovery of forest plant communities in post-agricultural landscapes. *Frontiers in Ecology and the Environment*, *3*(5), 243-250.

Forman, R. T. (1995). Some general principles of landscape and regional ecology. *Landscape Ecology*, *10*(3), 133-142.

Freckleton, R. P., & Watkinson, A. R. (2002). Large-scale spatial dynamics of plants: metapopulations, regional ensembles and patchy populations. *Journal of Ecology*, *90*(3), 419-434.

García-Valdés, R., Svenning, J. C., Zavala, M. A., Purves, D. W., & Araujo, M. B. (2015). Evaluating the combined effects of climate and land-use change on tree species distributions. *Journal of Applied Ecology*, *52*(4), 902-912.

Graae, B. J., & Sunde, P. B. (2000). The impact of forest continuity and management on forest floor vegetation evaluated by species traits. *Ecography*, *23*(6), 720-731.

Graae, B. J., Hansen, T., & Sunde, P. B. (2004). The importance of recruitment limitation in forest plant species colonization: a seed sowing experiment. *Flora-Morphology, Distribution, Functional Ecology of Plants*, *199*(3), 263-270.

Grilli, J., Barabás, G., & Allesina, S. (2015). Metapopulation persistence in random fragmented landscapes. *PLoS Computational Biology*, *11*(5), e1004251.

Grime, J. P. (1988). The CSR model of primary plant strategies—origins, implications and tests. In: Plant evolutionary biology, *Springer Netherlands*, *371-393.*

Hahs, A. K., McDonnell, M. J., McCarthy, M. A., Vesk, P. A., Corlett, R. T., Norton, B. A., ... & Williams, N. S. (2009). A global synthesis of plant extinction rates in urban areas. *Ecology Letters*, *12*(11), 1165-1173.

Halley, J. M., Sgardeli, V., & Monokrousos, N. (2013a). Species–area relationships and extinction forecasts. *Annals of the New York Academy of Sciences*, *1286*(1), 50-61.

Halley, J. M., Iwasa, Y., & Vokou, D. (2013b). Comment on" Extinction Debt and Windows of Conservation Opportunity in the Brazilian Amazon". *Science*, *339*(6117), 271-271.

Hanski, I. (1994). A practical model of metapopulation dynamics. *Journal of Animal Ecology*, 151-162.

Hanski, I. (1998). Metapopulation dynamics. *Nature*, *396*(6706), 41.

Hanski, I. (2000). Extinction debt and species credit in boreal forests: modelling the consequences of different approaches to biodiversity conservation. *Annales Zoologici Fennici*, 271-280.

Hanski, I., & Ovaskainen, O. (2002). Extinction debt at extinction threshold. *Conservation biology*, *16*(3), 666-673.

Harrison, S. (1991). Local extinction in a metapopulation context: an empirical evaluation. *Biological Journal of the Linnean Society*, *42*(1-2), 73-88.

Hautekèete, N. C., Frachon, L., Luczak, C., Toussaint, B., Van Landuyt, W., Van Rossum, F., & Piquot, Y. (2015). Habitat type shapes long‐term plant biodiversity budgets in two densely populated regions in north‐western Europe. *Diversity and*

Distributions, *21*(6), 631-642.

He, F., & Hubbell, S. P. (2011). Species-area relationships always overestimate extinction rates from habitat loss. *Nature*, *473*(7347), 368.

Hermy, M., Honnay, O., Firbank, L., Grashof-Bokdam, C., & Lawesson, J. E. (1999). An ecological comparison between ancient and other forest plant species of Europe, and the implications for forest conservation. *Biological Conservation*, *91*(1), 9-22.

Hermy, M., & Verheyen, K. (2007). Legacies of the past in the present-day forest biodiversity: a review of past land-use effects on forest plant species composition and diversity. *Ecological Research*, 22(3), 361-371.

Hiebeler, D. E., Houle, J., Drummond, F., Bilodeau, P., & Merckens, J. (2016). Locally dispersing populations in heterogeneous dynamic landscapes with spatiotemporal correlations. I. Block disturbance. *Journal of theoretical biology*, *407*, 212-224.

Hilborn, R., & Mangel, M. (1997). The ecological detective: confronting models with data (Vol. 28), *Princeton University Press.*

Hodgson, J. A., Moilanen, A., & Thomas, C. D. (2009). Metapopulation responses to patch connectivity and quality are masked by successional habitat dynamics. *Ecology*, *90*(6), 1608-1619.

Honnay, O., Bossuyt, B., Verheyen, K., Butaye, J., Jacquemyn, H., & Hermy, M. (2002). Ecological perspectives for the restoration of plant communities in European temperate forests. *Biodiversity and Conservation*, *11*(2), 213-242.

Hughes, T. P., Linares, C., Dakos, V., van de Leemput, I. A., & van Nes, E. H. (2013). Living dangerously on borrowed time during slow, unrecognized regime shifts. *Trends in Ecology & Evolution*, *28*(3), 149-155.

Hutchinson, G. E. (1957). Population studies-animal ecology and demography-concluding remarks. In: Cold Spring Harbor Symposia on Quantitative Biology.

Hylander, K., & Ehrlén, J. (2013). The mechanisms causing extinction debts. *Trends in Ecology & Evolution*, *28*(6), 341-346.

Jabot, F., Etienne, R. S., & Chave, J. (2008). Reconciling neutral community models and environmental filtering: theory and an empirical test. *Oikos*, *117*(9), 1308-1320.

Jackson, S. T., & Sax, D. F. (2010). Balancing biodiversity in a changing environment: extinction debt, immigration credit and species turnover. *Trends in Ecology & Evolution*, *25*(3), 153-160.

Jacquemyn, H., Butaye, J., & Hermy, M. (2003). Influence of environmental and spatial variables on regional distribution of forest plant species in a fragmented and changing landscape. *Ecography*, *26*(6), 768-776.

Johst, K., Brandl, R., & Eber, S. (2002). Metapopulation persistence in dynamic landscapes: the role of dispersal distance. *Oikos*, *98*(2), 263-270.

Johst, K., Drechsler, M., van Teeffelen, A. J., Hartig, F., Vos, C. C., Wissel, S., ... & Opdam, P. (2011). Biodiversity conservation in dynamic landscapes: trade‐offs between number, connectivity and turnover of habitat patches. *Journal of Applied Ecology*, *48*(5), 1227-1235.

Julve, P. H. (1998). Baseflor. Index botanique, écologique et chorologique de la flore de France. *Institut Catholique de Lille, Lille*.

Keil, P., Storch, D., & Jetz, W. (2015). On the decline of biodiversity due to area loss. *Nature communications*, *6*, 8837.

Keith, D. A., Akçakaya, H. R., Thuiller, W., Midgley, G. F., Pearson, R. G., Phillips, S. J., ... & Rebelo, T. G. (2008). Predicting extinction risks under climate change: coupling stochastic population models with dynamic bioclimatic habitat models. *Biology Letters*, *4*(5), 560-563.

Kéry, M., & Schmidt, B. (2008). Imperfect detection and its consequences for monitoring for conservation. *Community Ecology*, *9*(2), 207-216.

Kimberley, A., Blackburn, G. A., Whyatt, J. D., Kirby, K., & Smart, S. M. (2013). Identifying the trait syndromes of conservation indicator species: how distinct are British ancient woodland indicator plants from other woodland species? *Applied Vegetation Science*, *16*(4), 667-675.

Kimberley, A., Alan Blackburn, G., Duncan Whyatt, J., & Smart, S. M. (2014). Traits of plant communities in fragmented forests: the relative influence of habitat spatial configuration and local abiotic conditions. *Journal of Ecology*, *102*(3), 632-640.

Kimberley, A., Blackburn, G. A., Whyatt, J. D., & Smart, S. M. (2016). How well is current plant trait composition predicted by modern and historical forest spatial configuration?. *Ecography*, *39*(1), 67-76.

Kindlmann, P., & Burel, F. (2008). Connectivity measures: a review. *Landscape Ecology*, *23*(8), 879-890.

Kitzes, J., & Harte, J. (2015). Predicting extinction debt from community patterns. *Ecology*, *96*(8), 2127-2136.

Kleyer, M., Bekker, R. M., Knevel, I. C., Bakker, J. P., Thompson, K., Sonnenschein, M., ... & Klotz, S. R. G. M. (2008). The LEDA Traitbase: a database of life-history traits of the Northwest European flora. *Journal of Ecology*, *96*(6), 1266-1274.

Koerner, W., Cinotti, B., Jussy, J. H., & Benoît, M. (2000). Evolution des surfaces boisées en France depuis le début du XIXe siècle: identification et localisation des boisements des territoires agricoles abandonnés. *Revue Forestière Française*, *52*(3), 249-270.

Kolb, A., & Barsch, K. (2010). Environmental factors and seed abundance influence seedling emergence of a perennial forest herb. *Acta Oecologica*, *36*(5), 507-513.

Kolk, J., Naaf, T., & Wulf, M. (2017). Paying the colonization credit: converging plant species richness in ancient and post-agricultural forests in NE Germany over five decades. *Biodiversity and Conservation*, *26*(3), 735-755.

Kühn, I., Durka, W., & Klotz, S. (2004). BiolFlor: a new plant-trait database as a tool for plant invasion ecology. *Diversity and Distributions*, *10*(5/6), 363-365.

Kuussaari, M., Bommarco, R., Heikkinen, R. K., Helm, A., Krauss, J., Lindborg, R., ... & Stefanescu, C. (2009). Extinction debt: a challenge for biodiversity conservation. *Trends in Ecology & Evolution*, *24*(10), 564-571.

Lalechère, E., Jabot, F., Archaux, F., & Deffuant, G. (2017). Non-equilibrium plant metapopulation dynamics challenge the concept of ancient/recent forest species. *Ecological Modelling*, *366*, 48-57.

Lalechère, E., Jabot, F., Archaux, F., Deffuant, G., (in review). Effects of habitat turnover on time-delayed metapopulation dynamics. *Theoretical Ecology*.

Lele, S. R., Moreno, M., & Bayne, E. (2012). Dealing with detection error in site occupancy surveys: what can we do with a single survey?. *Journal of Plant Ecology*, *5*(1), 22-31.

Levins, R. (1969). Some demographic and genetic consequences of environmental heterogeneity for biological control. *American Entomologist*, *15*(3), 237-240.

Levins, R. (1970). Extinctions. Some Mathematical Questions in Biology. Lectures on Mathematics in the Life Sciences. *American Mathematical Society*, *2*, 77-107.

Liao, J., Ying, Z., Hiebeler, D. E., Wang, Y., Takada, T., & Nijs, I. (2015). Species extinction thresholds in the face of spatially correlated periodic disturbance. *Scientific Reports*, 5.

Liao, J., Ying, Z., Woolnough, D. A., Miller, A. D., Li, Z., & Nijs, I. (2016). Coexistence of species with different dispersal across landscapes: a critical role of spatial correlation in disturbance. *Proceedings of the National Academy of Sciences B*, 283(1830).

Lindborg, R., & Eriksson, O. (2004). Historical landscape connectivity affects present plant species diversity. *Ecology*, *85*(7), 1840-1845.

MacArthur, R. H., & Wilson, E. (1967). The theory of island biogeography, *Princeton University Press.*

Matlack, G. R. (2009). Long-term changes in soils of second-growth forest following abandonment from agriculture. *Journal of Biogeography*, *36*(11), 2066-2075.

Matuszkiewicz, J. M., Kowalska, A., Kozłowska, A., Roo-Zielińska, E., & Solon, J. (2013). Differences in plant-species composition, richness and community structure in ancient and post-agricultural pine forests in central Poland. *Forest Ecology and Management*, *310*, 567-576.

May, F., Giladi, I., Ristow, M., Ziv, Y., & Jeltsch, F. (2013). Metacommunity, mainland-island system or island communities? Assessing the regional dynamics of plant communities in a fragmented landscape. *Ecography*, *36*(7), 842-853.

McCune, J. L., & Vellend, M. (2015). Using plant traits to predict the sensitivity of colonizations and extirpations to landscape context. *Oecologia*, *178*(2), 511-524.

Mestre, F., Risk, B. B., Mira, A., Beja, P., & Pita, R. (2017). A metapopulation approach to predict species range shifts under different climate change and landscape connectivity scenarios. *Ecological Modelling*, *359*, 406-414.

Meeus, J. H. (1993). The transformation of agricultural landscapes in Western Europe. *Science of the Total Environment*, *129*(1-2), 171-190.

Moilanen, A. (1999). Patch occupancy models of metapopulation dynamics: efficient parameter estimation using implicit statistical inference. *Ecology*, *80*(3), 1031-1043.

Moilanen, A. (2002). Implications of empirical data quality to metapopulation model parameter estimation and application. *Oikos*, *96*(3), 516-530.

Naaf, T., & Kolk, J. (2015). Colonization credit of post-agricultural forest patches in NE Germany remains 130–230years after reforestation. *Biological Conservation*, *182*, 155-163.

Naaf, T., & Kolk, J. (2016). Initial site conditions and interactions between multiple drivers determine herb-layer changes over five decades in temperate forests. *Forest Ecology and Management*, *366*, 153-165.

Nagelkerke, K. C., Verboom, J., Van Den Bosch, F., & Van De Wolfshaar, K. (2002). Time lags in metapopulation responses to landscape change. In: Applying landscape ecology in biological conservation, *Springer New York*, 330-354.

Nelder, J. A., & Mead, R. (1965). A simplex method for function minimization. *The Computer Journal*, *7*(4), 308-313.

Newbold, T., Hudson, L. N., Hill, S. L., Contu, S., Lysenko, I., Senior, R. A., ... & Day, J. (2015). Global effects of land use on local terrestrial biodiversity. *Nature*, *520*(7545), 45-50.

Paltto, H., Nordén, B., Götmark, F., & Franc, N. (2006). At which spatial and temporal scales does landscape context affect local density of Red Data Book and Indicator species?. *Biological Conservation*, *133*(4), 442-454.

Parr, T. W., Ferretti, M., Simpson, I. C., Forsius, M., & Kovacs-Lang, E. (2002). Towards a long-term integrated monitoring programme in Europe: network design in

theory and practice. *Environmental Monitoring and Assessment*, *78*(3), 253-290.

Pellissier, V., Bergès, L., Nedeltcheva, T., Schmitt, M. C., Avon, C., Cluzeau, C., & Dupouey, J. L. (2013). Understorey plant species show long-range spatial patterns in forest patches according to distance-to-edge. *Journal of Vegetation Science*, *24*(1), 9-24.

Pereira, H. M., Ferrier, S., Walters, M., Geller, G. N., Jongman, R. H. G., Scholes, R. J., ... & Coops, N. C. (2013). Essential biodiversity variables. *Science*, *339*(6117), 277-278.

Peterken, G. F. (1996). Natural woodland: ecology and conservation in northern temperate regions, *Cambridge university press*.

Pimm, S. L., & Raven, P. (2000). Biodiversity: extinction by numbers. *Nature*, *403*(6772), 843-845.

Piqueray, J., Cristofoli, S., Bisteau, E., Palm, R., & Mahy, G. (2011). Testing coexistence of extinction debt and colonization credit in fragmented calcareous grasslands with complex historical dynamics. *Landscape Ecology*, *26*(6), 823-836.

Prugh, L. R., Hodges, K. E., Sinclair, A. R., & Brashares, J. S. (2008). Effect of habitat area and isolation on fragmented animal populations. *Proceedings of the National Academy of Sciences*, *105*(52), 20770-20775.

Purves, D. W., Zavala, M. A., Ogle, K., Prieto, F., & Benayas, J. M. R. (2007). Environmental heterogeneity, bird-mediated directed dispersal, and oak woodland dynamics in mediterranean Spain. *Ecological Monographs*, *77*(1), 77-97.

Quantum GIS Development Team. (2011). Quantum GIS Geographic Information System. Open Source Geospatial Foundation Project.

Rogers, D. A., Rooney, T. P., Hawbaker, T. J., Radeloff, V. C., & Waller, D. M. (2009). Paying the extinction debt in southern Wisconsin forest understories. *Conservation Biology*, *23*(6), 1497-1506.

Royle, J. A., Nichols, J. D., & Kéry, M. (2005). Modelling occurrence and abundance of species when detection is imperfect. *Oikos*, *110*(2), 353-359.

Rubin, D. B. (1984). Bayesianly justifiable and relevant frequency calculations for the applied statistician. *The Annals of Statistics*, *12*(4), 1151-1172.

Ruete, A., Fritz, Ö., & Snäll, T. (2014). A model for non-equilibrium metapopulation dynamics utilizing data on species occupancy, patch ages and landscape history. *Journal of Ecology*, *102*(3), 678-689.

Ruete, A., Jönsson, M. T., & Snäll, T. (2017). Conservation benefits of international Aichi protection and restoration targets for future epiphyte metapopulations. *Journal of Applied Ecology.*

Ruiz, L., Parikh, N., Heintzman, L. J., Collins, S. D., Starr, S. M., Wright, C. K., ... & McIntyre, N. E. (2014). Dynamic connectivity of temporary wetlands in the southern Great Plains. *Landscape Ecology*, *29*(3), 507-516.

Sala, O. E., Chapin, F. S., Armesto, J. J., Berlow, E., Bloomfield, J., Dirzo, R., ... & Leemans, R. (2000). Global biodiversity scenarios for the year 2100. S*cience*, *287*(5459), 1770-1774.

Stork, N. E. (2010). Re-assessing current extinction rates. *Biodiversity and Conservation*, *19*(2), 357-371.

Sutherland, C. S., Elston, D. A., & Lambin, X. (2014). A demographic, spatially explicit patch occupancy model of metapopulation dynamics and persistence. *Ecology*, *95*(11), 3149-3160.

Thioulouse, J., Chessel, D., Dole, S., & Olivier, J. M. (1997). ADE-4: a multivariate analysis and graphical display software. *Statistics and computing*, *7*(1), 75-83.

Tilman, D., May, R. M., Lehman, C. L., & Nowak, M. A. (1994). Habitat destruction and the extinction debt. *Nature*, *371*(6492), 65-66.

Tilman, D., Clark, M., Williams, D. R., Kimmel, K., Polasky, S., & Packer, C. (2017). Future threats to biodiversity and pathways to their prevention. *Nature*, *546*(7656), 22900.

Urban, D., & Keitt, T. (2001). Landscape connectivity: a graph‐theoretic perspective. *Ecology*, *82*(5), 1205-1218.

Van Teeffelen, A. J., Vos, C. C., & Opdam, P. (2012). Species in a dynamic world: consequences of habitat network dynamics on conservation planning. *Biological Conservation*, *153*, 239-253.

Vellend, M. (2005). Land-use history and plant performance in populations of Trillium grandiflorum. *Biological Conservation*, *124*(2), 217-224.

Vellend, M., Verheyen, K., Jacquemyn, H., Kolb, A., Van Calster, H., Peterken, G., & Hermy, M. (2006). Extinction debt of forest plants persists for more than a century following habitat fragmentation. *Ecology*, *87*(3), 542-548.

Vellend, M., Verheyen, K., Flinn, K. M., Jacquemyn, H., Kolb, A., Van Calster, H., ... & Brunet, J. (2007). Homogenization of forest plant communities and weakening of species–environment relationships via agricultural land use. *Journal of Ecology*, *95*(3), 565-573.

Vellend, M., Brown, C. D., Kharouba, H. M., McCune, J. L., & Myers-Smith, I. H. (2013). Historical ecology: using unconventional data sources to test for effects of global environmental change. *American Journal of Botany*, *100*(7), 1294-1305.

Verheyen, K., Honnay, O., Motzkin, G., Hermy, M., & Foster, D. R. (2003a). Response of forest plant species to land‐use change: a life‐history trait‐based approach. *Journal of Ecology*, *91*(4), 563-577.

Verheyen, K., Guntenspergen, G. R., Biesbrouck, B., & Hermy, M. (2003b). An integrated analysis of the effects of past land use on forest herb colonization at the

landscape scale. *Journal of Ecology*, *91*(5), 731-742.

Verheyen, K., & Hermy, M. (2004). Recruitment and growth of herb-layer species with different colonizing capacities in ancient and recent forests. *Journal of Vegetation Science*, *15*(1), 125-134.

Verheyen, K., Vellend, M., Van Calster, H., Peterken, G., & Hermy, M. (2004). Metapopulation dynamics in changing landscapes: a new spatially realistic model for forest plants. *Ecology*, *85*(12), 3302-3312.

Verheyen, K., Fastenaekels, I., Vellend, M., De Keersmaeker, L., & Hermy, M. (2006). Landscape factors and regional differences in recovery rates of herb layer richness in Flanders (Belgium). *Landscape Ecology*, *21*(7), 1109-1118.

Violle, C., Navas, M. L., Vile, D., Kazakou, E., Fortunel, C., Hummel, I., & Garnier, E. (2007). Let the concept of trait be functional!. *Oikos*, *116*(5), 882-892.

Vos, C. C., Verboom, J., Opdam, P. F., & Ter Braak, C. J. (2001). Toward ecologically scaled landscape indices. *The American Naturalist*, *157*(1), 24-41.

Wang, B. C., & Smith, T. B. (2002). Closing the seed dispersal loop. *Trends in Ecology & Evolution*, *17*(8), 379-386.

Warren, D. L. (2012). In defense of 'niche modeling'. *Trends in Ecology & Evolution*, *27*(9), 497-500.

Wearn, O. R., Reuman, D. C., & Ewers, R. M. (2012). Extinction debt and windows of conservation opportunity in the Brazilian Amazon. *Science*, *337*(6091), 228-232.

With, K. A., & King, A. W. (1997). The use and misuse of neutral landscape models in ecology. *Oikos*, 219-229.